ISOTOPIC RECORDS OF METEOROLOGICAL AND ATMOSPHERIC CONDITIONS FROM SUB-ANNUALLY RESOLVED TREE-RING CELLULOSE, PRECIPITATION, AND SURFACE WATERS

A Thesis Submitted to the College of
Graduate Studies and Research
In Partial Fulfillment of the Requirements
for the Degree of Master of Science
in the Department of Geological Sciences
University of Saskatchewan
Saskatoon

Justin P. Dodd

PERMISSION TO USE

In presenting this thesis in partial fulfilment of the requirements for a Postgraduate degree from the University of Saskatchewan, I, Justin Dodd, agree that the Libraries of this University may make it freely available for inspection. I further agree that permission for copying of this thesis in any manner, in whole or in part, for scholarly purposes may be granted by myself, Dr. William P. Patterson, Dr. Chris Holmden, or in my absence or Drs. Patterson and Holmden's absence, by the Head of the Department of Geological Sciences or the Dean of the College in which my thesis work was done. It is understood that any copying or publication or use of this thesis or parts thereof for financial gain shall not be allowed without my written permission. It is also understood that due recognition shall be given to me and to the University of Saskatchewan in any scholarly use which may be made of any material in my thesis titled *Isotopic Records of Meteorological and Atmospheric Conditions from Sub-Annually Resolved Tree-Ring Cellulose, Precipitation, and Surface Waters*

Requests for permission to copy or to make other use of material in this thesis in whole or part should be addressed to Justin P. Dodd or:

Head of the Department of Geological Sciences
University of Saskatchewan
Saskatoon, SK S7N 5E2
Canada

UNIVERSITY OF SASKATCHEWAN
College of Graduate Studies and Research

ABSTRACT
Submitted in partial fulfillment
of the requirements of the

DEGREE OF MASTERS OF SCIENCE
By

Justin P. Dodd
Department of Geological Sciences
University of Saskatchewan
June 6, 2006

Examining Committee:

Dr. K. Ansdell	Chair of Committee
Dr. W. Patterson	Co-Supervisor, Department of Geological Sciences
Dr. C. Holmden	Co-Supervisor, Department of Geological Sciences
Dr. J. Basinger	Department of Geological Sciences
Dr. N. Bélanger	Department of Soil Sciences

ISOTOPIC RECORDS OF METEOROLOGICAL AND ATMOSPHERIC CONDITIONS FROM SUB-ANNUALLY RESOLVED TREE-RING CELLULOSE, PRECIPITATION, AND SURFACE WATERS

In recent decades, there has been increased global concern about observed climate change; however for future climatic impacts and anthropogenic forcings of climate change to be realistically predicted, natural climate variability in the past needs to be better understood. The aim of this research is to develop quantifiable proxy records of past climate change through the calibration of isotope values in modern surface waters and tree-ring cellulose with meteorological and atmospheric records. Terrestrial proxy records that utilize oxygen and hydrogen isotope values to reconstruct paleoclimatic and paleohydrologic conditions are limited by a paucity of data on the modification of surface water isotope values prior to sequestration into proxy material. To address this gap in our knowledge and determine the most appropriate study sites, this research focuses on

isotopic records preserved in surface water reservoirs, precipitation, and tree-ring cellulose. In the first study, δD, $\delta^{18}O$, and deuterium-excess values were determined for lakes and rivers from Tasmania, southeastern Australia.

The second focus of this research was to calibrate the $\delta^{18}O$, δD, and $\delta^{13}C$ values of tree-ring cellulose from North America with instrumental records. A new high-resolution sampling procedure that uses a robotic micromilling device to very precisely map and sample along growth rings in trees is discussed. Additionally, a seasonally resolved (early/late wood) 110-year record of $\delta^{18}O$ values from tree-ring α-cellulose from spruce species (*Picea mariana* and *P. glauca*) from east-central Saskatchewan, Canada is compared to growing season precipitation $\delta^{18}O$ values, temperature, and relative humidity. The $\delta^{18}O$ time series from α-cellulose display a high correlation with growing season precipitation isotope values ($r = 0.86$). $\delta^{18}O$ α-cellulose time series from a white spruce (*Picea* glauca) also records seasonal changes in atmospheric circulation associated with the position of the circumpolar vortex and dominate modes of atmospheric variability such as the North Atlantic Oscillation and Pacific Decadal Oscillation.

Keywords: $\delta^{18}O$, δD, $\delta^{13}C$, surface water, hydrology, paleoclimate, tree-ring cellulose, micromill, high-resolution, atmospheric circulation

ACKNOWLEDGEMENTS

First and foremost I would like to acknowledge the support of my co-supervisors William Patterson and Chris Holmden. I am very grateful for the opportunity to conduct research all over the world on multiple projects. Without Bill's encouragement I would have never collected water samples from crocodile infested waters. I would also like to thank Breanna Uzelman for her support and patience when I have nothing but isotopes on my brain. Also I thank Aaron Diefendorf, without whose guidance I surely would have lost my mind, and Tim Prokopiuk, Kristin Dietrich, and Adam Csank for reading early drafts of the manuscript and helping with analyses at the Saskatchewan Isotope Laboratory. I would also like to thank Bob Deegan for his invaluable assistance collecting water samples in Australia and Tim Prokopiuk for his tree coring expertise.

This research was supported by a National Science Foundation – Graduate Research Fellowship and a Geologic Society of America Graduate Research Grant to J. Dodd, and Natural Sciences and Engineering Research Council of Canada Grant #203538 to W. Patterson.

TABLE OF CONTENTS

page

PERMISSION TO USE.....i

ABSTRACT..... ii

ACKNOWLEDGMENTS..... iv

LIST OF TABLES.....vii

LIST OF FIGURES..... ix

CHAPTER 1. INTRODUCTION.....1

1.1 Climate Overview and Motivation..... 1

1.2 Methodology..... 2

1.3 References..... 3

CHAPTER 2. SURVEY OF OXYGEN AND HYDROGEN ISOTOPES IN TASMANIAN SURFACE WATERS..... 6

2.1 Abstract..... 6

2.2 Introduction..... 6

2.3 Site Description..... 8

2.4 Methods..... 12

2.5 Isotope Values of Tasmanian Precipitation..... 13

2.5.1 IAEA/WMO Preciptation Data..... 13

2.5.2 Synoptic Pattern in Precipitation..... 18

2.6 Tasmanian Surface Water: Results and Discussion..... 19

2.6.1 Surface Water Lines and Data Correlations..... 20

2.6.2 Deuterium excess..... 22

2.6.3 Relevance to Paleoclimate and Hydrologic Studies..... 26

2.7 Summary..... 27

2.8 Acknowledgements 28

2.9 References 28

2.10 Manuscript's Relationship to Thesis 32

CHAPTER 3. A NEW TOOL FOR OBTAINING SUB-SEASONAL SAMPLES OF TREE-RING CELLULOSE FOR ISOTOPE STUDIES: ADVANTAGES OF ROBOTIC MICROMILLING 33

3.1 Abstract 33

3.2 Introduction 33

3.3 Experimental Section 34

3.3.1 Sample Preparation 34

3.3.2 Micromilling Apparatus 35

3.3.3 Alpha Cellulose Processing 37

3.3.4 Isotope Analyses 40

3.4 Results 40

3.5 Discussion and Conclusions 47

3.6 Acknowledgments 49

3.7 References 49

3.8 Manuscript's Relationship to Thesis 52

CHAPTER 4. A 110YR SEASONAL PRECIPITATION AND ATMOSPHERIC CIRCULATION RECORD: EVIDENCE FROM $\delta^{18}O$ VALUES OF TREE-RING α–CELLULOSE IN MODERN SPRUCE 53

4.1 Abstract 53

4.2 Introduction 53

4.2.1 Oxygen Isotope Values of Tree-Rings 55

4.3 Site Description 56

4.4 Methods 60

4.5 Results 61

4.5.1 Tree-ring oxygen isotopes 61

4.5.2 Reconstructing growing season $\delta^{18}O$ precipitation values 61

4.6 Discussion 63

4.6.1 Interpretation of $\delta^{18}O$ values in source water and precipitation 63

4.6.2 Meteorological and atmospheric interpretations from $\delta^{18}O$ values 67

2.7 Conclusions 74

2.8 Acknowledgements 75

2.9 References 75

2.10 Manuscript's Relationship to Thesis 81

CHAPTER 5. CONCLUSION AND RELATIONSHIP OF MANUSCRIPTS TO THE THESIS 82

APPENDIX A: SURFACE WATER δ D, $\delta^{18}O$, AND D-EXCESS DATA FOR TASMANIA, AUSTRALIA A1

APPENDIX B: TREE RING DATA FOR WHITE AND BLACK SPRUCE FROM LIMESTONE LAKE, SASKATCHEWAN B1

CURRICULUM VITAE CV1

LIST OF TABLES

Table 2.1 Salinity of Tasmanian Surface waters 23

Table 2.2 Correlations between surface sample δD, $\delta^{18}O$, and d-excess values and sample parameters. 24

Table 3.1 Homogeneity: Scalpel vs. Micromill Sampling of cellulose 45

Table 4.1 Correspondence analysis of $\delta^{18}O$ time series and environmental parameters .. 69

LIST OF FIGURES

Figure 2.1 Sample locations for Tasmanian surface water samples 9

Figure 2.2 Precipitation patterns and Streamhead Location 10

Figure 2.3 Surface temperature and precipitation amount recorded at Cape Grim 11

Figure 2.4 Weighted monthly averages δD and $\delta^{18}O$ values of precipitation at Cape Grim 15

Figure 2.5 The LMWL constructed from the Cape Grim precipitation data and SWL from Tasmanian surface water data 16

Figure 2.6 Weighted monthly values of d-excess in Cape Grim precipitation data 17

Figure 2.7 Detailed SWLs from Tasmanian surface water data 21

Figure 3.1 Screen capture during the milling of a white spruce 36

Figure 3.2 Micromilling Schematic 38

Figure 3.3 High-resolution $\delta^{18}O$ time series of white spruce 41

Figure 3.4 High-resolution $\delta^{18}O$ time series of tamarack 42

Figure 3.5 High-resolution $\delta^{18}O$, δD, and $\delta^{13}C$ time series of beech 43

Figure 3.6 Homogeneity of micromilled samples 46

Figure 3.7 Intra-ring $\delta^{18}O$ values of beech display a strong relationship with average monthly temperature 48

Figure 4.1 Map of western Canada depicting Limestone Lake and nearby meteorological stations 57

Figure 4.2 $\delta^{18}O$ time series constructed for early and late wood portions of a black and white spruce from Limestone Lake 62

Figure 4.3 $\delta^{18}O$ values of reconstructed source water are well correlated with growing season precipitation 64

Figure 4.4 $\delta^{18}O$ values of source water and snowfall amount 65

Figure 4.5 Correspondence analysis of $\delta^{18}O$ time series and environmental parameters 68

Figure 4.6 Continuous wavelet transform (CWT) analysis of white spruce $\delta^{18}O$ time series, PDO, NAO, temperature and precipitation..... 72

Figure 4.7 Cross wavelet transform analysis (XWT) of periods with common periodicities 73

CHAPTER 1. INTRODUCTION

1.1 Climate Overview and Motivation

Increasing global concern about observed climate change in recent decades has prompted a great deal of debate as to whether these changes are due to anthropogenic or natural forcings. In order for future climatic impacts and anthropogenic forcings of climate change to be realistically predicted, there is a great need for an examination of natural climate variability in the past (Oldfield and Alverson, 2003). Instrumental records of meteorological conditions cover, at most, the last few hundred years of Earth history. Additionally, poor geographical distribution of data stations, especially in the Southern Hemisphere and the high-latitudes of the Northern Hemisphere, present a significant weakness in the present understanding of natural climate variability (Ciais et al., 1992; Gibson, 2001, Schindler and Donahue, 2006).

Stable isotope values in natural systems have been demonstrated to reliably record a variety of meteorological and atmospheric parameters. A wide range of materials contain isotope proxies, including lacustrine sediment (e.g. Kirby et al., 2001), speleothems (e.g. McDermott et al., 2001), ice cores (e.g. Alley et al., 2003), bone phosphate (e.g. Zazzo et al., 2006), biogenic carbonate (e.g.Wurster and Patterson, 2001) and tree-rings (e.g. Anderson et al., 2002, McCarroll and Loader, 2004). However, isotope values recorded in tree-rings offer a significant advantage over other terrestrial isotope proxies in that annual rings in tree stem cellulose provide unambiguous age control (Waterhouse et al., 2002, Saurer, 2003). This perfect annual resolution facilitates direct comparison and calibration of tree-ring isotope time series (such as $\delta^{18}O$, δD, and $\delta^{13}C$) with instrumental records of air temperature, relative humidity, precipitation amount, the $\delta^{18}O/\delta D$ value of precipitation, and atmospheric circulation (Anderson et al., 2002; Saurer, 2003). Trees are abundant in many terrestrial environments and long (>5,000 years) tree-ring width chronologies have been developed in Europe (e.g. Eronen et al., 2002; Grudd et al., 2002), North America (e.g. Baillie, 1995), and Australia (Cook et al., 1992). Isotope values in tree cellulose provide additional information that is often not recorded in tree-ring width measurements, and therefore can potentially be used to

develop precise records of meteorological and environmental conditions (Saurer, 2003; McCarroll and Loader, 2004). Through development of tree-ring isotope time series, and calibration of these time series with instrumental data, it is possible to extend the (spatial and temporal) resolution of meteorological and atmospheric records.

Additionally, reconstruction of paleoclimate records contained in tree-ring cellulose hydrogen and oxygen isotope proxies is limited by a paucity of meteoric water $\delta^{18}O/\delta D$ data and information on the modification of $\delta^{18}O$ and δD values in water throughout hydrologic cycle (Kendall and Coplen, 2001). In order to better interpret modern and paleoclimatic conditions via tree-ring cellulose H and O isotope proxies that record meteoric and surface waters it is necessary to understand the causes of geographic variability in δD and $\delta^{18}O$ values of local meteoric waters. It is therefore beneficial to document the patterns of geographic variation in meteoric waters for each region of interest in order to document the concordance with and discordance from global meteorological /hydrologic models (Darling, 2004).

1.2 Methodology

Research discussed herein focuses on the use of $\delta^{18}O$, δD, and $\delta^{13}C$ values in tree-ring cellulose as records of environmental change. The body of the research is divided into three main chapters (2 – 4), and each of these chapters is a separate article for peer-reviewed publication. Each article consists of original work by the author with supervision by the author's co-supervisors. Chapter 2 introduces the theory behind $\delta^{18}O$ and δD values in meteoric waters and the modification of these values in surface water reservoirs through case study of surface waters collected by the author from Tasmania, Australia in the summer of 2004. Chapter 3 then shifts to North America and focuses on reconstructing time series of $\delta^{18}O$, δD, and $\delta^{13}C$ values in tree-ring cellulose from four modern tree species (*Picea glauca*, *P. mariana*, *Larix laricina*, and *Fagus grandiflora*) from central Saskatchewan, Canada and New York, USA. Chapter 3 also describes a high-resolution sampling method for tree-ring isotope studies that has been implemented for the first time by the author. Chapter 4 brings together the concepts discussed in Chapters 2 and 3 by using the $\delta^{18}O$ time series of two spruce species (*Picea glauca*, *P.*

mariana) from central Saskatchewan to reconstruct the $\delta^{18}O$ values of growing season precipitation. Additionally, Chapter 4 discusses the relationship between the $\delta^{18}O$ time series and meteorological and atmospheric conditions for the 20th century. Although the study areas in Chapter 2 and Chapters 3-4 vary significantly in geographical location and physical characteristics, all three studies examine different aspects of isotope records as climate proxies.

1.3 References

Alley, R.B., Mayewski, P.A., Sowers, T., Stuiver, M., Taylor, K.C., and Clark, P.U., 1997. Holocene climatic instability: A prominent, widespread event 8200yr ago, Geology 25, 483-486.

Anderson, W.T., Bernasconi, S.M., McKenzie, J.A., Saurer, M., and Schweingruber, F., 2002. Model evaluation for reconstructing oxygen isotopic composition in precipitation from tree ring cellulose over the last century, Chemical Geology 182: 121-137.

Baillie, M.G.L., 1995. A slice through time: Dendrochronology and precise dating, Batsford, London, pp. 176.

Barnett, T.P., Santer, B.D., Jones, P.D., Bradley, R.S., and Briffa, K.R., 1999. Comparison of near-surface air temperature variability in 11 coupled global climate models. J. of Clim. 12: 511-518.

Ciais, P. Petit, J.R., Jouzel, J., Lorius, C., Barkov, N.I., Lipenkov, V., and Nicolaïev, 1992. Evidence for an early Holocene climatic optimum in the Antarctic deep ice-core record, Climate Dynamics 6: 169 – 177.

Cook, E.R., Bird, T., Peterson, M., Barbetti, M., Buckley, B., D'Arrigo, R., Francey, R., 1992. Climatic change over the last millennium in Tasmania reconstructed from tree-rings, The Holocene 2: 205 – 217.

Darling, W.G., 2004. Hydrological factors in the interpretation of stable isotopic proxy data present and past: a European perspective, Quaternary Science Reviews 23: 743–770.

Eronen, M., Zetterberg, P., Briffa, K.R., Lindhom, M., Merilanen, J., and Timomen, M., 2002. The supra-long Scots pine tree-ring record for Finnish Lapland: Part 1, chorology, construction, and initial inferences, The Holocene 12: 673-680.

Gibson, J.J., 2001. Forest-tundra water balance signals traced by isotopic enrichment in lakes, J. of Hydro. 251: 1-12.

Grudd, H., Briffa, K.E., Karlen, W., Bartholin, T.S., Jones, P.D., and Kormer, B., 2002. A 7400yr tree-ring chronology in northern Swedish Lapland: natural climatic variability expressed on annual to millennial timescales, The Holocene 12: 657-665.

Kirby, M.E., Mullins, H.T., Patterson, W.P., and Burnett, A.W., 2002. Lacustrine isotopic evidence for multidecadal natural climate variability related to the circumpolar vortex over northeast United States during the past millennium, Geology 29: 807-810.

Kendall, C., and Coplen, T.B., 2001. Distribution of oxygen-18 and deuterium in river waters across the United States, Hydrological Processes 15: 1363–1393

McCarroll, D., and Loader, N.J., 2004. Stable isotopes in tree rings, Quat. Sci. Rev. 23: 771 – 801.

McDermott, F., Mattey, D.P., and Hawkesworth, C., 2001. Centennial-scale Holocene climate variability revealed by a high-resolution speleothem $\delta^{18}O$ record from SW Ireland, Science 294: 1328-1331.

Oldfield, F., and Alverson, K., 2003. The societal relevance of paleoenvironmental research, in Alverson, K.D., Bradley, R.S., Pedersen, T.F., (Eds), Global Change, the IGBP Series: Paleoclimate, Global Change and the Future, Springer-Verlag, Heidelberg, Germany, pp. 1 – 11.

Saurer, M., 2003. The influence of climate on the oxygen isotopes in tree rings, Isotopes Environ. Health Stud. 39: 105-112.

Schindler, D.W., and Donahue, W.F., 2006. An impending water crisis in Canada's western prairie provinces, Proc. Natl. Acad. Sci.:1-7. (www.pnas.org/cgi/doi/10.1073/pnas.0601568103)

Waterhouse, J.S., Switsur, V.R., Barker, A.C., Carter, A.H.C., and Robertson, I., 2002. Oxygen and hydrogen isotope ratios in tree rings: how well do models predict observed values? Earth and Planet. Sci. Lett. 201: 421-430.

Wurster, C.M., and Patterson, W.P., 2001, Seasonal variation in stable oxygen and carbon isotope values recovered from modern lacustrine freshwater mollusks: Paleoclimatological implications for sub-weekly temperature records. J. of Paleo. Lim.26: 305-218.

Zazzo, A., Balasse, M., Patterson, W.P. 2005. High-resolution $\delta^{13}C$ intratooth profiles in bovine enamel: Implications for mineralization pattern and isotopic attenuation. Geochim. Cosmochim. Acta 69: 3631–3642.

CHAPTER 2. SURVEY OF OXYGEN AND HYDROGEN ISOTOPE VALUES IN TASMANIAN PRECIPITATION AND SURFACE WATERS

2.1 Abstract

Terrestrial proxy records that utilize oxygen and hydrogen isotope values to reconstruct paleoclimatic and paleohydrologic conditions are limited by a paucity of data that quantify modification of surface water isotope values prior to sequestration into proxy material. To address this gap in our knowledge and determine the most appropriate study sites and proxy materials, δD, $\delta^{18}O$, and deuterium-excess (d-excess) values of lakes and rivers (*n*=72) from Tasmania, southeastern Australia, are presented. δD and $\delta^{18}O$ values of surface waters are compared to precipitation isotope values from Cape Grim, northwestern Tasmania from 1979 to 2000 (IAEA/WMO, 2001; *n*=195) and from Margate, southeastern Tasmania, from 1994 to 2000 (n=598; Treble et al, 2005). Local surface water lines and local meteoric water lines are defined by the relationships $\delta D = 5.90 (\pm 0.19) * \delta^{18}O + 1.48 (\pm 1.32)$ (*r*= 0.93) and $\delta D = 6.61 (\pm 0.16) * \delta^{18}O + 5.28 (\pm 0.63)$ (*r* = 0.95), respectively. Surface water isotope values are most significantly correlated with sample/stream head elevation and more weakly correlated with latitude/longitude. Tasmania is divided by northwest-southeast trending mountains that exert a strong orographic effect on Tasmanian precipitation amount and subsequent isotope values. Surface water isotope values record an altitude effect of 3‰/100m for δD and 0.4‰/100m for $\delta^{18}O$. This study provides the first regional analysis of isotope values of Tasmanian surface waters. Interpretation of proxy records of climate change in Tasmania and elsewhere will benefit from this type of surface water survey because it permits identification of the most appropriate study sites and proxy materials.

2.2. Introduction

Oxygen and hydrogen isotope values of a wide variety of materials including speleothems, lacustrine sediment, ice cores, tree-ring cellulose and terrestrial organic material have been demonstrated to be reliable paleoclimatic proxies. Similarly, oxygen

and hydrogen isotopes are used as tracers in animal migration studies (Hobson et al., 2004), wildlife forensics (Bowen et al., 2005), and mummified human remains (Sharp et al., 2003). A common goal of these studies is to characterize the hydrogen and oxygen isotope value of the source water, and consequently the rainfall that contributed to this water body (Darling, 2004). Although isotope values of global precipitation have been characterized by the IAEA/WMO and modeled by others (e.g. Bowen and Revenaugh 2003), a complete understanding of precipitation isotope values is limited by the low density of sampling stations. Additionally, the original isotope value of precipitation can be modified in surface, soil, and groundwater reservoirs prior to preservation by proxy material (Darling, 2004). Treble et al. (2005) note that to date there have been few in-depth studies of the modification and representation of δD and $\delta^{18}O$ values throughout the hydrologic cycle in the Australian region.

Isotope proxies used in the reconstruction of paleoclimate and as tracers of geographic origin are thus limited by a paucity of meteoric water isotope data and information on the isotopic modification of water in the hydrologic cycle (Kendall and Coplen, 2001). In order to better interpret modern and paleoclimatic conditions via proxies that record meteoric and surface waters it is necessary to understand the nature of spatial isotope variability in these waters. It is therefore beneficial to generate records for each region of interest that characterize the concordance with and discordance from global precipitation/hydrologic models.

Herein we present the spatial variability of $\delta^{18}O$ and δD values of surface waters and precipitation in Tasmania, Australia as a means to characterize the isotope values of water incorporated into proxies such as lake sediment, trees and speleothems. Similar studies have been conducted in the UK (Darling 2004), Ireland (Diefendorf and Patterson, 2005), North America (Kendall and Coplen, 2001), and Central America (Lachniet and Patterson, 2002, 2006); however, this is the first study of surface water isotope hydrology in Tasmania. Surface water isotope values presented in this study yield information on lake water residence time, and regional hydrologic processes and serve as a useful tool in selecting appropriate locations for gathering climate change proxy materials.

2.3 Site Description

The island of Tasmania is bordered by the Tasman Sea and the Southern Pacific Ocean to the east and the Southern Ocean to the south and west. The Bass Straight to the north separates Tasmania from mainland Australia. The island is divided by northwest-southeast trending mountains (Fig. 2.1) that exert a strong orographic influence on rainfall patterns, such that the west coast receives more than 3000 mm of precipitation per year whereas the central and eastern regions of the island are limited to less than 400mm per year (Fig. 2.2, Treble et al., 2005; Commonwealth of Australia Bureau of Meteorology, 2005). Precipitation in Tasmania is derived from cyclonic systems and associated fronts embedded in the southern mid-latitude circumpolar vortex (also referred to as the westerly front), with most of the storm systems tracking from the Southern Ocean in the west (Treble et al., 2005). The high pole-to-equator temperature pressure gradients between the South Pole and tropical Indian Ocean, and the lack of land between 60ºS and 40ºS latitude result in exceptionally strong westerly winds in the Southern Hemisphere (Shulmeister et al., 2004). Cyclonic activity and therefore precipitation in Tasmania is greatest in the austral winter (June – August) when the mid-latitude circumpolar vortex is positioned between 60ºS and 35ºS (Burnett and McNicoll, 2000). During the austral winter a persistent high-pressure system is centered over the Australian continent extending from the Indian Ocean to the Western Pacific between 20ºS and 40ºS, whereas the Tasman Sea and Southern Ocean to the east of Tasmania are dominated by a prevalent low pressure system (Struman and Trapper, 1996).

During the austral summer (December – February) the subtropical high moves southward toward the Great Australian Bight and Tasmania, deflecting the circumpolar vortex southward thereby causing the westerlies and cyclonic activity to be concentrated south of 60ºS (Burnett and McNicoll, 2000). The result is strong seasonal variation in air temperature and precipitation characterized by the meteorological station in Cape Grim, Tasmania (Figure 2.3). The relationship between Tasmanian precipitation/climate and the position of the westerly belt renders Tasmania ideal for characterizing atmospheric variability in the mid latitudes of the Southern Hemisphere. In addition, the position and strength of the westerly storm tracks are constrained by changes in sea surface temperatures related to Antarctic and low-latitude climate parameters such as El

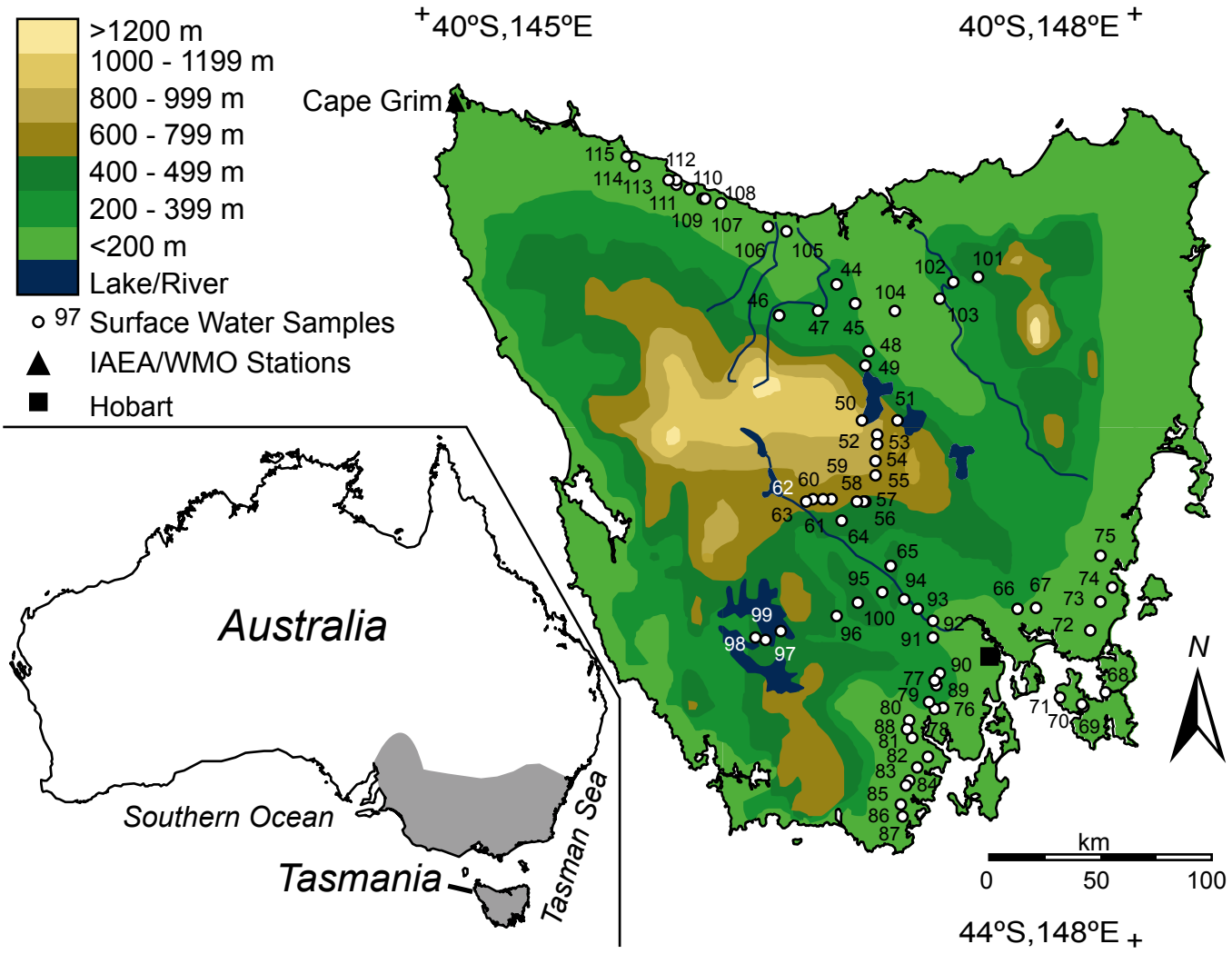

Figure 2.1. Sample locations and sample numbers for Tasmanian surface water samples. Elevation contours illustrate the altitudinal divide through the center of the island. The IAEA/ WMO GNIP station at Cape Grim is located in the northwest corner of the island. Gray area denotes the winter rainfall zone of southeast Australia.

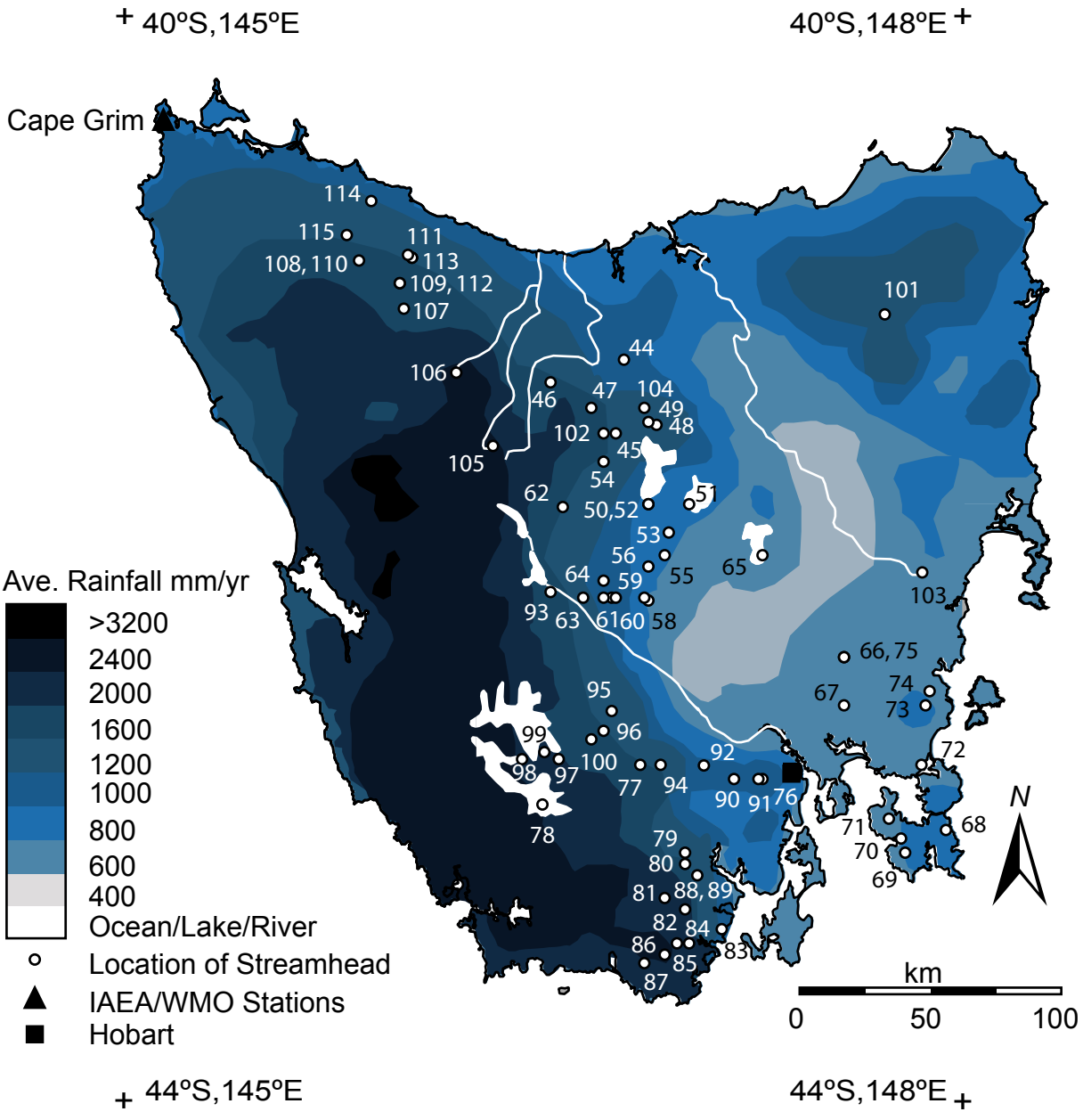

Figure 2.2. Precipitation patterns in Tasmania are strongly influenced by the orographic effects of the mountain ranges with more than 3000mm per year falling in the western side of the island and less than 400mm per year east of the mountains. Streamhead locations for surface water samples are also shown.

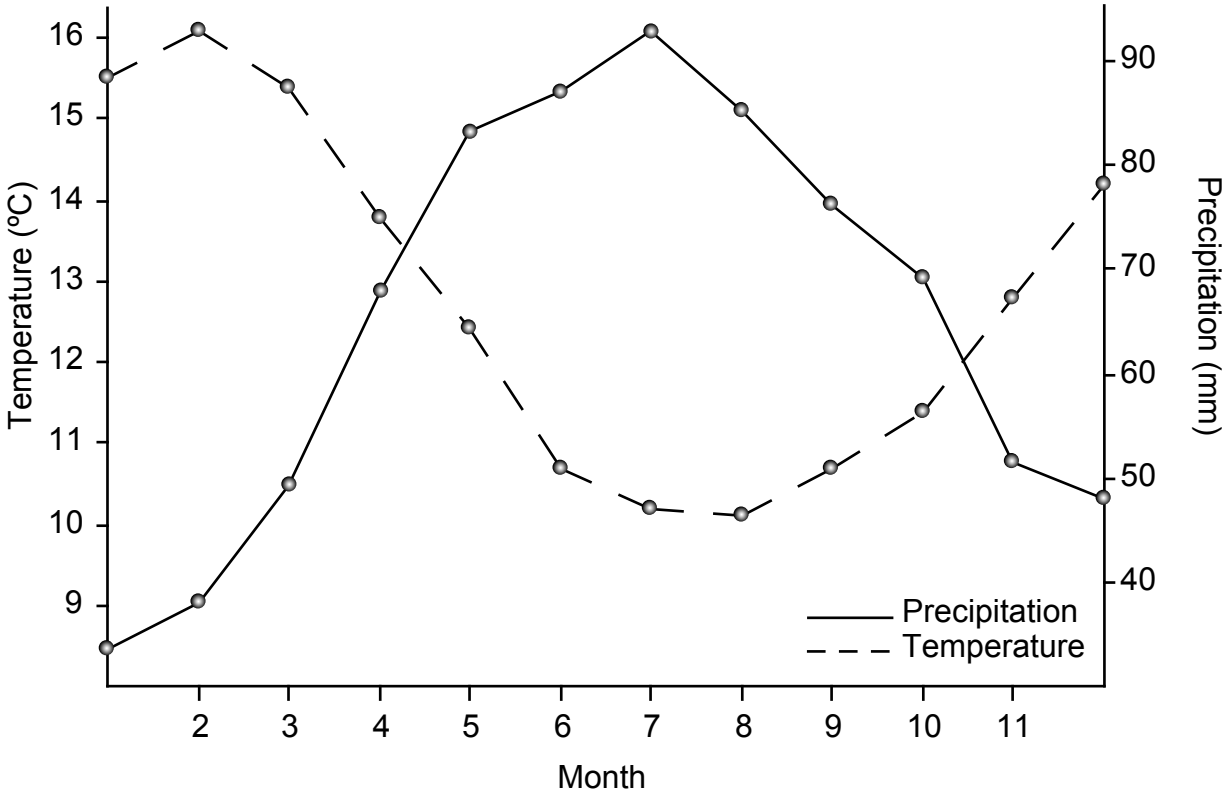

Figure 2.3. Surface temperature and precipitation amount recorded at Cape Grim are inversely related and display a strong seasonal signal. The lowest temperatures and greatest precipitation amounts are observed during austral winter (May - September).

Niño/Southern Oscillation (ENSO) and Indian Monsoon climate dynamics (Shulmeister et al., 2004).

Long-term terrestrial records of Southern Hemisphere climate are scarce. Consequently, there is a significant need to develop such records if we are to gain a better understanding of future climate change in the southern hemisphere (Villalba, 2000). Tasmania is well-positioned for the development of these kinds of records, having abundant tree-ring width chronologies covering the past few millennia (e.g. Cook et al. 1992, 2000), as well as cave and lake deposits that extend back prior to the last Ice Age (e.g. Goede et al., 1998; Calhoun, 2000).

2.4 Methods

Surface water samples were collected in July 2004 from Tasmania (Fig.2.1) as well as other areas in southeast Australia's winter rainfall zone (New South Wales, Victoria, and South Australia). Water samples were collected in 30 ml Nalgene® bottles and sample locations determined using a Magellan® GPS and Tasmanian Government 1:250,000 topographic maps (TASMAP Tasmanian Government, 2000).

δD and $\delta^{18}O$ analyses were conducted using a continuous flow pyrolysis technique at the Saskatchewan Isotope Laboratory. Water samples were injected in 1 μl aliquots into a Thermo Finnigan TC/EA containing a ceramic column lined with a glassy carbon tube and packed with glassy carbon fragments. Water was pyrolized at 1450ºC to H_2 and CO and was separated via a gas chromatograph. Gases were subsequently passed to a Conflo III for He dilution prior to analysis. Isotope ratios of D/H and $^{18}O/^{16}O$ were determined via continuous flow using a Thermo Finnigan Delta Plus XL mass spectrometer relative to H_2 and CO reference gases using the dual inlet port. Four internal standards calibrated with VSMOW, VSLAP, and GISP were used to normalize water isotope values. Sample values were corrected using a two-point calibration with two internal standards (δD/$\delta^{18}O$ values of -171/6.1‰ and –22/11.8‰) and corrected for internal drift using a third internal standard (δD/$\delta^{18}O$ values of –49/6.2‰). Intra-run drift was less than 2‰ for δD and 0.2‰ for $\delta^{18}O$. The fourth internal standard (δD/$\delta^{18}O$ values of –81/10.8‰) was used to test inter-run reproducibility. Sample precision is ±2.0‰ for δD and ±0.2 ‰ for $\delta^{18}O$ (1σ, n=48) with all values reported relative to

VSMOW. Conductivity of surface water samples was measured using a Radiometer Copenhagen CDM 80 Conductivity Meter calibrated at 25ºC.

2.5 Isotope Values of Tasmanian Precipitation

A number of climatological and physical processes result in fractionation of hydrogen and oxygen isotope values of precipitation. These effects cause the progressive fractionation of water vapor in air masses predicted by Rayleigh distillation ($R=R_0 f^{(\alpha-1)}$; Dansgaard, 1964). Temperature is one of the primary factors that constrain the rainout process (Dansgaard, 1964); however, studies of $\delta^{18}O$ values in Tasmanian precipitation have revealed little correlation between $\delta^{18}O$ values of precipitation and surface temperature at the time of precipitation. Instead, $\delta^{18}O$ values of Tasmanian precipitation appear to be best correlated with the amount of precipitation and seasonal variations in the westerly storm track (Treble et al., 2005). Studies of tropical precipitation have observed similar discrepancies between temperature and isotope values of precipitation (e.g. Fricke and O'Neill, 1999; Rozanski, 1993; Lachniet and Patterson, 2002, 2006). Although Tasmania (40 – 45ºS) is located well outside of the tropics, the large continental desert in western Australia deflects tropical air masses south resulting in a low latitudinal gradient in isotope values of precipitation over the Australian continent and Tasmania (Bowen and Revenaugh, 2003). In Tasmania, an elevation change of more than 1200 m exerts a strong orographic effect on the amount and isotope value of precipitation. Changes in topography force air upward resulting in adiabatic cooling of the air mass, driving the rainout process that produces a change in the δD ($\delta^{18}O$) in precipitation of –1 to –4‰ (–0.15 to – 0.5‰) per 100m increase in elevation (Clark and Fritz, 1997).

2.5.1 IAEA/WMO Precipitation Data

The International Atomic Energy Association and the World Meteorological Organization have operated a meteorological station in Cape Grim (40º41'S, 144º41'E; 94m elev.) in the northwestern corner of Tasmania as part of the Global Network of Isotopes in Precipitation (IAEA/WMO, 2001). The station was in operation from 1979 to 2000; however, data on precipitation amount, monthly weighted δD and $\delta^{18}O$ values, and

temperature were not recorded for periods of months to years in the dataset. Weighted monthly means have been calculated for all months for which sufficient data exist and display a distinct seasonal cycle in both δD and $\delta^{18}O$ values with highest values during austral summer and lowest values during austral winter (Fig 2.4). Weighted monthly average δD values range from –32‰ in June to –13‰ in December, whereas $\delta^{18}O$ values range from -5.1‰ in June to -2.1‰ in December (IAEA/WMO, 2001). A linear regression of the weighted monthly values (n = 195) in $\delta^{18}O$/δD space yields a local meteoric water line (LMWL) with the following equation:

$$\delta D = 6.61 (\pm 0.16) * \delta^{18}O + 5.28 (\pm 0.63) \text{ with } r = 0.95.$$

The Cape Grim LMWL has a lower slope and intercept than the Global Meteoric Water Line (GMWL), defined by $\delta D = (8.20 \pm 0.07)\ \delta^{18}O + (11.27 \pm 0.65)$ (Rozanski et al., 1993), indicating that $\delta^{18}O$ and δD values are influenced by secondary evaporation during precipitation (Fig 2.5). Kinetic evaporation of precipitation falling through the air column is primarily controlled by relative humidity; high relative humidity at Cape Grim (~80% annual average) causes the Cape Grim LMWL to have a of 6.61 (Clark and Fritz, 1997).

The deuterium-excess ($d = \delta D - 8 * \delta^{18}O$) has been calculated for the Cape Grim data and also displays a strong seasonal signal (Fig. 2.6). The global average d-excess in precipitation is about 10‰, but varies on a regional scale with local evaporative effects on precipitation such as variations in relative humidity, air temperature, wind speed, and sea surface temperature in the vapor source region. Recycling of surface waters via evaporative contributions of moisture to precipitation increases d-excess values (Fröhlich et al., 2002). Cape Grim data exhibits the highest average monthly d-excess from April to October, peaking at 13‰ in August and decreasing to 7.1‰ in November. For Cape Grim precipitation, the seasonal variation in d-excess is primarily a result of increased westerly wind velocity over Tasmania and lower temperatures in oceanic vapor source regions during austral winter. Increased wind velocity causes greater evaporation of surface water in the Southern Ocean west of Tasmania, resulting in increased precipitation. The greater evaporation that occurs at the oceanic vapor sources during

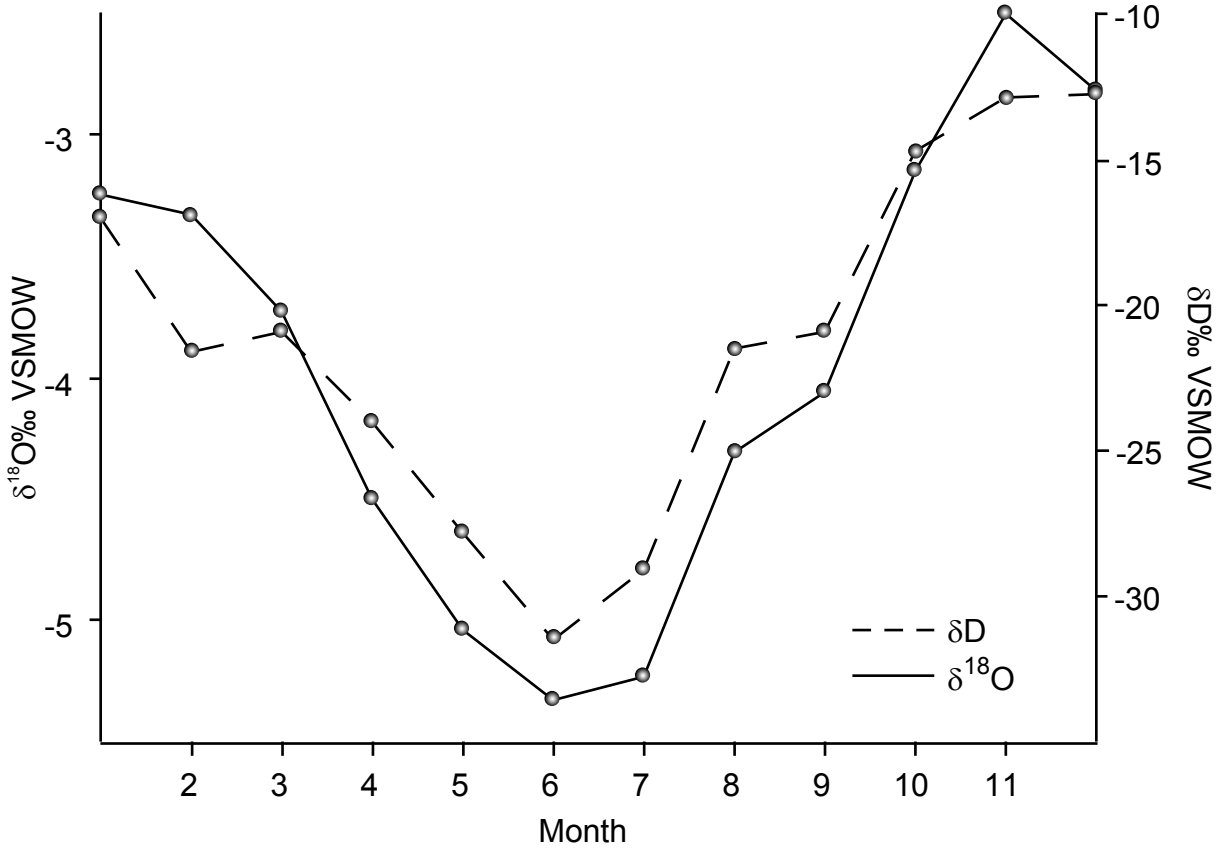

Figure 2.4. Weighted monthly averages of δD and $\delta^{18}O$ values of precipitation at Cape Grim between 1979 and 2000 display a seasonal cycle with the highest isotope values occurring during austral summer (October - March) and lowest values during austral winter (April - September).

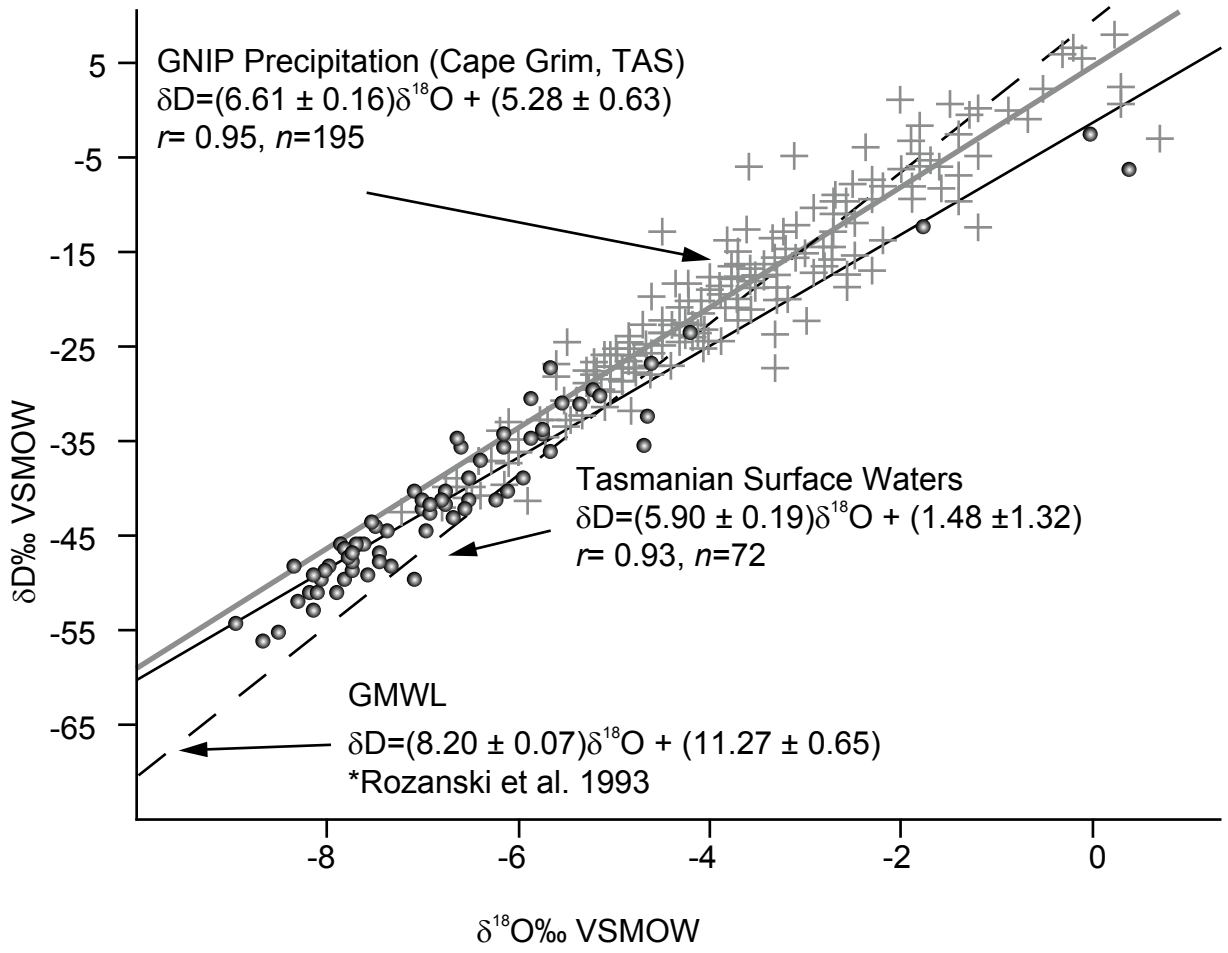

Figure 2.5. The LMWL constructed from the Cape Grim precipitation data (gray line) and SWL from Tasmanian surface water data (black) are shown with the GMWL (dashed) for comparison. The SWL displays a slightly lower slope than the LMWL indicating increased evaporation of surface water bodies as a whole.

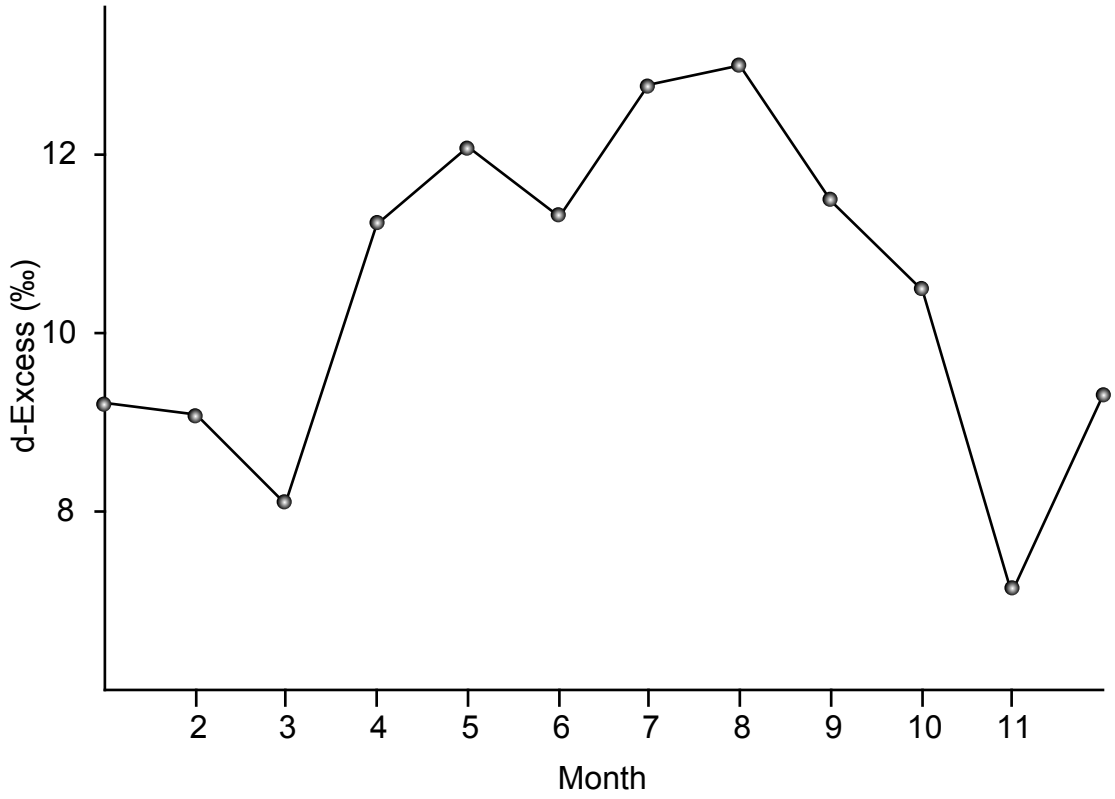

Figure 2.6. Weighted monthly values of d-excess in Cape Grim precipitation data. Cape Grim data exhibit the highest average monthly d-excess from April to October, peaking at 13‰ in August and decreasing to 7.1‰ in November.

austral winter results in higher d-excess values in austral winter and low d-excess values during austral summer.

2.5.2 Synoptic Pattern in Precipitation

In a study of precipitation $\delta^{18}O$ values from Cape Grim and Margate (42°57'S, 147°19'E; 1176m elev.), Treble et al. (2005) demonstrate that $\delta^{18}O$ values of Tasmanian precipitation are forced by the position of mid-latitude circumpolar vortex. Daily precipitation samples were collected from Margate in southeastern Tasmania for a 5-year period (1994 to 2000) to characterize event-to-event variation in precipitation $\delta^{18}O$ values. Monthly weighted means were also compared to monthly $\delta^{18}O$ records from an IAEA/GNIP station at Cape Grim. In the precipitation data from Margate for the period between 1994 and 2000, Treble et al. (2005) observed similar average seasonal variation in $\delta^{18}O$ values of ~3‰ (-6.1‰ in June to -3.0‰ in December), with values approximately 1‰ lower at Margate than at Cape Grim due to rainout as westerly systems pass over the Tasmanian mountain range. However, daily precipitation $\delta^{18}O$ values demonstrate a greater event-to-event variability, manifested as a range in daily precipitation $\delta^{18}O$ values that range from ~0‰ to –11.5‰ between January 1994 and December 2000 (Treble et al., 2005). As is more commonly observed in tropical sites, there is little correlation between $\delta^{18}O$ values of precipitation and surface temperature. Rather, the correlation between $\delta^{18}O$ values and temperature appears to be an artifact of seasonal variability in precipitation amount forced by the position of the westerly belt. If the seasonal cycle is removed, there appears to be very little correlation between $\delta^{18}O$ values and surface temperature (r = 0.12 daily, r = -0.07 monthly). $\delta^{18}O$ values do, however, appear to demonstrate an inverse relationship with rainfall amount (r = -0.35 to –0.51; Treble et al., 2005).

Low $\delta^{18}O$ precipitation values at the Margrate station correlate between high rainfall amounts that occur when the westerly track was shifted northward toward Tasmania. Lawrence et al. (1982) found a similar relationship between the position of cyclonic centers in the northern hemisphere circumpolar vortex and the isotope value of precipitation in New York State. When the mid-latitude vortex is positioned further south, Tasmania is located at the edge of the cyclonic activity and therefore receives

precipitation with higher $\delta^{18}O$ values. Due to the extreme convective processes and moisture recycling near the center of cyclonic low-pressure systems, precipitation that occurs near the centers of these systems will have a lower $\delta^{18}O$ value, whereas precipitation that occurs more distal to these low-pressure systems will have a higher $\delta^{18}O$ value. In addition, contribution of low latitude moisture will likely increase $\delta^{18}O$ values of precipitation.

When the mid-latitude circumpolar vortex is displaced to the south, high-pressure systems (warmer and drier air) move south along the east and west Australian coasts. In this scenario, precipitation consists of relatively more localized evaporation with higher $\delta^{18}O$ values than winter precipitation with values closer to that of seawater (~0‰; Treble et al, 2005). With the exception of the Cape Grim and Margate isotope data, however, there is little isotope data for Tasmanian precipitation and, to our knowledge these two sites provide the only isotope studies of precipitation on the island.

2.6 Tasmanian Surface Water: Results and Discussion

In order to gain a better understanding of hydrologic processes that influence isotope values of surface waters, we collected a suite of samples during the rainy season in July 2004 (Fig. 2.1) that provide a snapshot of isotope values of surface waters across Tasmania during the winter season (Appendix A). Rivers and other moving water bodies have comparatively short residence times and the relative effects of evaporation on these surface bodies is less than that on raindrops. Therefore riverine surface water samples are only slightly modified by evaporation and reflect, for the most part, the isotope values of precipitation averaged over short periods of time (Darling, 2004). Lakes and stagnant water bodies have a longer residence time and are therefore more significantly affected by evaporation. However, in regions with high relative humidity, evaporation has only a small effect on isotope values of lake water. In small or terminal lakes evaporation from the surface water body can greatly affect lake water isotope values, and thus significantly modify meteoric source isotope values (Gat, 1995).

δD values range from –56‰ at Arthur's Lake (elev. 954m) in central Tasmania to –3‰ in the Forth River on the northern coast of Tasmania (elev. 6m). $\delta^{18}O$ values of surface water samples range from –9.0‰ in an alpine lake on Projection Bluff in central

Tasmania (elev. 1070m) to 0.4‰ in a highly evaporative pond at the headwaters of the Saltwater River in the Tasman Peninsula. Despite its name, the Saltwater River pond is at an elevation of 94m and δD/ $\delta^{18}O$ values likely reflect evaporative enrichment rather than seawater mixing.

2.6.1 Surface Water Lines and Data Correlations

Surface water lines (SWL) were calculated using a linear regression of $\delta^{18}O$ and δD values in Tasmanian surface waters. For all surface water samples, the SWL is defined by $\delta D = 5.90\ (\pm 0.19) * \delta^{18}O + 1.48\ (\pm 1.32)$ $r = 0.93$, $n = 72$ (Fig. 2.5). Surface waters are subject to a greater degree of evaporation than meteoric waters and therefore the lower slope and intercept of the Tasmanian surface waters are expected. Surface water values also fall at the lower range of Cape Grim precipitation values because surface waters were collected during austral winter when $\delta^{18}O$ and δD values of Tasmanian precipitation are lower. Separate SWLs were calculated for lakes and rivers (Fig. 2.7), represented by the following equations:

a) Lakes and standing bodies of water

$\delta D = 6.25\ (\pm 0.41) * \delta^{18}O - 0.06\ (\pm 2.99)$, $r = 0.98$, $n = 12$

b) Rivers

$\delta D = 7.14\ (\pm 0.31) * \delta^{18}O + 7.59\ (\pm 2.14)$, $r = 0.95$, $n = 55$

Although they are not out of the range of isotope values recorded at Cape Grim, five surface samples (59, 71, 72, 75, 105) were excluded from SWL calculations and other comparisons because they appear to have abnormally high isotope values when compared to winter precipitation values. Samples 59 and 71 are stagnant bodies of water, and therefore likely reflect localized evaporative effects. Samples 72 and 75 were rivers from the extreme southeastern part of the island and likely reflect local evaporation effects as they flow through the drier region. For samples 71, 72, and 75 local evaporative effects are likely imprinted on the higher isotope value of meteoric water as air masses move across Tasmania (Treble et al., 2005). Samples 105 and 75 have been excluded because of tidal seawater (salinity ~35) mixing at the mouths of the Forth and Processor Rivers. Conductivity of these samples (59, 71, 72, 75, 105) was determined as a proxy for

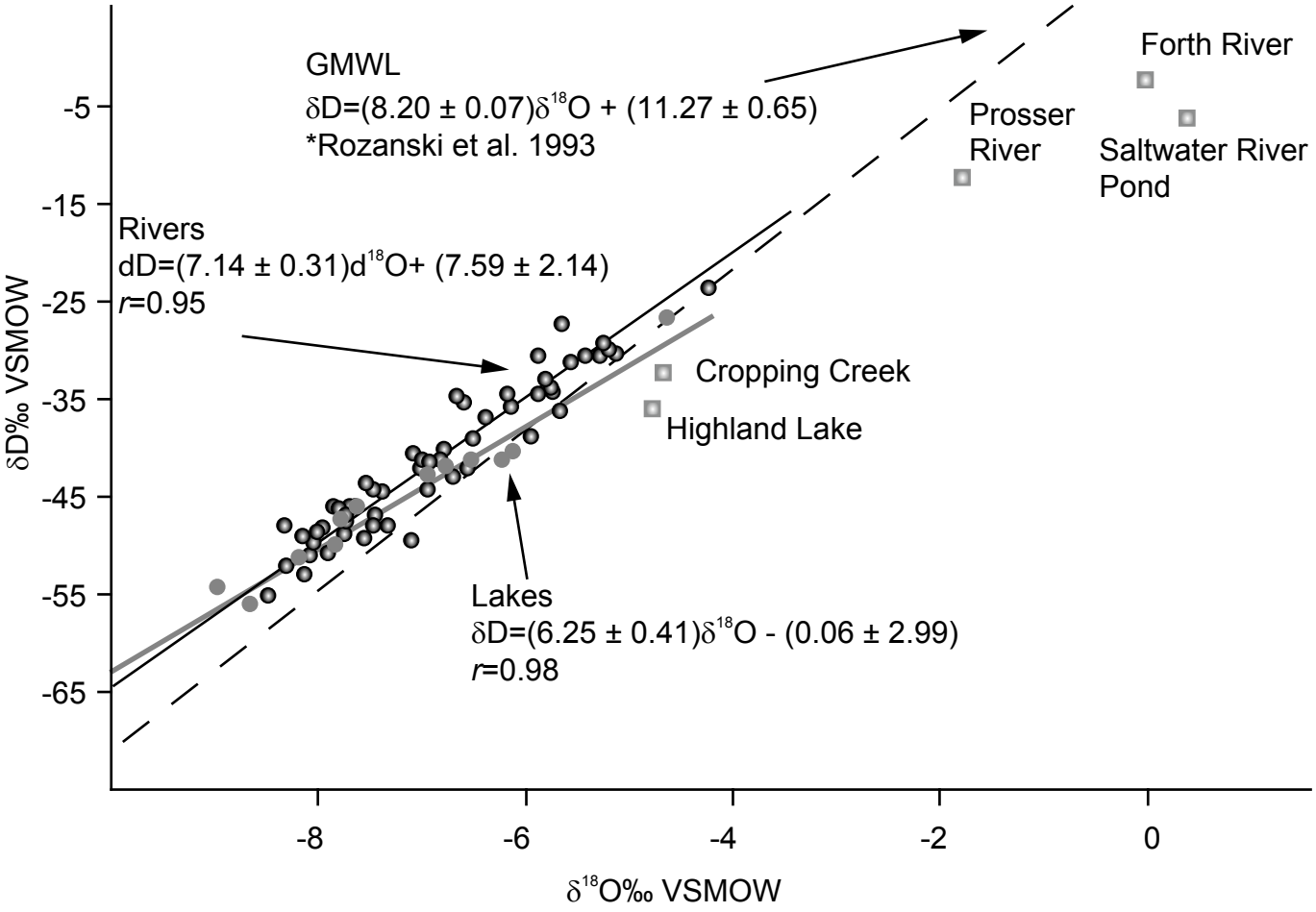

Figure 2.7. $\delta^{18}O$ and δD values of Tasmanian surface waters display a lower slope than the global and local meteoric water lines, reflecting the greater evaporation of surface water bodies. Lakes display greater evaporation than rivers, except for rivers in the extreme eastern part of the island (Prosser River and Cropping Creek). The eastern rivers as well as small-enclosed reservoirs (Saltwater River Pond and Highland Lake) plot below the meteoric water line as a result of evaporative effects on these water bodies. Saltwater mixing is likely in the Forth River.

salinity. Samples 59, 71, and 72 were significantly more saline compared to the average salinity for Tasmanian surface water samples, thereby suggesting increased evaporation of the water bodies. Samples 75 and 105 have relativity high salinity values of 22 and 31, respectively suggesting mixing with seawater (Table 2.1), therefore reaffirming the likelihood of seawater mixing in samples 75 and 105 (Linde, 2005).

When compared to physical and environmental parameters (Table 2.2), $\delta D/\delta^{18}O$ values of surface waters are most significantly correlated with stream head elevation (r = -0.51 and -0.55 for δD and $\delta^{18}O$, respectively). Stream head elevation was calculated for each river sampled, while the sample elevation was used for lakes and stagnant bodies (Fig. 2.2). The regression of stream head/sample elevation with $\delta D/\delta^{18}O$ values yields an altitude effect of 3‰/0.4‰ per 100 m rise in elevation. After sample elevation, surface water $\delta D/\delta^{18}O$ values correlate most strongly with latitude (r = -0.44/ -0.28) and longitude (r = -0.37/-0.24), reflecting fractionation associated with rainout as storms move across the island from west to east. Surface water isotope values show no significant correlation with the estimated precipitation amount at the sample site or at the stream head location (Table 2.2). Surface water bodies serve to average the large degree of variability in isotope values within and between individual storm events. In addition, surface water samples were collected during the austral winter when the evaporative modification of surface waters is less than it would be during the warmer and drier summer months.

2.6.2 Deuterium excess

Deuterium excess (d-excess) values of surface waters can be used as an indicator of surface water recycling through evapotranspiration, as well as precipitation source. However, variations in d-excess values of surface waters are complicated and, at present, the theoretical processes affecting d-excess values have not been fully explored. Uncertainties in the interpretation of d-excess values are in part due to uncertainties (<2‰) associated with δD measurements (Fröhlich et al, 2002). Tasmanian surface waters display d-excess values that range from –9.3‰ to 18.5‰ with an average value of 12.3‰ (Appendix A). The average value of 12.3‰ is slightly higher than the global average value of 10‰. However, the total range in d-excess values includes abnormally

Table 2.1. Salinity of Tasmanian surface waters.

Sample Site	Sample #	Conductivity (mS/cm)	Salinity
Highland Lake	59	0.43	0.1
Saltwater River Pond	71	1.25	0.4
Carlton River	72	1.18	0.4
Prosser River	75	34.6	21.6
Forth River	105	47.5	30.8
Ave. Tasmanian surface water	NA	0.05	<0.1

Table 2.2. Correlations between surface sample δD, $\delta^{18}O$, and d-excess values and sample parameters.

	Latitude (S) (dec. deg.)	**Longitude (E) (dec. deg.)**	**Sample Elevation (m)**	**Elevation of streamhead (m)**	**Estimated Mean Ann. Precip. (mm)**
δD	**-0.44**	**-0.28**	**-0.47**	**-0.51**	0.08
$\delta^{18}O$	**-0.37**	**-0.24**	**-0.46**	**-0.55**	0.00
d-excess	-0.09	-0.03	0.13	0.13	**0.27**

high and abnormally low values. Bowen and Revenaugh (2003) have modeled global d-excess values and noted that the area off the southwestern coast of mainland Australia has abnormally high d-excess values. They have attributed this anomaly to low relative humidity as a result of the dry continental Australia. The North and South Subtropical fronts that migrate across the Indian Ocean converge just south of western Australia before diverting southward toward Tasmania. As a result, storm systems imbedded in the subtropical front will contain a greater amount of recycled moisture and the subsequent precipitation that falls in Tasmania will therefore have d-excess values greater than the global average of 10‰.

The only correlation between the d-excess values of Tasmanian surface waters and physical/climatological parameters is that with mean annual precipitation (r = 0.27; Table 2.2). The same orographic effects that result in greater mean annual precipitation in western Tasmania also result in greater evaporative recycling of surface waters. Surface waters that receive more recycled precipitation are therefore located in areas that receive a greater amount of annual precipitation; however, the large error associated with δD measurements preclude more detailed comparisons of d-excess to physical/environmental parameters. In addition, increased rain, cloudiness, and orographic uplift of airmasses in the western part of the island will cause lower condensation temperatures and result in lower d-excess values (Clark and Fritz, 1997).

All of the surface water sample sites that exhibit abnormally high $\delta D/\delta^{18}O$ values also display abnormally low d-excess values that are likely the result of evaporative increases in surface water isotope values. Two of the surface sites, the Saltwater River Pond and the Forth River (71, 105), have extremely low d-excess values of -9.3 and -2.4 respectively (Appendix A). With the exception of the Forth River, all surface samples with a d-excess less than 10‰ (50, 57, 65, 66, 67) are in central to southeastern Tasmania. In southeastern Tasmania there is less recycling of moisture since the prevailing westerly winds carry the evaporated moisture away from the island and thus cause lower d-excess values in surface waters of this region. This is in stark contrast to the western region of the island where high d-excess values and high annual precipitation is observed. The orographic barrier imposed by the Tasmanian mountains that run northwest-southwest likely captures much of the moisture evaporating from western

Tasmanian surface waters, depositing it again on the west side of the mountains and thereby increasing moisture recycling and d-excess values as well as the amount of precipitation in the western region. Additionally, precipitation that does fall on the east side of the island may come from a more southerly oceanic source. Low d-excess values have been demonstrated to correspond with high relative humidity in oceanic vapor source regions (Merlivat and Jouzel, 1979; Bowen and Revenaugh, 2003). Low d-excess values are also found in Tierra del Fuego and the Antarctic Peninsula, thus lower d-excess values in southeastern Tasmania might also be attributed to input of Southern Ocean derived precipitation.

2.6.3 Relevance to Paleoclimate and Hydrologic Studies

Tasmanian surface waters analyzed in this study characterize isotope values of precipitation over a period of weeks to months. Rainfall amount is greatest and isotope values of precipitation are lowest during austral winter. As a result, surface water values are generally weighted toward winter precipitation values. However, in drier areas such as the eastern part of the island, or in small terminal lakes (i.e. Highland Lake and Salt Water River Pond), isotope values are higher and reflective of greater evaporation of both meteoric and surface water. Consequently, paleoclimatic proxies from eastern Tasmania that utilize surface and/or ground water will reflect more evaporative conditions than those from western Tasmania. The changing position of the circumpolar vortex and imbedded westerly front is presently the dominant control on meteoric water and, in turn, surface water isotope values. Today, the circumpolar vortex and resultant westerly winds are proximal to Tasmania during winter months, resulting in more precipitation between June and August. However, changes in the seasonal position of the westerly front through time would cause dramatic changes in annual precipitation amount in Tasmania. For example, deflection of the circumpolar vortex to the south would result in drier than average conditions in Tasmania and more positive isotope values of meteoric and surface waters. Therefore, changes in precipitation isotope values, and proxies that utilize meteoric water, would likely be observed during periods such as the Little Ice Age, when the circumpolar vortex contracted toward the southern pole, or the Last Glacial Maximum when the circumpolar vortex is believed to have expanded northward

(Shulmeister et al., 2004). The d-excess of surface waters in different regions can be used to ascertain the oceanic source region of Tasmanian precipitation as there is a large difference between the d-excess values of Indian Ocean derived precipitation and Southern Ocean derived precipitation (Bowen and Revenaugh, 2003). In addition, surface water d-excess indicates that moisture recycling through evapotranspiration is greater in regions where annual precipitation amount is high. In proxy materials that record both hydrogen and oxygen isotope values of source waters, such as tree-ring cellulose, changes in the relative δD and $\delta^{18}O$ values would therefore record additional information on storm tracks and evapotranspiration.

2.7 Summary

This study is the first survey of the spatial distribution of isotope values in Tasmanian surface water. Waters analyzed range from –56‰ to –2‰ in δD and from -9.0‰ to 0.4‰ in $\delta^{18}O$ values. Isotope values of Tasmanian precipitation reflect seasonal variability in storm tracks and moisture source; however δD and $\delta^{18}O$ values of precipitation also record physical processes, most notably rainout due to altitudinal gradients. As a result, the δD and $\delta^{18}O$ values of Tasmanian surface waters demonstrate the highest correlation with sample/stream head elevation (r = –0.51 for δD and –0.55 for $\delta^{18}O$). Isotope values of surface water correlate with latitude and longitude as well; however, this effect is also associated with the island's topography. As air masses travel over Tasmania from west/southwest to east/northeast precipitation isotope values decrease. This trend is produced by the island's northwest-southeast trending topographic highs that drive the rainout process. d–excess values indicate that they are most closely related to precipitation amount, and moisture recycling is likely a significant component along the west coast of Tasmania. Our data also indicate that considerable mixing of precipitation occurs in surface water bodies, although the isotope values of Tasmanian surface waters are weighted toward winter precipitation values as expected.

Isotope values of Tasmanian surface waters provide useful information about modern meteorological and physical parameters that influence Tasmanian precipitation. Additionally, this study provides critical information about the modification of precipitation isotope values by surficial processes such as evaporation, hydrologic

residence time, and the time averaging of seasonal variability. Perhaps most importantly, development and interpretation of multi-proxy records of climate change in Tasmania and elsewhere will benefit significantly by surface water surveys such as this, in that they permit selection of the most appropriate study sites and proxy materials.

2.8 Acknowledgements

This research was supported by a National Science Foundation – Graduate Research Fellowship J. Dodd, a Geologic Society of America Graduate Research Grant J. Dodd, and National Sciences and Engineering Research Council of Canada Grant #203538 W. Patterson. I would like to thank Bob Deegan for his invaluable assistance in the collecting of samples as well as Aaron Diefendorf, Tim Prokopiuk, Kristin Dietrich, Adam Csank, and Breanna Uzelman for reading early drafts of the manuscript and help with analyses at the Saskatchewan Isotope Laboratory.

2.9 References

Barker, P.F., Thomas, E., 2004. Origin, signature, and palaeoclimatic influence of the Antarctic circumpolar current. Earth-Science Reviews 66, 143–162.

Bowen, G.J., Wassenaar, L.I., Hobson, K.A., 2005. Global application of stable hydrogen and oxygen isotopes to wildlife forensics. Oecologia 143, 337–348.

Bowen, G.J., Revenaugh, J., 2003. Interpolating the isotopic composition of modern meteoric precipitation. Water Resources and Research 39, 1299–1312.

Burnett, A.W., McNicoll, A.R., 2000. Interannual variations in the Southern Hemisphere winter circumpolar vortex: relationships with the semiannual oscillation. Journal of Climate 13, 99 –999.

Calhoun, E.C., 2000. Vegetation and climate change during the last interglacial-glacial cycle in western Tasmania, Australia. Palaeogeography, Palaeoclimatology, and Palaeoecology 155, 195–209.

Clark, I., Fritz, P., 1997. Environmental isotopes in hydrology. Lewis Publishers, New York, p. 328.

Commonwealth of Australia Bureau of Meteorology, 2005. GOES-9: Satellite image originally processed by the Bureau of Meteorology from the geostationary GOES-9 operated by the National Oceanographic & Atmospheric Administration (NOAA) for the Japan Meteorological Agency. (http://www.bom.gov.au).

Cook, E.R., Bird, T., Peterson, M., Barbetti, M., Buckley, B., D'Arrigo, R., Francey, R., 1992. Climatic change over the last millennium in Tasmania reconstructed from tree-rings. The Holocene 2, 205–217.

Cook, E.R., Buckley, B.M., D'Arrigo, R.D., Peterson, M.J., 2000. Warm-season temperature since the 1600BC reconstructed from Tasmanian tree rings and their relationship to large-scale sea surface temperature anomalies. Climate Dynamics 16, 79–91.

Dansgaard, W., 1964. Stable isotopes in precipitation. Tellus 16, 436–468.

Darling, W.G., 2004. Hydrological factors in the interpretation of stable isotopic proxy data present and past: a European perspective. Quaternary Science Reviews 23, 743–770.

Diefendorf, A.F., and Patterson, W.P., 2005. Survey of stable isotope values of Irish surface waters. Journal of Paleolimnology 34, 257–269.

Fricke, H.C., O'Neill, J.R., 1999. The correlation between $^{18}O/^{16}O$ ratios of meteoric water and surface temperature: its use in investigating terrestrial climate change over geologic time. Earth and Planetary Science Letters 170, 181–196.

Fröhlich, K., Gibson, J.J., Aggarwal, P., 2002. Deuterium excess in precipitation and its

climatological significance. Study of environmental change using isotope techniques. C&S Papers Series 13/p, International Atomic Energy Agency, Vienna, Austria, 54–66.

Gat, J.R., 1995. Stable Isotopes of Fresh and Saline Lakes. In: Lerman, A., Imboden, D., Gat, J. (Eds.), Physics and Chemistry of Lakes, Second Edition. Springer-Verlag, New York, pp. 139–162.

Goede, A., McCulloch, M., McDermott, F., Hawkesworth, C., 1998. Aeolian contribution to strontium and strontium isotope variations in a Tasmanian speleothem. Chemical Geology 149, 37 – 50.

Hobson, K.A., Bowen, G.J., Wassenaar, L.I., Ferrand, Y., Lormee, H., 2004. Using stable oxygen and hydrogen isotope measurements of feathers to infer geographical origins of migrating European birds. Oecologia 141, 477 – 488.

IAEA/WMO, 1998. Global Network for Isotopes in Precipitation. The GNIP Database. Release 3. International Atomic Energy Agency /World Meteorological Organization. Available at http://www.iaea.org/programs/ri/gnip/gnipmain.htm. (Accessed 10/05).

Kendall, C., Coplen, T.B., 2001. Distribution of oxygen-18 and deuterium in river waters across the United States. Hydrological Processes 15, 1363–1393.

Lachniet, M.S., Patterson, W.P., 2002. Stable isotope values of Costa Rican surface waters. Journal of Hydrology 260, 123–150.

Lachniet, M.S., Patterson, W.P., 2006. Use of correlation and stepwise regression to evaluate physical controls on the stable isotope values of Panamanian rain and surface waters. Journal of Hydrology, in press.

Lawrence, J.R., Gedzelman, S.D., White, J.W.C., Smiley, D., Lazov, P., 1982. Storm trajectories in eastern US D/H isotopic composition of precipitation. Nature 296, 638-640.

Linde, D.R. (Ed.), 2005. CRC Handbook of Chemistry and Physics, 86th edition. Taylor and Francis Group, Boca Raton, pp. 14-15–14-16.

Merlivat, L., Jouzel, J., 1979. Global climatic interpretation of the deuterium – oxygen 18 relationship for precipitation, Journal of Geophysical Research 84, 5029–5033.

Rozanski, K., Araguas-Araguas, L., Gonfiantini, R., 1993. Isotopic patterns in modern global precipitation. In: Swart, P.K., Lohmann, K.C., McKenzie, J., Savin, S. (Eds.), Climate change in continental isotope records. Am. Geophys. Union. Washington, DC, pp. 1- 37.

Shulmeister, J., Goodwin, I., Renwick, J., Harle, K., Armand, L., McGlone, M.S., Cook, E., Dodson, J., Hesse, P.P., Mayewski, P., Curran, M., 2004. The Southern Hemisphere westerlies in the Australasian sector over the last glacial cycle: a synthesis. Quaternary International 118 – 119, 23 – 53.

Sharp, Z.D., Atudorei, V., Panarello, H., Fernandez, J. and Douthitt, C., 2003. Hydrogen isotope systematics of hair: archeological and forensic applications. Journal of Archeological Science 30, 1709-1716.

Struman, A.,Trapper, N., 1996. The weather and climate of Australia and New Zealand. Oxford University Press, Melbourne, 476 pp.

TASMAP Tasmanian Government, 2000. Topographic Maps of Tasmania, 1:250,000, Third Edition. Government of Tasmania, Hobart, Tasmania.

Treble, P.C., Budd, W.F., Hope, P.K., Rustomji, P.K., 2005. Synoptic-scale climate patterns associated with rainfall $\delta^{18}O$ in southern Australia. Journal of Hydrology 302, 270 – 282.

Villalba, R., 2000, Dendroclimatology: A Southern Hemisphere perspective. In: Smolka, P., Volkheimer, W. (Eds.), Southern Hemisphere paleo- and neoclimates: key sites, methods, data and models. Springer-Verlag, New York, pp. 27 – 58.

2.10 Manuscript's Relationship to Thesis

Chapter 2 discusses modification $\delta^{18}O$ and δD values in precipitation by surface water processes. Although Tasmania is vastly different, geographically and physically, than the other areas discussed Ch 2 and 3, modification of precipitation $\delta^{18}O$ and δD values through the hydrologic cycle is a critical component of other isotope proxies, such as those preserved in tree-ring cellulose.

CHAPTER 3. A NEW TOOL FOR OBTAINING SUB-SEASONAL SAMPLES OF TREE-RING CELLULOSE FOR ISOTOPE STUDIES: ADVANTAGES OF ROBOTIC MICROMILLING

3.1 Abstract

High-resolution, intra-ring analysis of $\delta^{18}O$, δD, and $\delta^{13}C$ values of modern tree species (*Picea glauca*, *P. mariana*, *Larix laricina*, and *Fagus grandiflora*) were sampled using a robotic micromill. The micromilling apparatus allows growth bands to be accurately mapped and sampled at a resolution of few μm. Milling produces a fine, homogenous powder that facilitates the chemical processing and analyses of very small samples (~100μg). Considerable intra-ring isotope variability observed in all tree samples correlates with temperature, relative humidity, and precipitation data indicating that intra-ring variability in $\delta^{18}O$, δD, and $\delta^{13}C$ has great potential for reconstructing high-resolution variations in meteorological conditions throughout the growing season.

3.2 Introduction

Isotope studies of tree-ring cellulose (e.g. δD, $\delta^{18}O$, and $\delta^{13}C$ analyses) are increasingly used as proxies for terrestrial climate variability (Epstien et al., 1977; Wilson and Grinsted, 1977; Saurer et al., 1997; Switsur and Waterhouse, 1998; McCarroll and Loader, 2004). Isotope time series developed from tree-ring cellulose have advantages over other proxies such as speleothems and lake sediments in that they provide annual and even sub-seasonal samples that can be precisely dated. Developments in online, continuous flow gas isotope ratio mass spectrometry technology permit analysis of increasingly smaller samples (~100μg). Intra-ring sampling of cellulose for H, O and C isotope analyses provides records of meteorological and atmospheric conditions at monthly or even weekly resolution (Leavitt and Long, 1991; Loader et al., 1995, Evans and Schrag, 2004). High-resolution studies are particularly useful for reconstructing seasonal variability in precipitation source (i.e. monsoonal rain and tropical storm activity), temperature and relative humidity (Loader et al., 1995; Evans and Schrag, 2004,

Poussart et al., 2004, Miller et al., *in press*). Additionally, researchers have used high-resolution isotopic time-series to elucidate seasonality in tropical trees where growth banding does not necessarily record annual cycles (Evans and Schrag, 2004, Poussart et al, 2004).

Traditionally, high-resolution sampling has been conducted with a fixed blade and rotary microtome (Loader et al., 1995; Evans and Schrag, 2004; Poussart et al., 2004). Microtomes are capable of extracting small wood slivers (~20-30μm thick), although there are drawbacks to this method. First, because microtomes utilize a rotary blade, samples must be removed as linear segments parallel to each other. As a result, only rings or ring segments that are linear or nearly linear can be sampled. Rings that are very narrow or rings that have tight curvatures cannot be reliably sampled with out crosscutting growth rings, thereby mixing material from adjacent time periods and reducing the temporal resolution of sampling. Secondly, microtomes compress tree-ring cellulose and distort the true sample thickness. Robotic micromills are increasingly used for high-resolution sampling of gastropod and mollusk shells (e.g. Wurster and Patterson, 2001), fish otoliths (e.g. Patterson et al. 1993), animal teeth (e.g. Zazzo et al., 2005), and speleothems (e.g. Lachniet et al., 2004); however, to our knowledge, this is the first time it has been applied to tree ring cellulose. Herein, we describe the use of a robotic micromilling device that recovers high-resolution time-specific subseasonal samples of cellulose concordant with growth rings. An additional advantage of micromilling is that it generates a fine, homogenous powder that facilitates the processing and analyses of small samples.

3.3. Experimental Section

3.3.1 Sample Preparation

In order to compare methods for recovery of high-resolution cellulose samples, trees were sampled using a 1.2cm Haglof™ increment bore tree corer and by cutting disks from felled trees. Samples discussed herein include spruce (*Picea glauca* and *P. mariana*), and tamarack (*Larix laricina*) from central Saskatchewan, Canada as well as beech (*Fagus grandiflora*) from the Green Lake region of upstate New York, USA. Increment core samples were trimmed into 10 to 15cm lengths by slicing along ring

boundaries with a scalpel while disks where cut with a band saw into blocks approximately 15 x 5 x 2cm (length x width x height). Samples were sanded with 100- to 500-grit sand paper to facilitate identification of rings and prevent sampled powder from becoming caught in pores and cracks. Subsequently, specimens were affixed to glass dissection slides and attached to a moveable stage for micromilling.

3.3.2 Micromilling Apparatus

Wood specimens were milled using a computer-controlled micromilling apparatus that facilitates micron-scale sampling of tree-rings (Wurster et al., 1999). Increment cores and sections were attached to a movable stage beneath a fixed micro drill. Stage motion is controlled by three linear actuators with a step resolution of 0.05 μm on the x- and y-axis, and 1μm on the z-axis. The apparatus is manipulated by a computer via a motion controller with a range of x, y, and z- axis motion of 17.78 x 7.62 x 4.54 cm, respectively.

Tree-rings, though generally sequentially concordant, often display complex patterns or curves that are difficult if not impossible to sample at high-resolution using standard techniques. Tree-rings are thus mapped using a real-time digital color camera mounted on a fourth linear actuator. Digital characterization of tree-rings entails touching the tip of the drill to the surface of the sample at several points along the growth ring and recording these points in x-y-z space. We then employ a cubic spline interpolation between the digitized points that mimics the characteristics of growth rings. By characterizing two successive growth rings multiple intermediate paths can be interpolated (Fig. 3.1). Spacing of intermediate paths can be regulated to insure that adequate material is recovered to generate sufficient gas for analyses. Due to the removal of up to 70% of wood material (lignin, resins, and other non-cellulose compounds) during α-cellulose processing, we found that approximately 600μg of raw wood is necessary for each isotope analysis. For the increment core samples this generally requires a minimum thickness of 400μm; however for the slabs where longer sample paths could be milled, individual path widths of 100μm were possible.

Samples were milled using coarse cut carbide burs from Advanced Carbide Tool Company™. The total bur diameter (2.4mm) is significantly greater than sample path

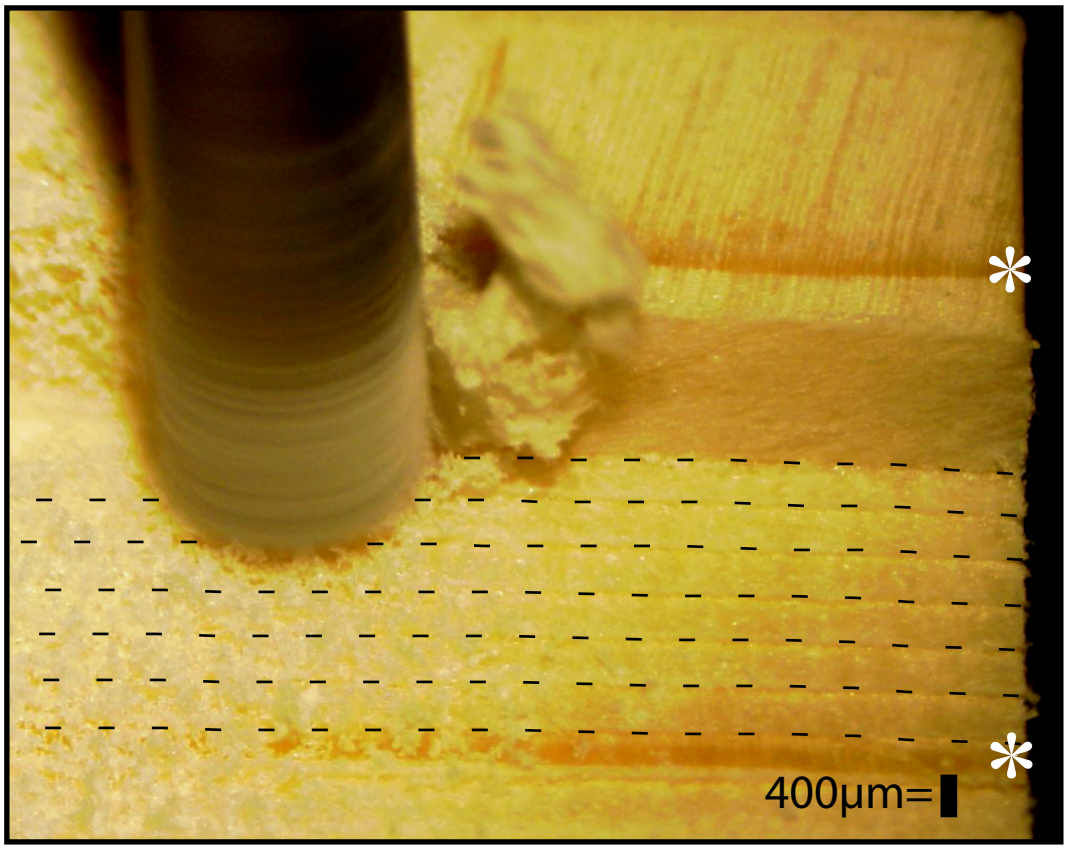

Figure 3.1. Screen capture during the milling of a white spruce 12mm core sample from central Saskatchewan. The growth ring boundaries (marked by white asterisks) are easily distinguished as well as previous sample paths (dashed lines). By discretely sampling with only the edge of the drill, samples that are much smaller than the diameter of the drill are collected. In this image, sample paths are 400µm in width and the drill is moving left to right parallel to the ring boundaries.

widths. However, recovery of much smaller increments is made possible by milling (rather than drilling) concordant with ring boundaries such that only the edge of the bit comes in contact with the sample (Fig. 3.2). Milling depth is dependent upon the three-dimensional characteristics/orientation of growth rings and the amount of powder that must be obtained for analyses. For example, longer paths allow for minimal milling depths (less than 200μm). Alternatively, when path length is limited, as in tree core samples, greater depths are required to obtain sufficient powder for isotope analyses. The resulting wood powder is collected into 1.5ml polypropylene microcentrifuge tubes. Wood powder particles generated by the micromill are approximately 150 to 500 μm (100- to 35-mesh sieve).

3.3.3 Alpha-cellulose processing

Tree rings are principally composed of cellulose and several other compounds such as lignin, waxes, lipids, oils, and resins. Non-cellulose compounds can vary significantly in relative abundance and isotope values throughout a given tree ring (Wilson and Grinsted, 1977; Brendel et al., 2000). Most studies that make use of isotope records of tree rings isolate purified cellulose (commonly referred to as α-cellulose) to derive paleoclimatic signals (Gaudinski et al., 2005). α-cellulose is ideally suited for paleoclimatic studies because once formed, carbon and oxygen atoms in the cellulose molecule do not exchange with other environmental compounds and therefore preserve the isotope values at the time of cellulose formation (Sternberg et al., 1986).
Waxes, resins and lipids were removed from milled whole wood powder by solvent extraction using 2:1 toluene and methanol and rinsed with ethanol and deionized water (Leavitt and Danzer, 1993). α-cellulose was subsequently isolated following a modified Brendel et al. (2000) procedure reported by Evans and Schrag (2004) for small samples. One hundred and twenty μl of 80% acetic acid and 12μL of 69% nitric acid were added to batches of 48 powdered wood samples that ranged between 600μg and 1000μg in 1.5ml polypropylene microcentrifuge tubes. Samples were then capped and heated to 120ºC in convection oven for 30 minutes and allowed to cool. Samples were subsequently rinsed in four successive steps using 400μl of 100% ethanol, 300μl of deionized water, and 150 μl of 100% ethanol, followed by a final rinse with acetone. Between each rinse samples

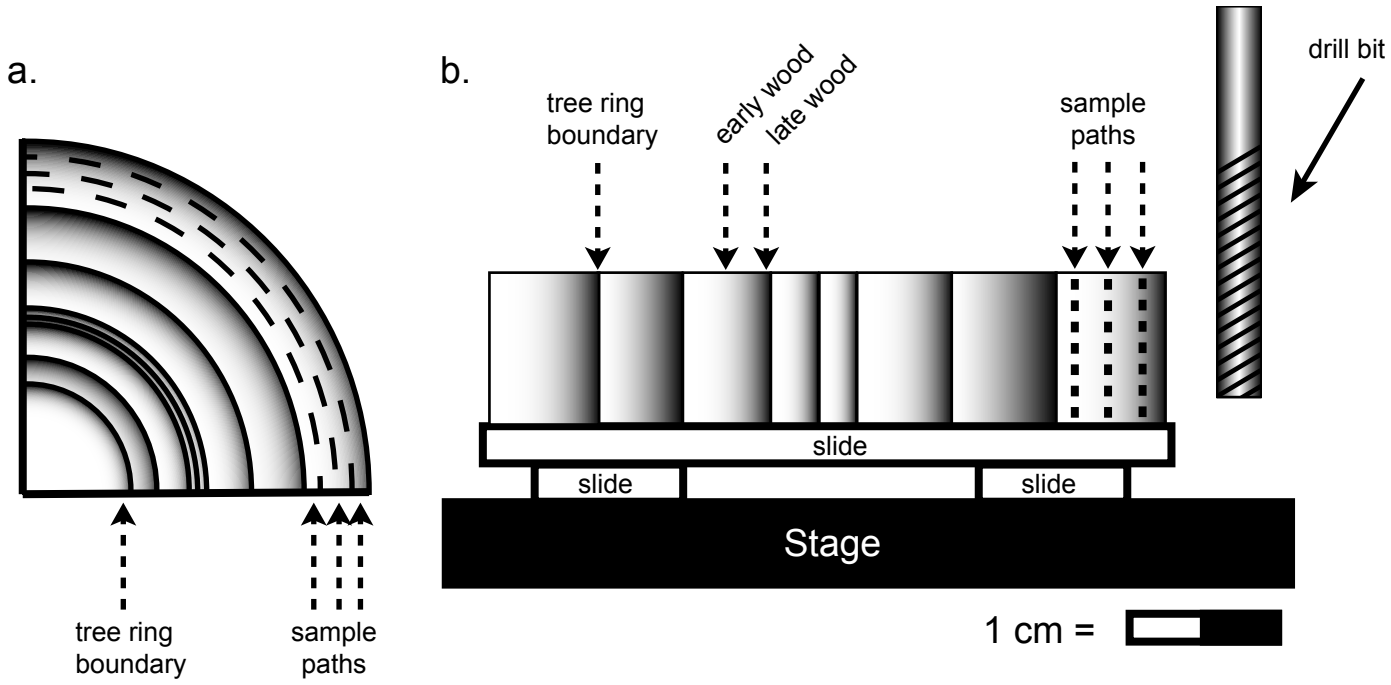

Figure 3.2. Tree-rings (a) can be mapped and sampled using a computer-controlled robotic micromilling apparatus (b). A section of a tree slab or core sample is fixed to a glass slide and attached to a movable stage. The stage then moves past the drill along a digitized sample path so that only the edge of the drill scraps the sample. Full range of motion in x-y-z space allows rings to be followed with resolution of 0.05μm.

were centrifuged at 15,000rpm for 10min. Samples were then dried at 70ºC for 1 hr and overnight in a vacuum desiccator. The resulting α-cellulose was a pure white cotton-like, fibrous material with a processing yield of 35 (±3)% the original volume, that is in agreement with other studies (Brendel et al., 2000; Evans and Schrag, 2004).

Gaudinski et al. (2005) have suggested that the modified Brendel method does not sufficiently remove lipids and waxes in comparison to other methods. They noted that samples processed with the Brendel method had higher $\delta^{18}O$ values than the samples processed with the Jayme-Wise method as reported by Green (1963), but could not explain the difference. Lignin, lipids, and other non-cellulose compounds generally have lower $\delta^{18}O$ and $\delta^{13}C$ values and therefore incomplete removal should result in lower, rather than higher values (Leavitt and Danzer 1993; Schmidt et al., 2001; Loader et al., 2003). Leavitt and Danzer obtained similar unexpected results when samples were exposed to sodium chlorite for extended periods of time and suggested that extreme chlorite delignification processes might be too harsh for fine samples and result in cellulose degradation (Leavitt and Danzer, 1993). Additionally, Gaudinski et al. (2005) did not use the toluene/alcohol solvent extraction prior to α-cellulose conversion, perhaps explaining the presence of resins and waxes in their samples. We believe the method described by Evans and Schrag (2004) is suitable for α-cellulose conversion in our study because the same process was applied to $\delta^{18}O$ time series in spruce species from central Saskatchewan (not shown) which appear to be well correlated with growing season source water values.

Hydrogen atoms in α-cellulose are not as strongly bound as carbon and oxygen in that 30% of the hydrogen atoms can exchange with xylem and other waters subsequent to cellulose production (Epstein et al., 1976; Grinsted and Wilson, 1977). α-cellulose in samples analyzed for δD, were converted to cellulose nitrate using the acetic anhydride method to remove exchangeable hydrogen atoms (Sternberg, 1989). One ml of 40% fuming nitric acid and 60% reagent grade acidic anhydrite was added to samples that were capped and placed on ice for 4 hours, after which the reaction was terminated by adding deionized ice water. Samples were subsequently rinsed with deionized water and methanol and centrifuged between each rinse. Because nitrated cellulose has a rather low

combustion temperature (65ºC), samples were freeze-dried under vacuum at –50ºC over night (12 to 20 hours).

3.3.4 Isotope analyses

Isotope analyses were conducted at Saskatchewan Isotope Laboratory on 150 to 200 μg of α-cellulose, or cellulose nitrate. Oxygen and hydrogen analyses were preformed by online pyrolysis using a Thermo Finnigan Thermal Conversion Elemental Analyzer (TC/EA) at 1450ºC. Isotope ratios of $^{18}O/^{16}O$ and D/H of the resulting CO and H_2 gases were determined via continuous flow using a Thermo Finnigan Delta Plus XL mass spectrometer relative to CO and H_2 reference. Sample reproducibility is constrained by international benzoic standards (IAEA-601 and IAEA-602) for $\delta^{18}O$ analyses (±0.1‰, 1σ) and IAEA-CH-7 and NBS-22 for δD analyses (±2‰, 1σ). Carbon isotope values were determined using a continuous flow online combustion technique on a Thermo Finnigan Elemental Analyzer (EA) coupled to a Thermo Finnigan Delta Plus XL mass spectrometer. Sample reproducibility for $\delta^{13}C$ is ±0.2‰ 1σ) and constrained by international cellulose and sucrose standards (IAEA-CH-3 and IAEA-CH-6). All isotope values are reported relative to VSMOW ($\delta^{18}O$ and δD) and VPDB ($\delta^{13}C$) in delta notation ($\delta_{sample} = \{R_{sample}/R_{standard} - 1\} \times 1000$).

3.4 Results

Considerable intra-ring variability is observed in $\delta^{18}O$ values of all trees analyzed in this study (Fig. 3.3-5). White spruce and tamarack from central Saskatchewan, Canada, were collected with a 1.2cm increment borer and milled at a resolution of 2 to 12 samples per ring (average of 4). Ring widths in the white spruce range from <0.5mm to 4mm and from 1 to 3mm in the tamarack. Each core contained only enough material for $\delta^{18}O$ analyses at this resolution. By collecting multiple cores the milling process could be repeated to generate $\delta^{13}C$ and δD values at the same resolution as the $\delta^{18}O$ time series. Both white spruce and tamarack $\delta^{18}O$ values display a seasonal cycle with highest values generally early in the growing season and lower values in the late growing season (Fig. 3.4). In years when average growing season $\delta^{18}O$ values do not change from year to year (for example 1993 to 1997 in Fig. 3.4), intra-ring variability is often quite high, thus

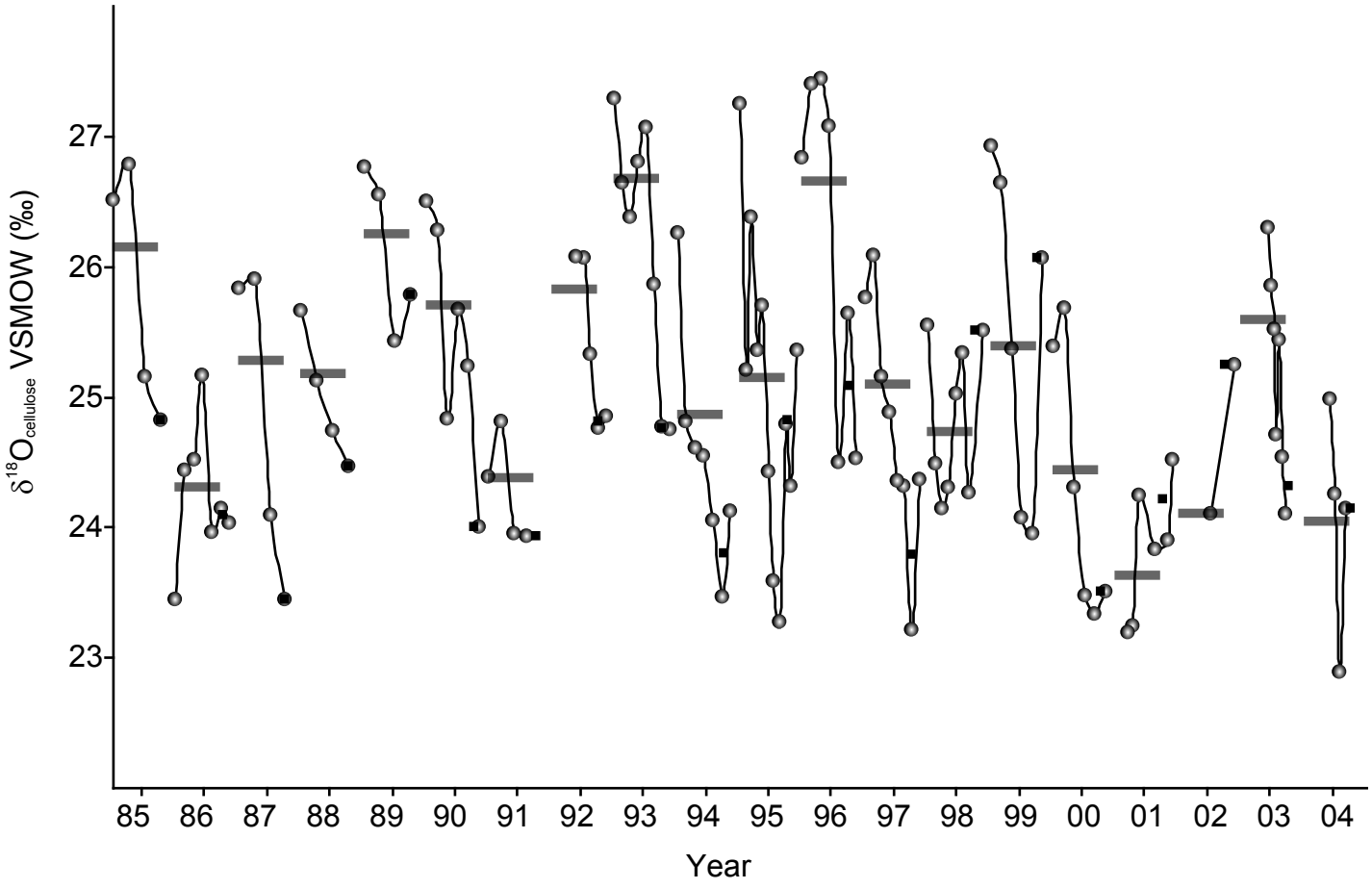

Figure 3.3. High-resolution sampling of white spruce from Prince Albert, Saskatchewan, Canada (53°13' N, 105° 40'W). Individual samples represent 400µm thickness and between 2 and 12 samples were collected per ring between 1985 and 2004. The average $\delta^{18}O$ value for each growing season as well as the time span represented by those average values are depicted as gray boxes (early wood) and black boxes (late wood). In most cases the late wood portion is much only one or two samples (< 800µm) and therefore boxes are much larger than the actual time represented. $\delta^{18}O$ values are generally highest early in the growing season and lowest late in the growing season. Analytical error is smaller than the dots that represent each sample.

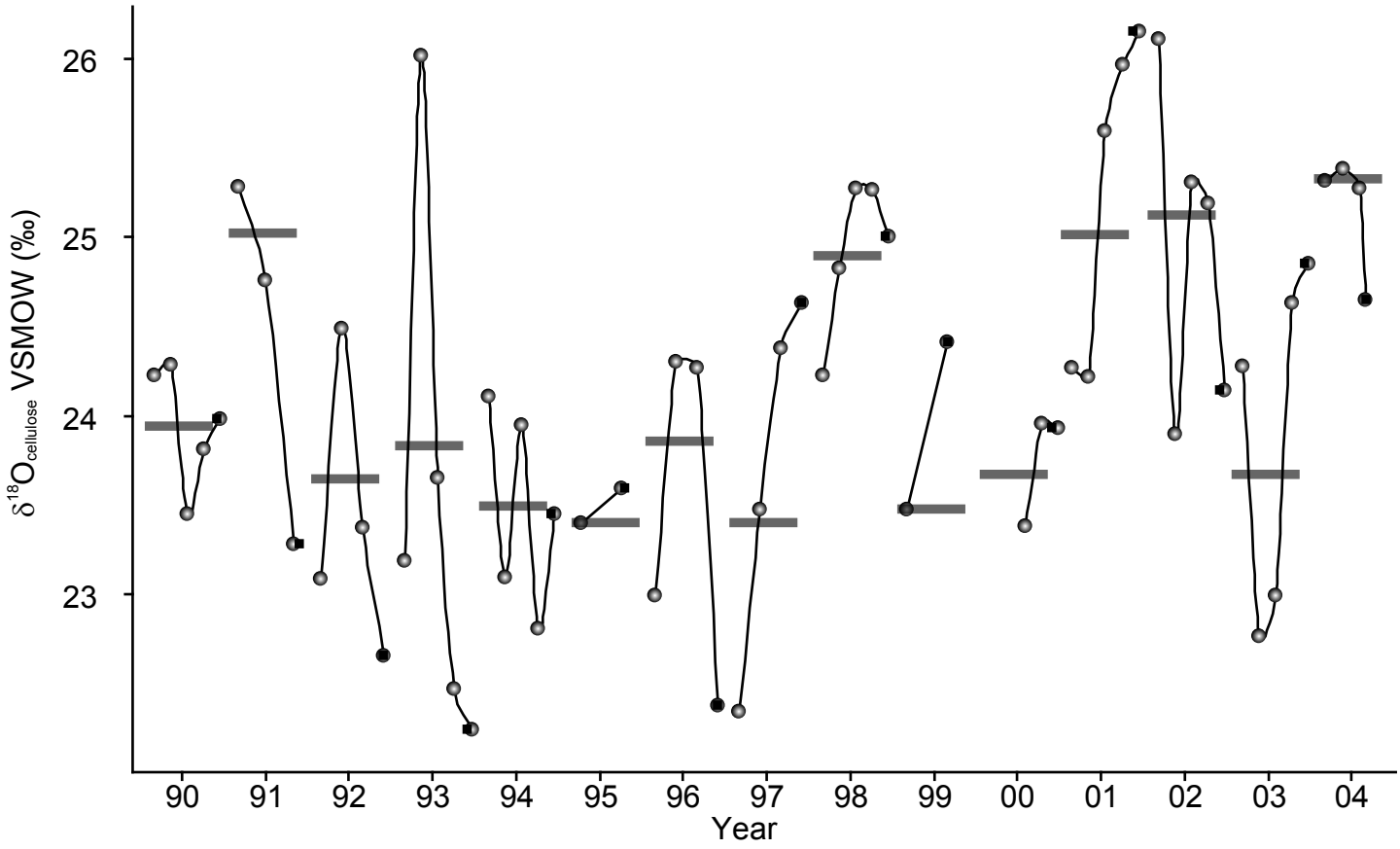

Figure 3.4. High-resolution $\delta^{18}O$ time series of tamarack from east central Saskatchewan, Canada (54° 40' 37 N, 103° 11'11W) from 1990 to 2004. Similar to the white spruce in figure 3.3, the tamarack $\delta^{18}O$ time series display a general seasonal pattern; however there is more seasonal variation than observed in the white source. Again the average $\delta^{18}O$ value for each growing season as well as the time span represented by those average values are depicted as gray boxes (early wood) and black boxes (late wood). Note that between 1993 and 1997 average $\delta^{18}O$ values change very little, yet intra-annual variation remains quite high (e.g.~4‰ in 1993).

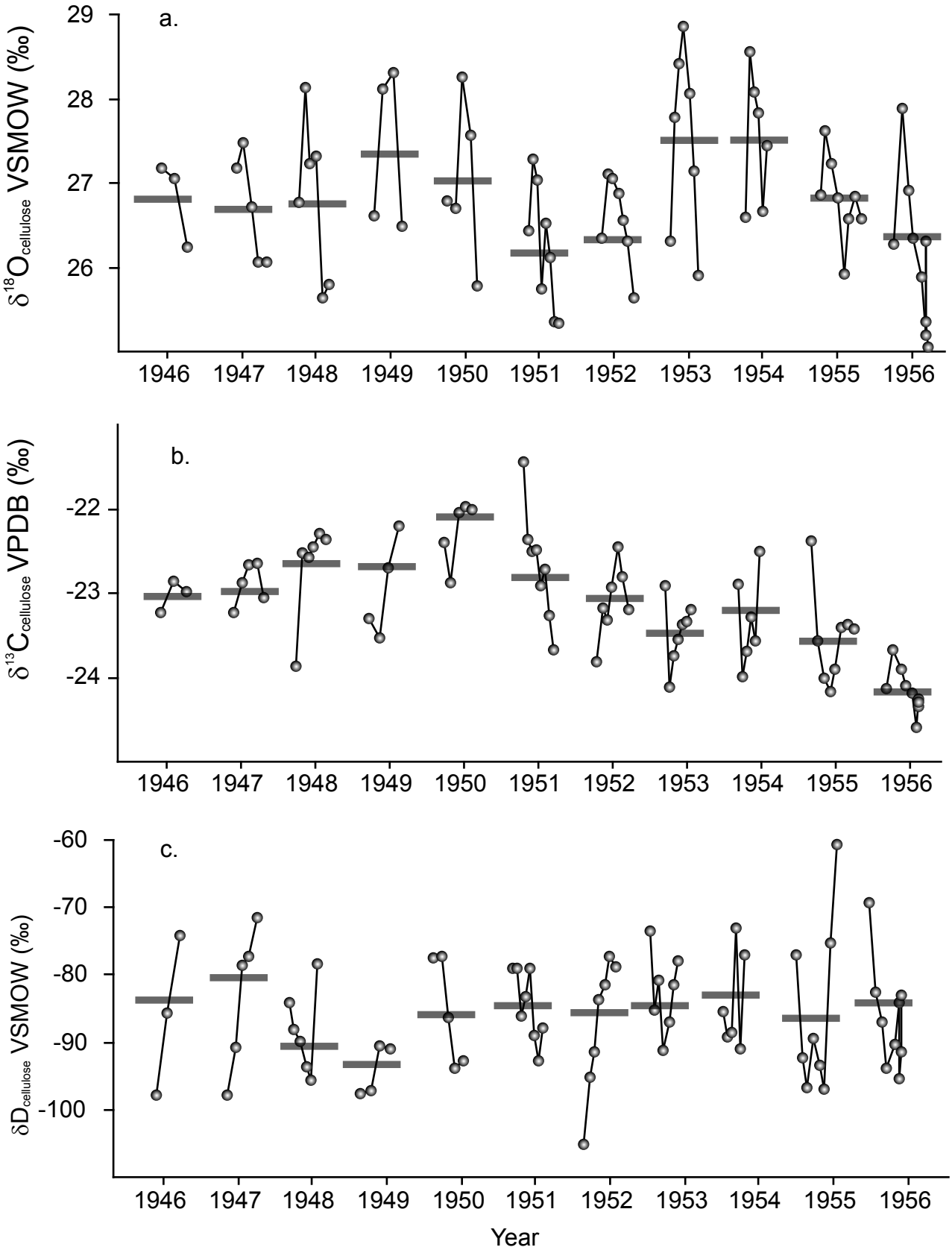

Figure 3.5. Unlike the white spruce and tamarack presented in figures 3.3 and 3.4, the beech tree used in this study was from a complete disk rather than a tree core from the Green Lakes region of central New York, USA. The disk allowed for recovery of more material and therefore analyses of $\delta^{18}O$ (a) as well as $\delta^{13}C$ (b) and δD (c) for the same sample. Between 1944 and 1998, 388 samples were collected with an average of 6 samples per ring. Shown here are a portion of those data from 1946 to 1956. The average isotope value for each growing season as well as the time span represented by those average values are depicted as gray boxes.

years that have extreme, but oppositely trending $\delta^{18}O$ values in the early and late wood would appear to be "normal" or "average" in $\delta^{18}O$ values if cellulose comprising the entire width of the annual rings were sampled.

For the beech tree from upstate New York, a complete slab (or cookie) was available, allowing for recovery of more material and therefore $\delta^{18}O$, δD, and $\delta^{13}C$ analyses were conducted on cellulose from each sample path (Fig 3.5). The micromill proved particularly useful for sampling slabs as it allowed for the curvature of growth bands to be mapped across several centimeters of the disk (see Fig. 3.2). A total of 383 samples were collected between 1944 and 1998 in the beech tree. Average sample width for the beech tree was 200μm, and up to 12 samples were collected per growth ring. The range of δD, $\delta^{18}O$, and $\delta^{13}C$ values in the beech is 36‰, 4.5 and 2.3‰, respectively. The intra-ring $\delta^{18}O$, δD, and $\delta^{13}C$ time series in the beech tree therefore also display considerable variability that is not recorded by annual or even late wood/ early wood portions of the ring. Additionally, all the intra-ring variability in $\delta^{18}O$, δD, and $\delta^{13}C$ in the beech specimen display a strong seasonal cycle. $\delta^{18}O$ and $\delta^{13}C$ values in the beech are generally low in the earliest and latest parts of the season with the highest values occurring in the midsummer, when temperature is highest and relative humidity is the lowest; however δD values for the beech tree display a less coherent seasonal pattern.

A major issue associated with isotopic analyses of very small (<200μm) samples of α-cellulose or cellulose nitrate is sample heterogeneity (Rinne et al., 2005). Much of this heterogeneity is the result of the high intra-ring variability that is observed in $\delta^{18}O$, δD, and $\delta^{13}C$ values. High-resolution, intra-ring sampling generates very small amounts of material and therefore often prevents multiple analyses of single samples. In order to assess the homogeneity of the micromilled samples at the 100μg scale, multiple $\delta^{18}O$ analyses were conducted on 25 samples of early and late wood from a black spruce from central Saskatchewan (Table 3.1). Micromilled samples have also been compared to the same 25 samples collected with the traditional scalpel method (Fig. 3.6; Table 3.1). Samples collected using the traditional scalpel method were homogenized using an agate mortar and pestle, while powder from the micromilled samples required no further grinding. Samples collected with the micromill display considerably less variability (average *s.d.* = 0.1‰, 1σ) than those collected by scalpel (average *s.d.* = 0.5‰,1σ).

Table 3.1. Homogeneity: Scalpel vs. Micromill Sampling of cellulose

		Sampled with Micromill			Sampled with Scalpel		
Year	**Season**	**$\delta^{18}O$ (‰)**	**s.d. (1σ)**	**n**	**$\delta^{18}O$ (‰)**	**s.d. (1σ)**	**n**
1951	Early	22.2	0.3	3	22.4	NA	1
1951	Late	21.6	0.1	2	22.4	0.3	3
1952	Early	21.9	NA	1	22.0	NA	1
1952	Late	22.1	0.1	2	23.3	0.6	2
1953	Early	22.8	0.2	3	22.3	0.3	3
1953	Late	22.7	NA	1	23.5	NA	1
1954	Early	24.5	0.1	2	24.1	0.6	2
1954	Late	23.4	0.1	2	23.6	0.1	2
1955	Early	22.0	0.1	2	22.6	0.3	3
1955	Late	23.9	0.1	2	24.2	0.3	3
1956	Early	22.9	NA	1	22.4	NA	1
1956	Late	24.1	0.1	2	24.2	0.6	4
1957	Early	24.8	0.1	5	25.4	1.4	3
1957	Late	NA	NA	NA	25.4	0.1	3
1958	Early	23.7	0.1	2	24.5	0.8	4
1958	Late	24.2	0.3	2	24.7	0.7	4
1959	Early	24.4	0.2	2	24.9	0.6	6
1959	Late	24.1	0.1	2	24.1	0.5	4
1960	Early	24.5	0.1	2	24.3	0.5	3
1960	Late	23.2	0.1	2	23.6	0.2	3
1961	Early	23.3	0.1	2	23.0	0.2	3
1961	Late	23.9	0.1	3	22.7	0.5	3
1962	Early	25.7	NA	1	25.0	NA	1
1962	Late	24.0	NA	1	23.6	NA	1
1963	Early	26.7	0.1	2	27.4	0.3	3
Average			**0.1**			**0.5**	

* Note most sample reruns were analyzed in the same run and standard deviations reflect sample heterogeneity not analytical reproducibility.

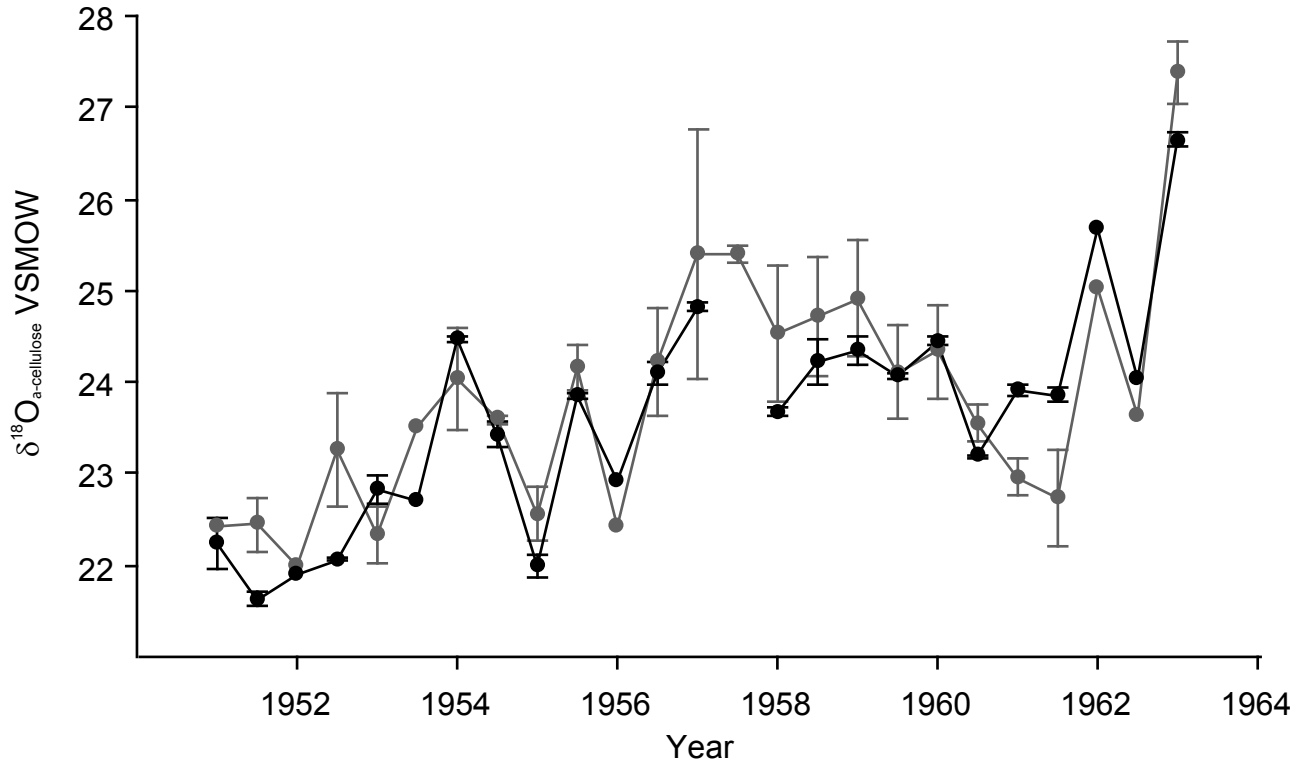

Figure 3.6. In order to asses the homogeneity of $\delta^{18}O$ values in the micromilled samples we analyzed early wood and late wood portions from a black spruce from east central Saskatchewan, Canada (54° 40' 37 N, 103° 11'11W) that had been collected using both micromill and scalpel techniques. The micromilled samples (black line) were considerably more homogeneous than those collected with a scalpel (gray line). The average standard deviation (depicted by vertical bars on each sample point) of the micromilled samples was 0.1‰, while samples collected with a scalpel had an average standard deviation of 0.5‰ (1s; Table 1). Analytical error for $\delta^{18}O$ analyses is 0.2‰ and therefore the error associated with the heterogeneity of the scalpel sampled cellulose is significantly higher. Note sample reruns were often analyzed in the same run and therefore do not reflect true analytical reproducibility.

Micromilled samples are therefore very homogenous and appear to represent the average value of the given sample interval within the range of analytical error.

3.5 Discussion and Conclusions

Seasonal cyclicity observed in the intra-ring variations in $\delta^{18}O$, δD, and $\delta^{13}C$ values indicate that high-resolution sampling of tree-ring cellulose offers the potential to reconstruct variation in meteorological conditions throughout the growing season. The climate of a region is characterized not only by the average growing season conditions but also the seasonal extremes; high-resolution reconstructions of intra-ring isotope variability can therefore provide critical information about the timing and magnitude of changes in past meteorological conditions such as temperature, relative humidity, precipitation amount, and precipitation $\delta^{18}O/\delta D$ values. Additionally, many major climate events such as monsoonal rain and tropical storm activity occur during small portions of the growing season and would therefore not be apparent in samples averaged over the entire growing season (Poussart et al., 2004, Miller et al., *in press*). Although some seasonal information can be ascertained from studies that divide wood into early wood and late wood portions, the division along the late wood boundaries is sometimes problematic. In white spruce and tamarack from central Saskatchewan, the late wood growth period is very short and results in late wood widths that are often less than 400μm in thickness. It is therefore difficult to discretely sample the late wood in these, and other boreal trees, even by micromilling. However, by sampling at a very high-resolution across the growth ring it is possible to reconstruct isotope time series of the entire season regardless of the early wood late wood boundary.

Intra-ring $\delta^{18}O$ time series from Saskatchewan trees are well correlated with relative humidity and temperature. The early growing season conditions are typically characterized by low relative humidity and high temperatures, whereas the late growing season is higher in relative humidity and lower in temperature. This causes tree-ring $\delta^{18}O$ values to be high in the early part of the growing season and lower near the end. A similar seasonal cycle is observed in $\delta^{18}O$ values of precipitation in central Saskatchewan with the highest $\delta^{18}O$ values in the early growing season (May – July) and lowest $\delta^{18}O$ values in the late growing season (Sep. – Oct.; Fritz et al., 1987). Intra-ring $\delta^{18}O$, δD, and

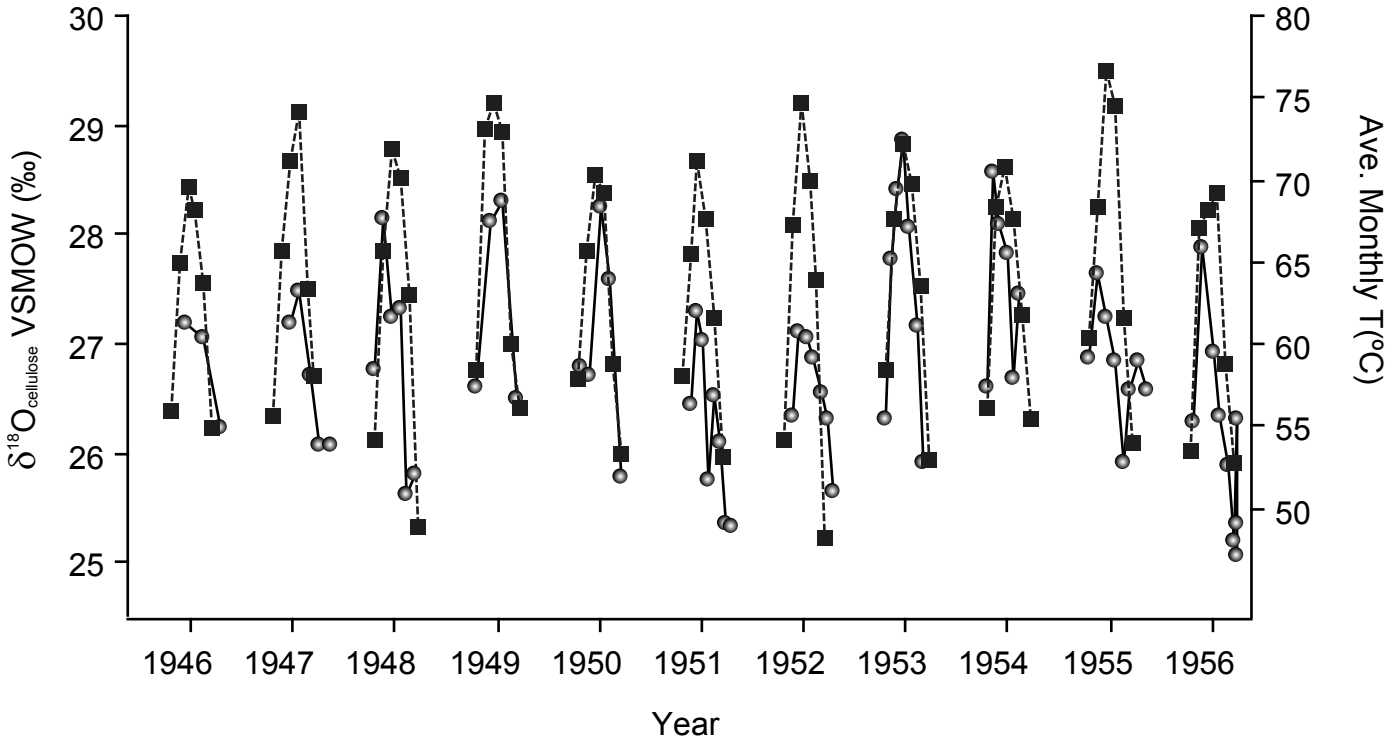

Figure 3.7. Although intra-ring samples of equal width may not represent equal periods of time, it does appear that they are very close to equal. Intra-ring $\delta^{18}O$ values from the beech tree have a strong relationship with the average monthly temperature recorded during the growing season (April to October). Both temperature and $\delta^{18}O$ values display a similar seasonal cycle with highest values occurring in the early part of the growing season and lowest values late in the growing season.

$\delta^{13}C$ values in the beech from central New York are well correlated with relative humidity, temperature, precipitation $\delta^{18}O/\delta D$ values, and precipitation amount. For example, there is a strong relationship between the seasonal variations in intra-ring $\delta^{18}O$ values of the beech tree and average monthly temperatures (Fig. 3.7).

A robotic micromilling device has many advantages over other methods of high-resolution sampling such as a microtome. The micromilling approach allows for growth bands to be accurately mapped and sampled, preventing crosscutting of growth bands as would often be the case if a scalpel or microtome were used. Micromilling of tree-ring wood also produces a very fine, isotopically homogeneous powder, which would benefit sampling of wood at any spatial resolution. Continuing work is focused on relating the seasonal changes in the $\delta^{18}O$, δD, and $\delta^{13}C$ time series to meteorological and atmospheric data. Once calibrated, high-resolution isotope time series can provide valuable information about seasonal and sub-seasonal changes in relative humidity, temperature, and precipitation.

3.6 Acknowledgments

This research was supported by a National Science Foundation – Graduate Research Fellowship J. Dodd, a Geologic Society of America Graduate Research Grant for J. Dodd, and National Sciences and Engineering Research Council of Canada Grant #203538 to W. Patterson. I would like to thank T. Prokopiuk for his invaluable assistance in the collection of samples as well as A. Diefendorf, T. Prokopiuk, K. Dietrich, and A. Csank for reading early drafts of the manuscript and help with analyses at the Saskatchewan Isotope Laboratory. Thanks also to J. Miller and K. Dietrich for help with the micromilling apparatus and software.

3.7 References

Brendel, O., Iannetta, P.P.M., Stewart, D., 2000. A rapid and simple method to isolate pure alpha-cellulose. Phytochem. Anal. 11, 7-10.

Epstein, S., Thompson, P., Yapp, C.J., 1977. Oxygen and hydrogen isotopic ratios in plant cellulose. Science 198, 1209-1215.

Evans, M.N., Schrag, D.P., 2004. A stable isotope-based approach to tropical dendroclimatology. Geochim. Cosmochim. Acta 68, 3295-3305.

Fritz, P., Drimmie, R.J., Frape, S.K., O'Shea, K., 1987. The isotopic composition of precipitation and groundwater in Canada, in: Proceedings of an international symposium on the use of isotope techniques on water resource development. IAEA, Vienna, pp. 539-550.

Gaudinski, J.B., Dawson, T.E., Quideau, S., Schuur, E.A.G., Roden, J.S., Trumbire, S.E., Sandquist, D.R., Oh, S., Waslishen, R.E., 2005. Comparative analysis of cellulose preparation techniques for use with ^{13}C, ^{14}C, and ^{18}O isotopic measurements. Anal. Chem. 77, 7212-7224.

Green, J.W., 1963. Wood cellulose, In: Whistler, R.L. (Ed.), Methods in Carbohydrate Chemistry, vol. III. Academic Press, pp. 9-21.

Lachniet, M.S., Asmerom, Y., Burns, S.J., Patterson, W.P., Polyak, V.J., Seltzer, G.O., 2004. A tropical early Holocene dry event and decadal scale variability in the Central American Monsoon from speleothem calcite. Geology 32, 957-960.

Leavitt, S.W., Danzer, S.R., 1993. Method for batch processing small wood samples to holocellulose for stable-carbon isotope analysis. Anal. Chem. 65, 87-89.

Leavitt, S.W., and Long, A., 1991. Seasonal stable carbon-isotope variability in tree rings: possible paleoenvironmental signals. Chem. Geo. Isotope Geoscience Sec. 87, 59-70.

Loader, N.J., Switsur, V.R., and Field, E.M., 1995. High-resolution stable isotope analysis of tree rings: implications of "microdendroclimatology" for palaeoenvironmental research. Holocene 5, 457 – 460.

Loader, N.J., Robertson, I., McCarroll, D., 2003. Comparison of stable carbon isotope ratios in the whole wood, cellulose and lignin of oak tree-rings, Palaeogeo., Palaeoclim., Palaeoeco. 196, 395-407.

McCarroll, D., Loader, N.J., 2004. Stable isotopes in tree rings. Quat. Sci. Rev. 23, 771-801.

Miller, D.L., Mora, C.I., Grissino-Mayer, H.D., Mock, C.J., Uhle, M.E., Sharp, Z., 2006. Tree-ring isotope records of tropical cyclone activity Proc. Natl. Acad. Sci.(in press).

Patterson, W.P., Smith, G.R., and Lohmann, K.C., 1993. Continental paleothermometry and seasonality using the isotopic composition of aragonite otoliths of freshwater fishes. In: P. Swart, K.C Lohmann, J. McKenzie and S. Savin (Eds.) Amer. Geophys. Union Monogr. Continental Climate Change from Isotopic Indicators, pp. 191-202.

Poussart, P.F., Evans, M.N., Schrag, D.P., 2004. Resolving seasonality in tropical trees: multi-decade, high-resolution oxygen and carbon isotope records from Indonesia and Thailand. Earth and Planet. Sci. Lett. 218, 301-316.

Rinne, K.T., Boettger, T., Loader, N.J., Robertson, I., Switsur, V.R., Waterhouse, J.S., 2005. On the purification of α-cellulose from resinous wood for stable isotope (H, C, and O) analysis. Chem. Geo. 222, 75-82.

Saurer, M., Aellen, K., Siegwold, R., 1997. Correlating $\delta^{13}C$ and $\delta^{18}O$ in cellulose of trees. Plant. Cell Environ. 20, 1543-1550.

Schmidt, H.-L., Werner, R.A., Roßmann, A., 2001. ^{18}O pattern and biosynthesis of natural plant products. Phytochem. 58, 9-32.

Sternberg, L.S.L., 1989. Oxygen and hydrogen isotope measurements in plant cellulose analysis, in: Linskens, H.F., Jackson, J.F. (eds.), Modern methods of plant analysis, 10, Springer-Verlag, Berlin, pp. 89-99.

Switsur, R., Waterhouse, J., 1998. Stable isotopes in tree ring cellulose. Stable Isotopes, Integration of Biological, Ecological, and Geochemical Processes. BIOS Scientific Publishers Ltd., pp. 303-321.

Wilson, A.T., Grinsted, M.J., 1977. 12C/13C in cellulose and lignin as paleothermimeters. Nature 265, 133-135

Wurster, C.M., Patterson, W.P., Cheatham, M.M., 1999. Advances in micromilling techniques: a new apparatus for acquiring high-resolution oxygen and carbon stable isotope values and major/minor elemental ratios from accretionary carbonate. Computers & Geosciences 25, 1159-1166.

Wurster, C.M., and Patterson, W.P., 2001, Seasonal variation in stable oxygen and carbon isotope values recovered from modern lacustrine freshwater mollusks: Paleoclimatological implications for sub-weekly temperature records. J. of Paleo Lim Paleobio. 26, 305-218.

Zazzo, A., Balasse, M., Patterson, W.P. 2005. High-resolution $\delta^{13}C$ intratooth profiles in bovine enamel: Implications for mineralization pattern and isotopic attenuation. Geochim. Cosmochim. Acta 69, 3631–3642.

3.8 Manuscript's Relationship to Thesis

Chapter 3 provides a detailed examination of the methods used in sampling and processing tree-ring cellulose for $\delta^{18}O$, δD, and $\delta^{13}C$ analysis. Chapter 3 also explains the justification for using a robotic micromilling apparatus to sample tree rings and demonstrates the applicability of intra-ring variations in $\delta^{18}O$, δD, and $\delta^{13}C$ to studies of sub-seasonal meteorological and atmospheric variability.

CHAPTER 4. A 110YR SEASONAL PRECIPITATION AND ATMOSPHERIC CIRCULATION RECORD: EVIDENCE FROM $\delta^{18}O$ VALUES OF TREE-RING α–CELLULOSE IN MODERN SPRUCE

4.1 Abstract

A seasonally resolved (early/late wood) 110-year time series of $\delta^{18}O$ values from tree-ring α-cellulose from modern spruce species (*Picea mariana* and *P. glauca*) from east-central Saskatchewan, Canada is presented as a record of growing season precipitation and atmospheric circulation. Isotope values of source-water utilized by the trees are reconstructed using a modified leaf-water equation (Anderson et al., 2002) that incorporates relative humidity and temperature measurements to account for leaf water modification through stomatal evaporation. The reconstructed $\delta^{18}O$ source water values display a high correlation with growing season precipitation isotope values (r = 0.86) recorded at The Pas, Manitoba approximately 150 km to the southeast. $\delta^{18}O$ α-cellulose time series also record seasonal changes in atmospheric circulation associated with the position of the circumpolar vortex and dominate modes of atmospheric variability such as the North Atlantic Oscillation and Pacific Decadal Oscillation.

4.2 Introduction

Oxygen isotope records preserved in tree ring α-cellulose are valuable proxies of environmental change that are particularly useful for reconstructing secular records of oxygen isotope values in precipitation (Epstein et al., 1977, DeNiro and Epstein, 1979, Roden et al., 2000, Anderson et al., 2002, Waterhouse et al., 2002, Saurer, 2003, McCarroll and Loader, 2004, Weigou et al. 2004, Miller et al., in press). Although the IAEA/WMO have constructed an extensive database of precipitation isotope values and others have modeled the spatial distribution of isotopes in global precipitation (Bowen and Revenaugh 2003), precipitation isotope records are only available for the later part of the 20th century, at best, and for only a few years at many stations. Tree-ring isotope studies have the potential to extend the record of precipitation isotope variability well

beyond the range of IAEA/WMO data and thus provide indispensable records of past variation in the hydrologic cycle (Darling, 2004). Unlike other terrestrial climate proxies such as lacustrine sediment, speleothems, and ice cores, tree-rings isotope studies provide unambiguous age control in the form of annual rings (Waterhouse et al., 2002, Saurer, 2003). The perfect annual resolution in tree-rings facilitates direct comparison with instrumental records of air temperature, relative humidity, precipitation amount, and the $\delta^{18}O$ value of precipitation. In addition, the abundance of trees in many terrestrial environments provides an opportunity to characterize the spatial distribution of precipitation isotope values over much of the Earth for the past several thousand years (Saurer, 2003).

Recent studies have demonstrated that high latitude environments may be particularly sensitive to global climate change, yet our understanding of natural climate variability in these regions is hindered by the poor temporal and spatial resolution of paleoclimate records (Gibson, 2001; Schindler and Donahue, 2006). Instrumental records of temperature and precipitation amount for western Canada are only available for the most recent 100 to 150 years; weather patterns that were experienced during the 20th century are generally considered as "normal" climate conditions. However, other proxies such as drought sensitive tree-ring chronologies indicate that western Canada was considerably drier prior to the 20th century (Sauchyn and Skinner, 2001; Schindler and Donahue, 2006).

Presented herein is a detailed (early/late wood) 110-year record of seasonal $\delta^{18}O$ values in tree-ring α-cellulose of boreal forest white and black spruce (*Picea mariana* and *P. glauca*) from east-central Saskatchewan, Canada. The $\delta^{18}O$ cellulose record is compared to meteorological data measured at The Pas, Manitoba and Prince Albert, Saskatchewan (Environment Canada, 2005) and $\delta^{18}O$ values in precipitation recorded by the International Atomic Energy and the World Meteorological Organization (IAEA/WMO) at The Pas, Manitoba (IAEA/WMO, 2001). The $\delta^{18}O$ records are compared to secular changes in the position of the circumpolar vortex (NCEP/NCAR Reanalysis Project, 2000) and other records of atmospheric circulation such as the Pacific Decadal Oscillation (PDO) and the North Atlantic Oscillation (NAO) indices (Hurrell, 1995, 1996; Mantua et al, 1997; Zhang et al., 1997)

Using a modified leaf-water equation (after Anderson et al., 2002) $\delta^{18}O$ values of water utilized by the trees during the growing season have also been reconstructed and are well correlated with $\delta^{18}O$ values of growing season (April – October) precipitation at the Pas, Manitoba. The modified leaf-water equation (Anderson et al., 2002) used in the $\delta^{18}O$ source water reconstruction is empirically calibrated with daily relative humidity and temperature measurements, and therefore accounts for isotopic modification of source water $\delta^{18}O$ values in a manner that is broadly applicable for reconstruction of the $\delta^{18}O$ values of growing season precipitation from tree-ring α-cellulose.

4.2.1 Oxygen isotope values of tree-rings

The woody tissue of tree rings consists of multiple compounds such as lignin, lipids, resins, and other non-cellulose compounds that generally have lower $\delta^{18}O$ values relative to cellulose (Wilson and Grinsted, 1977; Brendel et al., 2000). Most studies that make use of isotope studies of tree rings have focused on purified cellulose (commonly referred to as α-cellulose) to derive paleoclimatic and paleoenvironmental signals (Gaudinski et al., 2005). α-cellulose is ideally suited for paleoclimatic studies because once formed, carbon and oxygen atoms in the cellulose molecule do not exchange with other environmental compounds and therefore preserve the $\delta^{13}C$ and $\delta^{18}O$ values at the time of cellulose formation (Sternberg et al., 1986).

The oxygen atoms in tree-ring α-cellulose are primarily derived from water taken into the tree by the roots, which in the case of shallow rooted trees is predominantly derived from soil moisture. The $\delta^{18}O$ value of soil moisture reflects local precipitation, averaged over some period of time prior to utilization by the tree. Evaporation of water from the soil, long soil moisture residence times, and mixing of groundwater can distort the precipitation $\delta^{18}O$ signal; therefore in studies that attempt to reconstruct past $\delta^{18}O$ values of precipitation, it is desirable to study trees growing in shallow, well-drained soil with limited evaporation (Tang and Feng, 2001, Buhay and Edwards, 1995). The $\delta^{18}O$ value of water in the tree is subsequently modified by: (1) evaporation of water in the leaf through the stomata during transpiration (Dogmann et al. 1974), (2) biologic fractionation between water and cellulose (DeNiro and Epstein, 1979, Sternberg et al. 1986), (3) and exchange of oxygen atoms between sucrose produced during photosynthesis and water in

the leaf and stem-wood cellulose (Sternberg et al., 1986). For an in-depth discussion of fractionation processes see Yakir and DeNiro (1990), Roden et al. (2000), Waterhouse et al. (2002), and McCarroll and Loader (2004).

Anderson et al. (2002) reconstructed $\delta^{18}O$ values of the source water ($\delta^{18}O_{sw}$) utilized by the tree using a modified-leaf water equation (Eq. 1) developed from equations by Dogmann et al. (1974) and Aucour et al. (1996) that accounts for evaporative modification of $\delta^{18}O$ values during transpiration constrained by temperature (t), relative humidity (h), and tree growth rate (represented by measured tree-ring index values, r_x) to calculate a variable damping factor f (Eq. 2).

$$\delta^{18}O_{sw} \approx \delta^{18}O_{cellulose} - (1 - f)(1-h)(\varepsilon_e + \varepsilon_k) - \varepsilon_{biochem} \quad (1)$$

$$f = -1.47(h) + 0.03\,(t) + 0.11\,(r_x) + 0.62 \quad (2)$$

As used in this equation, the water liquid-vapor kinetic fractionation across the leaf boundary (ε_k) and the biologic fractionation factor ($\varepsilon_{biochem}$) are 28‰ and 27‰, respectively. A value of 28‰ for ε_k reflects the nearly stagnant boundary layer conditions observed in fine spruce needles (Anderson et al, 2002; Allison et al., 1985, Buhay et al., 1996). The biologic fractionation factor accounts for the fractionation of oxygen isotopes in leaf water during photosynthesis and a value of 27‰ is most common in the literature (DeNiro and Epstien, 1979; Roden et al., 2000, Yakir and DeNiro, 1990). ε_e is the liquid-vapor equilibrium fractionation factor for water from Manjoube (1971) and can be calculated using the average growing season temperature at the sample site. The damping factor f provides an estimate of the modification of the precipitation $\delta^{18}O$ value of water utilized by the tree through soil and leaf evaporation, groundwater mixing, and exchange of oxygen atoms between xylem water and photosynthate. Relative humidity and temperature are dynamic environmental parameters and by calculating a variable f factor that incorporates these processes, the equation developed by Anderson et al. (2002) is able to more accurately predict the $\delta^{18}O$ value of water utilized by the tree than equations that assume fixed value for f.

4.3 Site Description

Modern tree samples were collected near the north end of Limestone Lake in east-central Saskatchewan, Canada (54° 40' 37 N, 103° 11'11W; Fig. 4.1) at about 350m

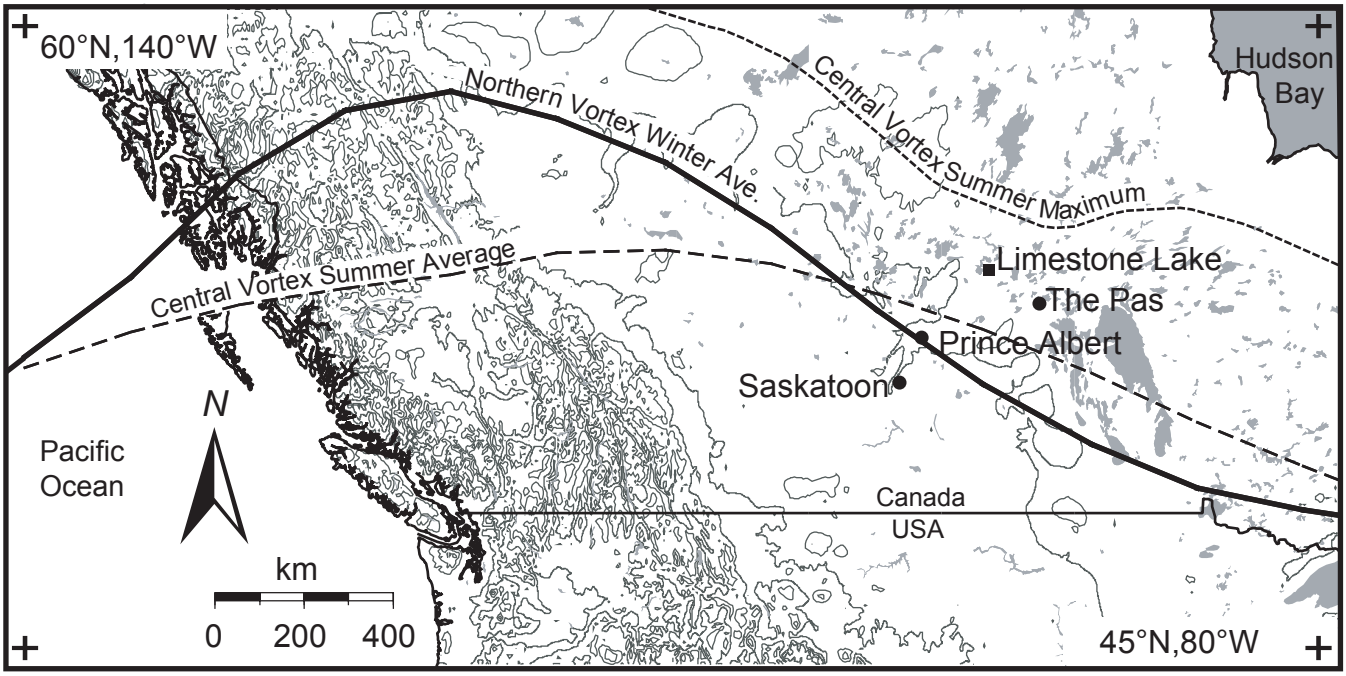

Figure 4.1. The position of the Limestone Lake sample site (54° 40' 37 N, 103° 11'11W) as well as meteorological stations at Prince Albert, Saskatchewan (53°13' N, 105° 40'W, ~300km southwest of Limestone Lake) and The Pas, Manitoba (53º 58'N, 101º 6'W~150km to the southeast). These sites are positioned between the Northern and Central contours of the circumpolar vortex. Both vortex contours seasonally contract to the north during the summer and expand to the south during the winter. Summer conditions are therefore dominated by the position of the central vortex contour.

above sea level. The sample area is part of the southern boreal forest/aspen plains transition zone with mixed wood boreal forests containing softwood (spruce, pine, fir, and tamarack) and hardwood (birch, aspen, and balsam poplar) growing in muskeg bog and shallow acidic soil underlain by metavolcanic and metasedimentary bedrock at the southern edge of the Canadian Shield.

Instrumental records from Prince Albert, Saskatchewan are available since 1889 for precipitation and temperature and since the early 1950s for relative humidity, sky conditions, and wind speed. Meteorological data for The Pas are less complete with reliable records from 1943 to present (Environment Canada, 2005). Monthly $\delta^{18}O$ values of precipitation are available from the IAEA/WMO at The Pas somewhat sporadically from 1975 to 1982 (IAEA/WMO, 2001; Fritz et al, 1987). Over the period of instrumental data (1889 – 2005), the study area received an average of 327mm of precipitation a year, with most (175mm on average) falling during the summer months (June - August). Sub-freezing temperatures are generally observed from late October through early April, and therefore April – October represents the maximum possible growing season for trees in the area.

The central Canadian boreal forest is dominated by three climate regimes influenced by Pacific, Arctic and Tropical/Atlantic air masses (Fritz et al, 1987). The relationship of these air masses to the study site is largely influenced by the position and strength of westerlies associated with the jet stream (Burnett, 1993; Frauenfeld and Davis, 2003; Fig. 4.1). The main band of westerly winds generally encircles the polar region and is therefore also referred to as the circumpolar vortex (Burnett, 1993). The center of the circumpolar vortex is defined as the region with the strongest meridional gradient within the main belt of westerly flow (Frauenfeld and Davis, 2003). To better characterize the geometry and circulation on the circumpolar vortex at higher and lower latitudes, the main westerly belt is divided into three contours, the central, northern and southern. The central contour of the circumpolar vortex best describes the core of the westerly flow while the northern and southern contours generally describe the northern and southern limits of the main westerly belt. Continental scale variations in the circumpolar vortex have strong geographic preferences and have a dominant influence on mid-latitude climates. In North America, the position of the circumpolar vortex is

confined by Canadian Rockies in the west and thermal contrast between the Atlantic Ocean and continental North America in the east. The geographic boundary conditions result in a relatively stable ridge, or northward deflection of the vortex, over the mountains and a trough over northeastern North America. The average position of the vortex varies seasonally, with a general expansion to the south during the winter months and a contraction to the north in the summer (Burnett, 1993). When the circumpolar vortex moves southwards during the winter months, the study area is dominated by cold, dry Arctic and Pacific air masses. Warmer and wet conditions persist as the circumpolar vortex migrates northwards in the spring (Burnett, 1993; Frauenfeld an Davis, 2003). Seasonal changes in the position of the circumpolar vortex cause seasonal changes in temperature and precipitation patterns across Canada (Burnett, 1993; Frauenfeld and Davis, 2003; Girardin et al., 2004; Girardin and Tardif, 2005), and longer-term secular periodicities have been related to global modes of atmospheric circulation such as the North Atlantic Oscillation (NAO) and the Pacific Decadal Oscillation (PDO)(Girardin et al, 2004).

Black spruce and white spruce were selected for isotope analyses because of their prevalence throughout northern boreal forests and similar physiological characteristics. There are however differences in site and stand conditions between the two species. Black spruce generally grow in cold, low-nutrient, poorly drained soils and Muskeg bog, while white spruce prefer moderate- to well-drained, moist soils. Black spruce are commonly found in stands of similar size trees, and all black spruce in the study area were ~10 to 15cm in diameter and ~10m tall. White spruce have higher shade tolerance and are found in stands of much greater size variation (Johnson et al., 1995). In our study area, white spruce ranged in size from a basal diameter of a few centimeters to greater than 50cm and from heights of less than 1m to more than 20m. Since these two species grow in soil with significantly different hydrologic characteristics, both species were analyzed to assess the degree to which the differences in soil moisture conditions influence $\delta^{18}O$ values of tree-ring α-cellulose.

4.5 Methods

Samples were collected using a 12mm increment borer or by felling smaller trees where permitted. Core samples were collected from near the base of large (> 50cm in diameter) white spruce trees (*n*=11) in early June 2005. Care was taken to ensure that the center and therefore the earliest rings were recovered in the core. Discs were cut from the base of freshly felled black spruce in September 2003. Ring width measurements were conducted on all tree samples using a 5x power dissection microscope and ocular scale. For the samples in which a disc was available, ring width measurements were conducted in four directions at 90º angles and the values used herein are the average of those four transects. Rings were divided into early (spring growth, lighter color) and late wood (late season growth, darker color) based on the transition from light/less dense to dark/more dense wood. In northern boreal forests, late wood growth is very short and therefore produces very small late wood rings (generally < 1mm thick; Fritts, 1976). Growth rings were subsequently digitized and sampled using a robotic micromilling device. This process has advantages over traditional scalpel and microtome methods as it produces a fine, homogenous powder and facilitates the processing and analyses of small samples. Additionally, it permits recovery of material concordant with growth banding to greater precision.

Waxes, resins and lipids were removed from cellulose by solvent extraction using 2:1 toluene and 100% methanol (Leavitt and Danzer, 1993). Cellulose samples were then converted to α-cellulose following a modified Brendel et al. (2000) procedure reported by Evans and Schrag (2004). $\delta^{18}O$ analyses were conducted using a continuous flow pyrolysis technique at the Saskatchewan Isotope Laboratory on 150 – 200 μg of α-cellulose samples loaded into silver capsules. Samples were then converted to CO gas via online pyrolysis in a Thermo Finnigan Thermal Conversion Elemental Analyzer (TC/EA) at 1450ºC. Isotope ratios of $^{18}O/^{16}O$ were determined via continuous flow using a Thermo Finnigan Delta Plus XL mass spectrometer relative to CO reference gases. Within each run (*n*=48), samples were bracketed by benzoic acid standards of known $\delta^{18}O$ values. Sample precision is constrained with a third internal benzoic acid standard and sample reproducibility ±0.2 ‰ (1σ) for $\delta^{18}O$ values with all values reported relative to VSMOW in delta notation ($\delta^{18}O = {}^{18}O/{}^{16}O_{sample}/{}^{18}O/{}^{16}O_{standard} - 1 \times 1000$).

4.5 Results

4.5.1 Tree-ring oxygen isotopes

In all, 207 early and late wood samples were analyzed for the white spruce between 1894 and 2004 and 100 samples between 1951 and 2003 for the black spruce. $\delta^{18}O$ values of black (*Pieca mariana*) and white (*P. glauca*) spruce α-cellulose show considerable variability with a total range of values from ~21‰ to ~28‰ , respectively (Fig. 4.2). The $\delta^{18}O$ time series derived from the black spruce α-cellulose yielded $\delta^{18}O$ values that are consistently lower than in the white spruce time series and the difference between the $\delta^{18}O$ values of the two species are shown in figure 4.2 ($\delta^{18}O$ value of black spruce – white spruce). Early and late wood $\delta^{18}O$ values generally display a similar trend in the black spruce sample (r = 0.66) and tend to follow similar patterns from one year to the next (Fig. 4.2); however, there is less correlation between $\delta^{18}O$ values of early and late wood in the white spruce (r = 0.43).

4.5.2 Reconstructing growing season $\delta^{18}O$ precipitation values

$\delta^{18}O$ values of source water utilized by the tree during cellulose production were calculated from the $\delta^{18}O$ α-cellulose values of both trees using the modified leaf-water equation (Eq.1) after Anderson et al. (2002). Seasonal averages of daily relative humidity and temperature measurements from The Pas (1953 – 2005), and tree ring index measurements were used to calculated the damping factor (f) for both the early and late wood components of the two trees (see Appendix B for table of values). Average daily relative humidity values proved more successful in reconstructing observed $\delta^{18}O$ values of precipitation than midday relative humidity and where therefore used in this study. The liquid to vapor fractionation factor (ε_e; Manjoube, 1971) was calculated using the average seasonal temperatures for the period between 1953 and 2005 and determined to be 10.4‰. Calculations of ε_e using maximum and minimum growing season temperature were also calculated to assess the possible range of ε_e at both temperature extremes, resulting in a ε_e values from 10.2‰ to 10.6‰. Propagation of the 0.4‰ uncertainty through the equation results in changes in the source water $\delta^{18}O$ value by an amount that is less than the analytical uncertainties of the α-cellulose measurements and is therefore

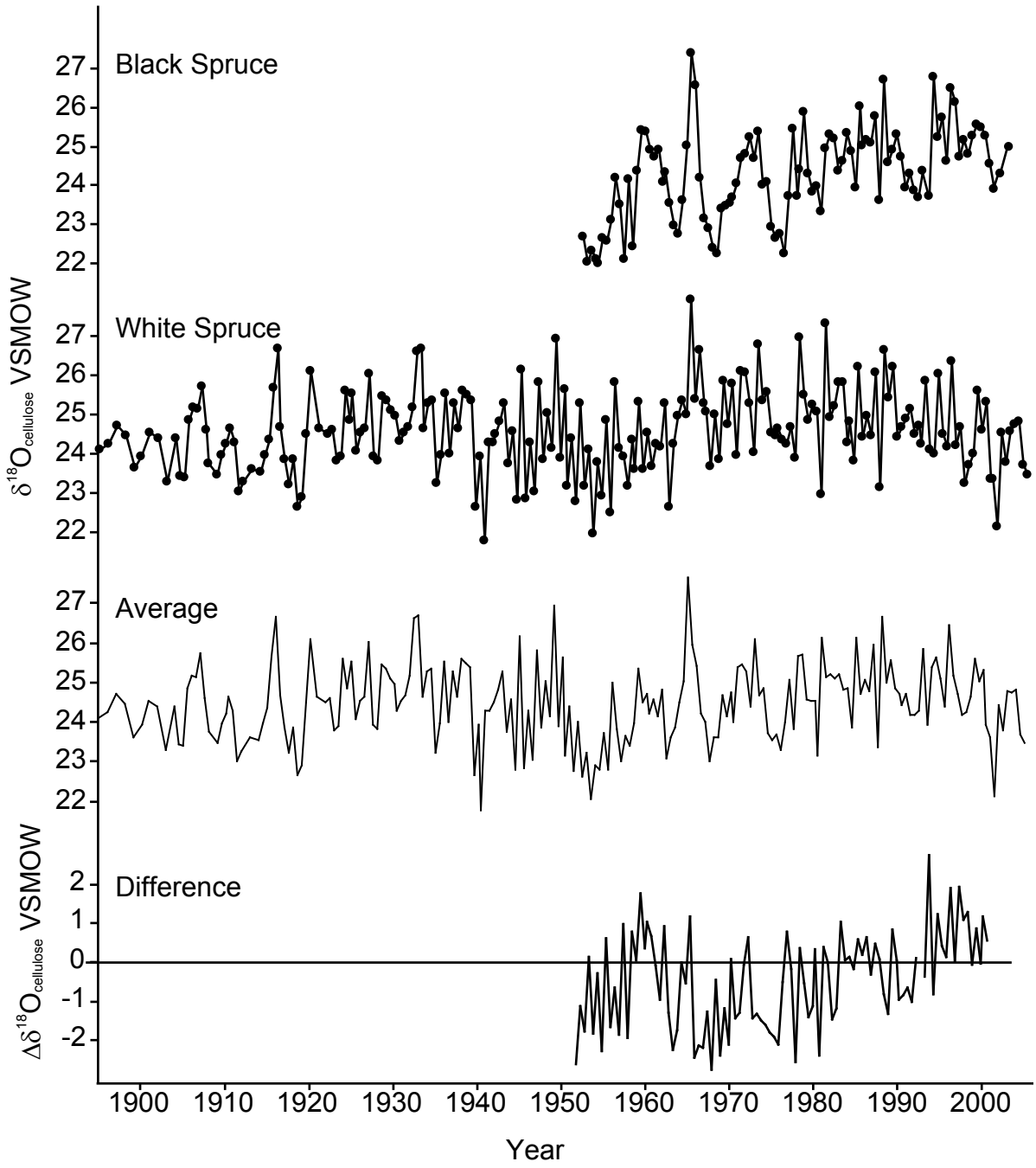

Figure 4.2. $\delta^{18}O$ time series constructed for early and late wood portions of a black spruce and white spruce from Limestone Lake. Both trees follow the same general trend as is shown by the average value; however the black spruce often has lower $\delta^{18}O$ values as a result of longer soil residence time in the poorly drained bog. Therefore, there is generally a negative difference between the black spruce and white spruce $\delta^{18}O$ values.

negligible. The calculated *f* values range from 0.02 to 0.38 for the black spruce and 0.01 to 0.34 for the white spruce, with average values of 0.13 for both trees. Allison et al. (1985) estimated *f* to be constant at 0.2 and Anderson et al. (2002) estimated *f* range between 0.27 and 0.49, and the *f* values in this study are on the lower range of values reported by other studies (Roden et al., 2000, Allison et. al, 1985, Waterhouse et al., 2002).

4.6 Discussion

4.6.1 Interpretation of $\delta^{18}O$ values in source water and precipitation

Source water $\delta^{18}O$ values calculated from black and white spruce display a relatively high correlation with growing season precipitation values (r = 0.79 and 0.82, respectively) from The Pas, Manitoba (1975 to 1982). However inferred source water values calculated from the average $\delta^{18}O$ values from the two trees yields an even higher correlation with the $\delta^{18}O$ values of precipitation (r = 0.86; Fig. 4.3). Reconstructed source water values range between about -17.4‰ to -13.5‰ in the black spruce and from -15.9‰ to -13.2‰ in the white spruce (Fig. 4.4a). Since most of the recharge in the study area occurs as a result of spring snowmelt, average groundwater values are weighted toward winter precipitation and range between -16‰ and -18‰ (Fritz et al., 1987), whereas growing season precipitation $\delta^{18}O$ values for The Pas are between -15.3‰ and -11.4‰. Trees that were utilizing significant amounts of groundwater would therefore be expected to have $\delta^{18}O$ source water values that are several per mil lower than growing season precipitation. Additionally, groundwater values remain relatively constant (Fritz et al., 1987), and if the trees were obtaining water from groundwater, there would be little change in the $\delta^{18}O$ values of α-cellulose from year to year. Snow melt water does likely persist as soil moisture into the early part of growing season, and years of high snow runoff will result in lower than average $\delta^{18}O$ value in the early part of the season.

The snow melt $\delta^{18}O$ signature also persists longer in poorly drained soils, such as the bog where the black spruce sample was collected. Surface water samples collected from the Limestone Lake/bog water had $\delta^{18}O$ values of -9.8‰ in September 2003 and -18.3‰ early June 2005. The bog water $\delta^{18}O$ values are lower than precipitation $\delta^{18}O$

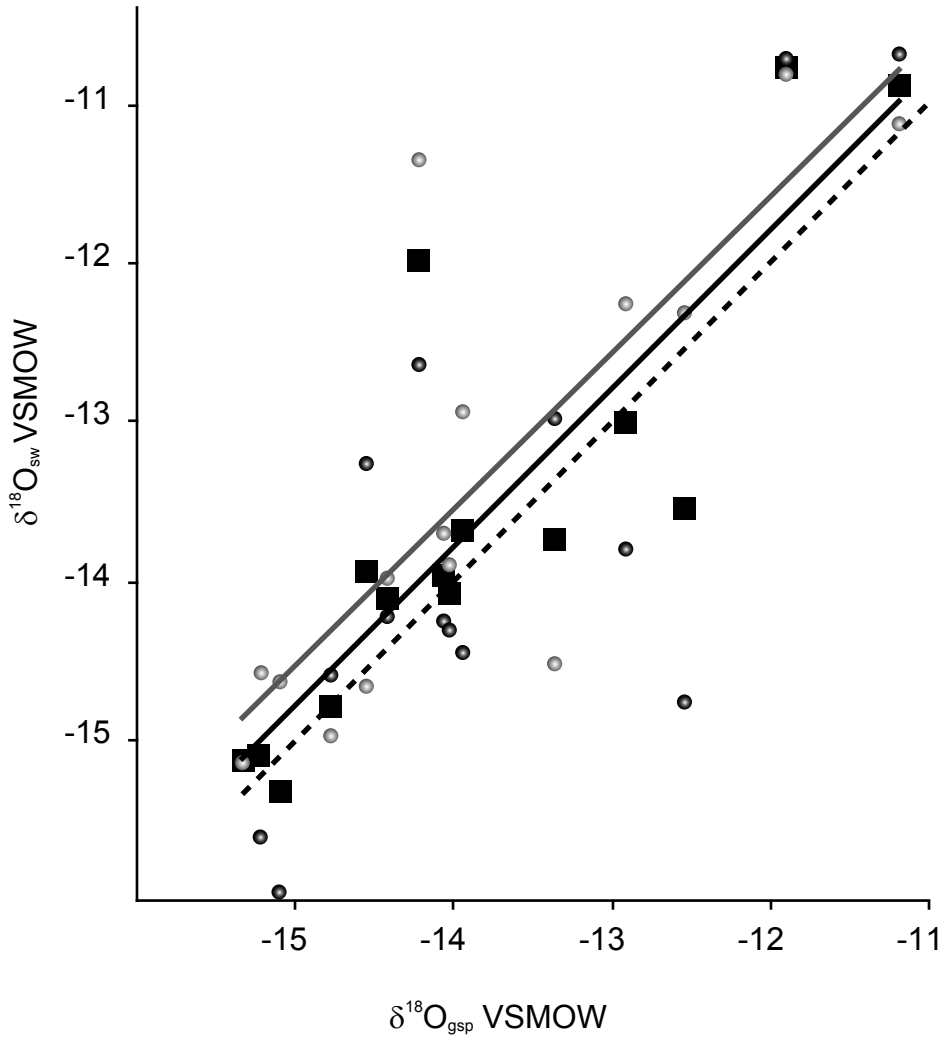

Figure 4.3. Reconstructed source water (sw) $\delta^{18}O$ values using the modified leaf-water equation (Anderson, 2002) are well correlated with weighted mean growing season precipitation (gsp) from The Pas, Manitoba for both early (April to August) and late (September to October) wood periods. Source water values reconstructed from black spruce values (dashed line/ black circles) display the lowest correlation with growing season precipitation $\delta^{18}O$ values ($r = 0.79$) while the white spruce (gray line/ circles) is slightly higher ($r = 0.82$). The source water $\delta^{18}O$ values reconstructed from the average of the two time series display the highest correlation (black line/ black squares) with $r = 0.86$.

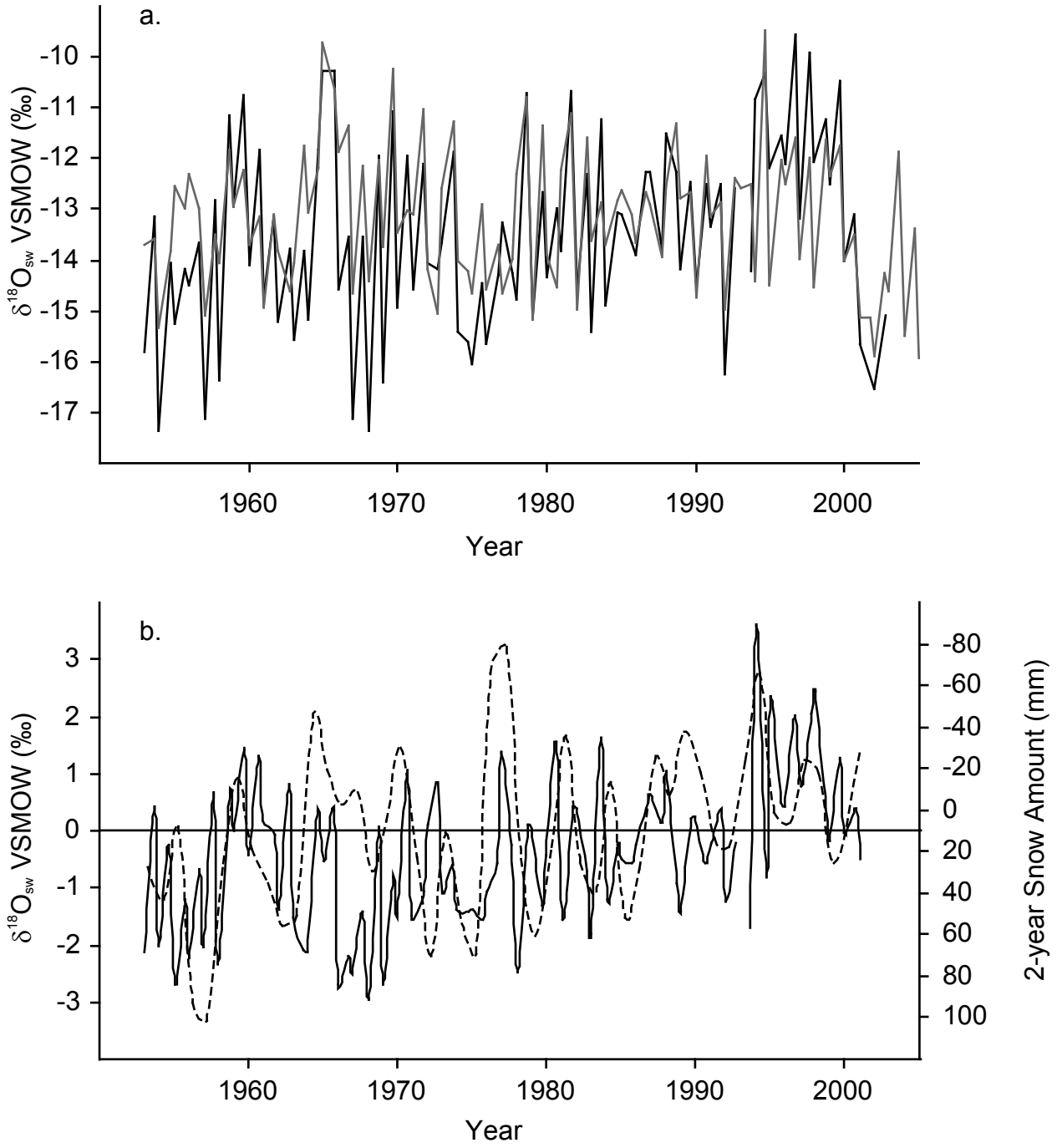

Figure 4.4 (a) $\delta^{18}O$ values of source water (sw) utilized by the black spruce (black) and white spruce (gray) from Limestone Lake display similar variability throughout the record from 1953 to 2005; however the black spruce source water is consistently lower than that of the white spruce as a result of snowmelt runoff and longer soil residence times. (b) Years in which the black spruce source water $\delta^{18}O$ values are higher than in the white spruce (Black spruce - white spruce values plotted in 4.4b are inversely correlated with the amount of snowfall in the 2 years prior to cellulose formation (dashed line, values reversed). Lower snowfall amounts cause the lake and bog water to be weighted toward summer precipitation values while in years with high snowfall amounts the low $\delta^{18}O$ snow signal persists longer into the growing season.

values in the summer and most likely record spring snow runoff. Conversely, the bog water $\delta^{18}O$ values are higher than the precipitation in the late growing season as a result summer precipitation and surface water evaporation. Since the black spruce is growing in the bog water and the white spruce is not, differing source water $\delta^{18}O$ values observed between the black and white spruce are therefore most likely due to differences in soil hydrology (Tang and Feng, 2001). The white spruce was growing further upslope, where no standing water was present, and the soil was much better drained. In addition, Jack pine (*Pinus banksiana*) were found in the same stand (<5m) from the white spruce. Jack pine grow in very well drained sandy soil supporting a change from the poorly drained soil in the black spruce location to a moderate to well drained soil up slope at the white spruce sample site. The longer residence time associated with bog/lake water therefore results in black spruce $\delta^{18}O$ values that are lower than the white spruce in the early summer and higher in the fall as a result of summer evaporation of the bog/lake water.

An alternate interpretation for the difference between the black and white spruce $\delta^{18}O$ time series is different periods of growth for the two species. Recent studies have demonstrated that black spruce growth retards as early as June or July, where white spruce is likely to continue growing on into the fall. The shorter period of growth, and therefore cellulose production, would cause the black spruce $\delta^{18}O$ values to be weighted toward spring and early summer precipitation $\delta^{18}O$ values. Both the shorter growing season and longer residence time of soil moisture in the black spruce bog would therefore be similarly recorded in the black spruce cellulose as $\delta^{18}O$ values that were lower than those observed in the white spruce. Additionally, better constraints on the growing season timing in both species would facilitate comparisons between the $\delta^{18}O$ α-cellulose records and meteorological/ environmental parameters.

Extended periods when the black spruce $\delta^{18}O$ time series is higher than the white spruce for both early and late wood occur from 1959 to 1961, 1984 to 1988, and 1994 to 2003 and coincide with snowfall deficits over the 2 years prior to cellulose growth (Fig. 4.4b). Soil water used by the black spruce records less of the snow $\delta^{18}O$ signature in low snowfall years resulting in higher $\delta^{18}O$ values in lake and bog water than in years where snowfall amount is high. Thus, in years when snowfall is low, the black spruce bog consists mainly of summer precipitation and reflects higher $\delta^{18}O$ values throughout the

early as well as the late growing season than the $\delta^{18}O$ value of precipitation recorded by the white spruce.

The shorter residence time associated with the white spruce soil would preclude the damping of the $\delta^{18}O$ values in the soil water associated with the black spruce. The white spruce $\delta^{18}O$ time series is therefore more responsive to growing season precipitation $\delta^{18}O$ values; however, the soil moisture in the white spruce stand would be more susceptible to modification of $\delta^{18}O$ values by evaporation. By averaging $\delta^{18}O$ time series from the two trees, the extreme effects of soil water residence time and soil water evaporation may be accounted for, and result in a more reliable estimate of the $\delta^{18}O$ values of growing season precipitation.

4.6.2 Meteorological and atmospheric interpretations from $\delta^{18}O$ values

Relative humidity data is only available from 1953 to 2005, thus confining source water reconstructions to that time period; however the $\delta^{18}O$ time series from the white spruce still records changes in relative humidity and temperature conditions from 1895 to 2005. Multiple studies have indicated that relative humidity and temperature are the dominant environmental forcers of $\delta^{18}O$ values in tree ring cellulose. Modification of the $\delta^{18}O$ precipitation values is largely depended evaporation in the leaves during transpiration as a result of relative humidity and temperature (Buhay et al, 1996; Roden et al., 2000, Anderson et al., 2002). Although the empirical relationship between $\delta^{18}O$ cellulose and changes in temperature/ relative humidity cannot be thoroughly examined without knowing the changes in the $\delta^{18}O$ values of the water used by the tree, changes in the $\delta^{18}O$ cellulose time series also record general variations in temperature and relative humidity through time. Correspondence analysis demonstrates that growing season relative humidity generally has a strong inverse relationship with the $\delta^{18}O$ cellulose time series, while growing season temperature and circumpolar vortex position are positively correlated with $\delta^{18}O$ values (Fig. 4.5, Table 4.1). Growing season temperatures in the study area display a strong relationship with the position of the circumpolar vortex (Frauenfeld and Davis, 2003), with the strongest correlation between the central vortex position and June through July temperature (r = 0.84). Since about 1970, there has been a general northward contraction of the circumpolar throughout the Northern Hemisphere

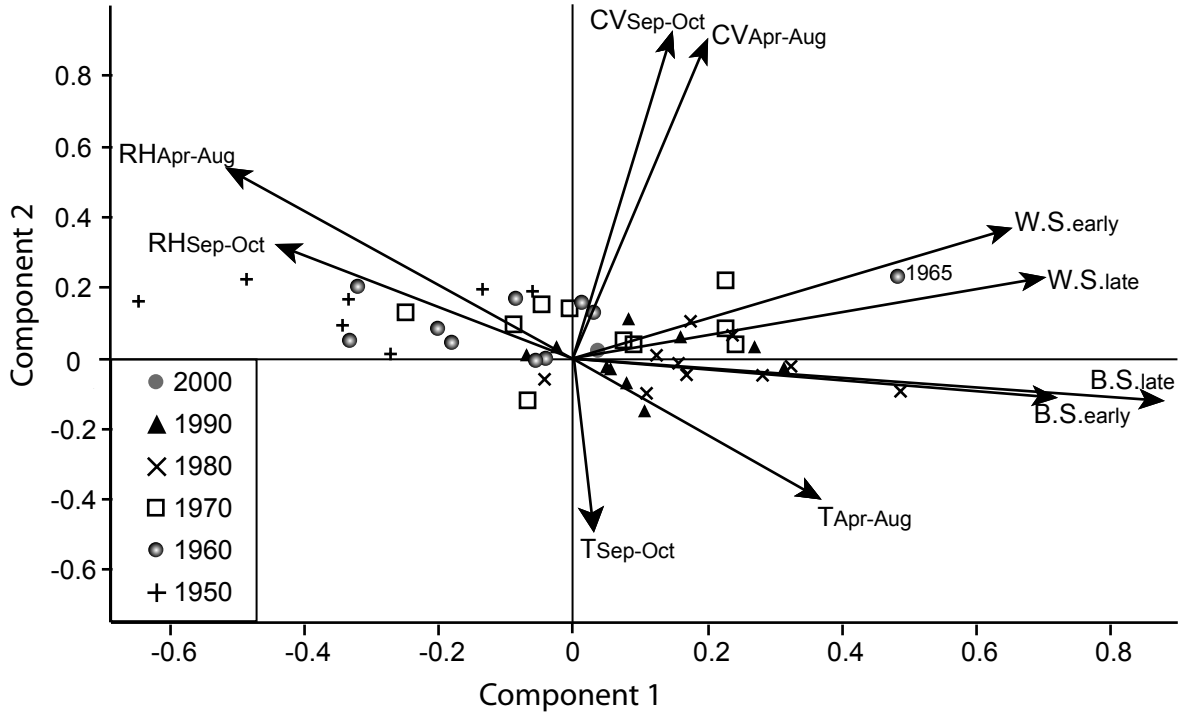

Figure 4.5. Components 1 and 2 of R- and Q- mode correspondence analysis are plotted above as a visual representation of the relationship between the $\delta^{18}O$ time series from black (B.S.) and white spruce (W.S.) early and late wood, growing season temperature (T), relative humidity (RH), and circumpolar vortex position (CV). This procedure allows both the variables (arrows) and the sample years (symbols) to be plotted on the same axis in eigenvector space (Gabriel, 1971). For example, April to August relative humidity (RH Apr-Aug) has a value of -0.50 for component 1 and +0.52 for component 2. Sample years are plotted in the same fashion; however they have been separated by year (decade) to depict changes in the relationship between sample loadings through time. Components 1-4 account for 69.1% of the total variance and variable loadings for these components are shown in Table 4.1. Vectors with acute relationships are positively correlated (i.e. cos 0° = 1 or perfect correlation) where as obtuse relationships indicate negative correlations (i.e. cos 180° = -1 or perfect correlation). All of the variables except relative humidity have positive values in component 1 and are therefore positively related to each other. As would be expected, relative humidity displays a strong negative relationship with temperature and the $\delta^{18}O$ cellulose values. Note the nearly perfect negative relationship between the April to August relative humidity and temperature. With the exception of 1965, most of the variance in years between 1950 and 1969 is explained by relative humidity and these years plot on the left side of the y axis along the relative humidity trend. The 1970s appear to be a transition with some years following the relative humidity trend and some years trending more toward the $\delta^{18}O$ values and temperatures, but from 1980 to 2000 nearly all of the variance is due to temperature and vortex position. The effects of temperature and vortex position on the sample variance in essence cancel each other out and result in the clustering of the samples years along the same trend as the $\delta^{18}O$ values.

Table 4.1. Variable loadings for components 1 through 4 from R- and Q- mode correspondence analysis conducted on $\delta^{18}O$ time series from black and white spruce and instrumental meteorological data from The Pas, Manitoba. Meteorological variables are air temperature (T), relative humidity (RH), and precipitation amount (P). The position of the central contour of the circumpolar vortex (CV) is also included as well as white spruce (W.S.) and black spruce (B.S.) early and late wood $\delta^{18}O$ values. Components 1 through 4 account for 69.1% of the total variance.

Variable	Comp. 1	Comp. 2	Comp. 3	Comp. 4
Apr-Aug T	0.34	-0.37	-0.56	0.43
Sep-Oct T	0.03	-0.44	-0.22	0.38
Apr-Aug RH	-0.50	0.52	0.24	-0.17
Sep-Oct RH	-0.42	0.31	0.62	0.42
Apr-Aug CV	0.19	0.86	-0.43	0.15
Sep-Oct CV	0.14	0.87	-0.42	0.13
W.S. early	0.64	0.35	0.23	-0.06
W.S late	0.68	0.21	0.19	-0.10
B.S. early	0.85	-0.12	0.14	-0.09
B.S. late	0.70	-0.11	0.40	0.16
% of total variance	27.22	17.95	13.39	10.56

resulting in higher annual temperatures in central Canada (Frauenfeld and Davis, 2003); however, in the study area the vortex position began shifting to the north in the mid-1960s (NCEP/NCAR, 2000). The localized northward contraction of the circumpolar vortex has resulted in decreased growing season relative humidity and increased temperatures from the mid-1960s to present (Environment Canada, 2005). The contraction of the vortex also appears to coincide with a shift from relative humidity forced variance (from 1953 – 1965) to more temperature forced values (1965 –2000) in the $\delta^{18}O$ time series in this study (Fig 4.5). The $\delta^{18}O$ time series also display a general increase in $\delta^{18}O$ values between the mid-1960s and 1999 (Fig 4. 2.) that coincides with the northward contraction of the circumpolar vortex, the increase in surface temperatures, and decrease in relative humidity. Additionally, the $\delta^{18}O$ cellulose values from 1964 to 1966 are among the highest in the entire record. The most likely explanation for these years is a combination of low winter precipitation the early 1960s followed by warm conditions that persisted late into the growing season as a result of a northward contraction of the circumpolar vortex during the mid-1960s (Environment Canada, 2005; NCEP/NCAR, 2000).

Circumpolar vortex data is available from 1948 to present; and other studies have shown that the position of the circumpolar vortex is largely related to the changes in the strength and phase of the North Atlantic Oscillation (NAO) and the Pacific Decadal Oscillation (PDO; Hurrell 1995, 1996; Frauenfeld and Davis, 2003). The observed surface temperature warming and circumpolar vortex contraction in the Northern Hemisphere coincide with phase shifts in the NAO and PDO. Between the mid-1970s and the early 1980s, the NAO changed from a negative to positive phase, indicated by increased westerly strength in the mid-latitudes of the North Atlantic ocean as a result of greater pressure gradient between the Icelandic Low and the high-pressure system near the Azores in the subtropical Atlantic (Hurrell, 1996). A similar shift also occurred in the PDO in the mid-1970s as a result of a strengthening and eastward migration of the Aleutian Low (Frauenfeld and Davis, 2003). Additionally, the white spruce $\delta^{18}O$ time series in this study displays periodicities that are similar in frequency and duration to those observed in the PDO and NAO indices.

Continuous wavelet analyses (CWT) were performed on the first differences (one year minus the previous year) of $\delta^{18}O$ α-cellulose values, temperature, precipitation, NAO, and PDO indices from 1900 to 2000. Winter (December to March) station based NAO indices and annual PDO indices from 1900 to 2004 were used in this study (Hurrell, 1995, 1996; Mantua et al, 1997; Zhang et al., 1997). All time series display a pervasive 2 to 8 year periodicity that is significant at the 95% confidence level against the corresponding red noise spectrum (Fig. 4.6; e.g. Torrence and Compo, 1998). Cross wavelet transform (XWT) analyses were preformed on $\delta^{18}O$, PDO, and NAO to emphasize periods of coherence between the white spruce $\delta^{18}O$ time series and NAO/PDO indices, and show that the 2-8 year period is common in all time series for much of the time between 1900 and 2004 (Fig .4. 7; e.g. Grinsted et. al., 2004). Girardin et al. (2004) also noted a 2-8 year oscillation during much of the 20th century in tree-ring width chronologies from central Manitoba. Ring width measurements from trees in our study area do display similar periodicities; however the ring width data appear to be much more patchy than the $\delta^{18}O$ time series and several decades in the 20th century display no significant periodicity (data not shown). In addition to the 2-8 year periodicity, there is an intensification of a more decadal scale oscillation (8-11 years) from the early1950s to present in both $\delta^{18}O$ values and the NAO/PDO indices (Fig. 4.7 b &d). This shift toward a more decadal pattern has also been noted by several other studies including tree-ring chronologies from the Gulf of Alaska (D'Arrgio et al., 2001) and eastern Canada (Girardin et al., 2004). Periodicities are similar between early and late wood $\delta^{18}O$ time series; however there is generally greater coherency between the $\delta^{18}O$ values of early wood and NAO/PDO indices indicating that changes in the NAO/PDO exert a stronger influence on early season $\delta^{18}O$ values. Cross wavelet analyses also allow for the interpretation of phase relationships between time series, with time series being in phase when they are both operating in the same direction (i.e. both positive; Grinsted et. al., 2004). $\delta^{18}O$ values and PDO indices generally display strong anti-phase relationships, depicted by arrows to the left while the $\delta^{18}O$ time series and NAO indices are generally in phase (arrows to the right). However, between 1990 and 2000, there is a strong anti-phase relationship between the $\delta^{18}O$ time series and the NAO at the 2-3 year frequency. The early wood portion of the $\delta^{18}O$ time series display common periodicities with the NAO

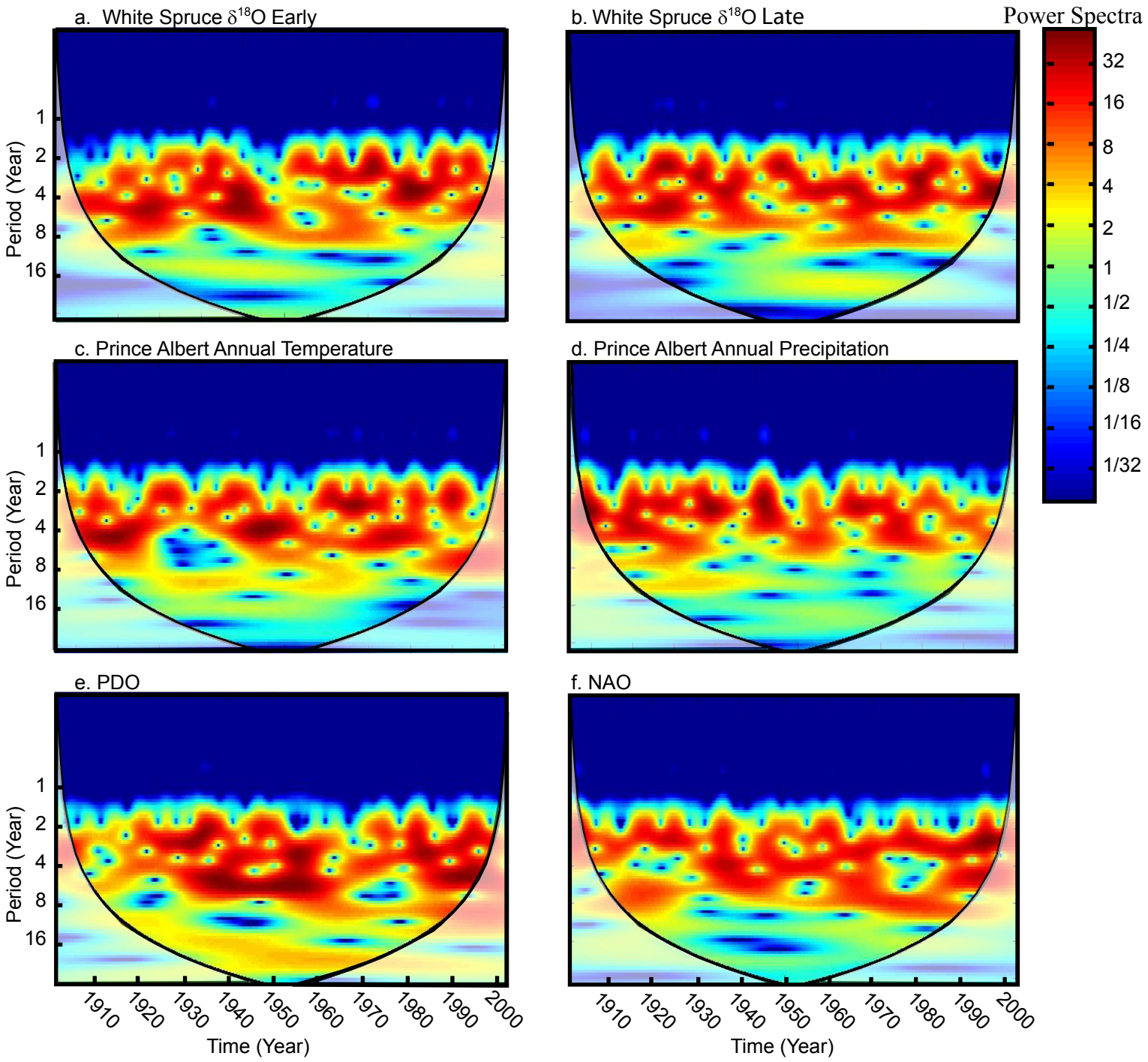

Figure 4.6. Continuous wavelet transform (CWT) analysis is a useful tool for examining cycle frequency in time series. CWT analyses of white spruce early (a) and late (b) wood $\delta^{18}O$, Prince Albert annual temperature (c), Prince Albert annual precipitation (d), and NAO (e) /PDO (f) indices show a common high power cycle with a frequency between 2 and 8 years. The highest powers appear as dark red areas and are significant at the 95% confidence interval against corresponding red noise spectra.

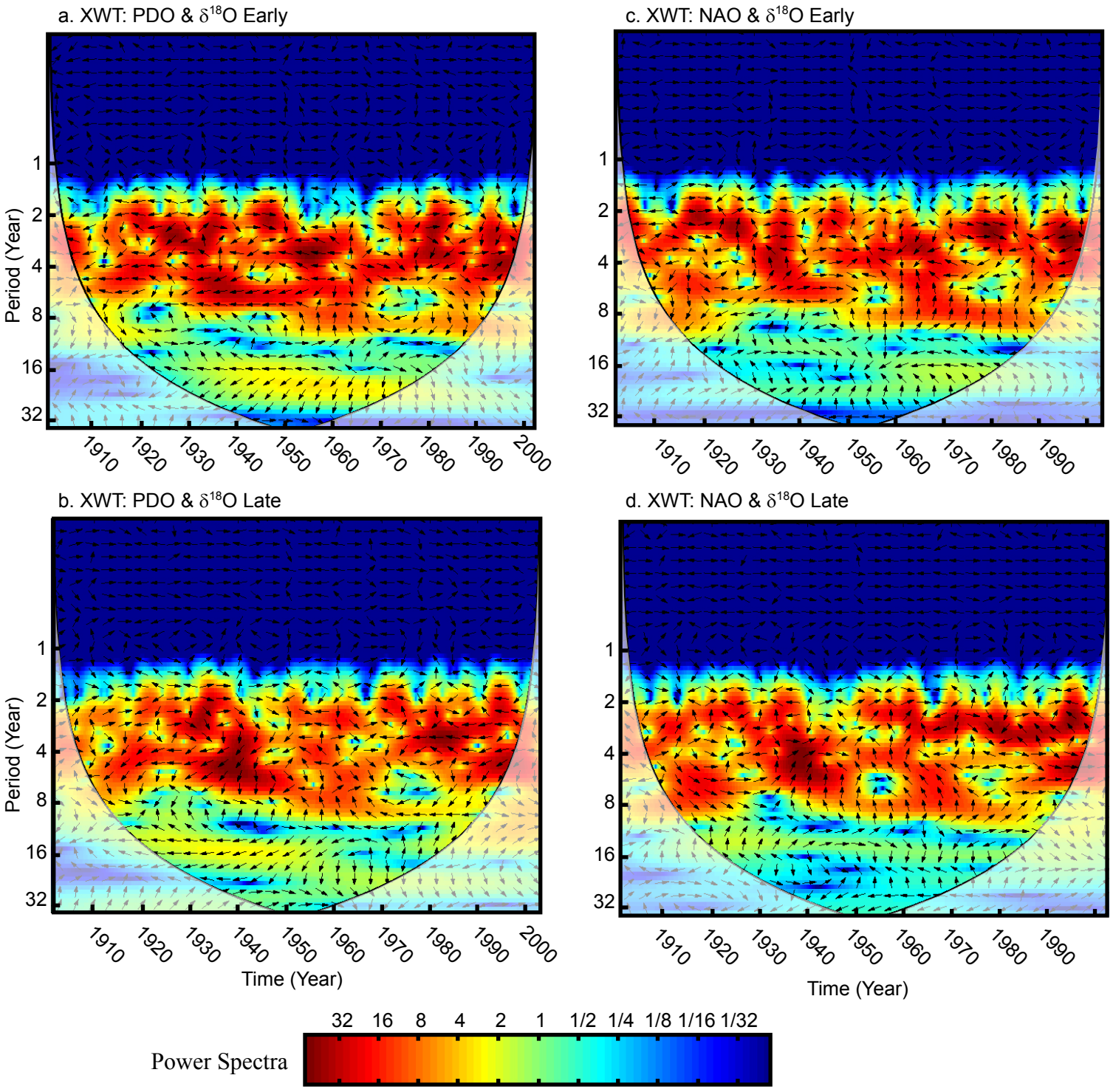

Figure 4.7. Cross wavelet transform analysis (XWT) is similar to CWT and exposes periods with common high powers and the relative phase relationship of the data. For example, the dark red area in Figure 10d shows a prominent common periodicity of 3 to 6 years between the NAO and the $\delta^{18}O$ values of white spruce late wood from 1930 to 1950. Arrows indicate the relative phase relationship between the two time series. Right arrows indicate an in-phase relationship while left arrows indicate that the time series have an anti-phase relationship. Arrows pointing straight up or down at 90° indicate that the first or second time series, respectively, leads the other.

and PDO throughout most of the 20th century. The mid-1960s to -1970s presents the only time when there $\delta^{18}O$ time series and the PDO/NAO indices do not appear to be operating under the same periodicity. During the mid-1960s, localized contraction of the circumpolar vortex was observed; however the change in circumpolar vortex appears to be largely independent of the factors forcing the changes in the NAO and PDO. There are fewer time segments with common periodicity between the late wood $\delta^{18}O$ time series and the NAO/PDO indices. The pressure and temperature gradients between the high and low latitudes in the Pacific and Atlantic Oceans that force changes in the position of the circumpolar vortex, the NAO, and the PDO are strongest during winter months (Hurrell 1995, 1996; Frauenfeld and Davis, 2003); therefore changes in the strength and phase of the NAO and PDO are therefore greatest during the winter months and are more likely to influence weather patterns during the early spring and summer than during the late season when late wood is produced.

4.7. Conclusions

Source water $\delta^{18}O$ values calculated from early and late wood $\delta^{18}O$ α-cellulose values of two spruce species indicates that $\delta^{18}O$ values in tree-ring α-cellulose record seasonal (early and late wood growth periods) variations in the $\delta^{18}O$ value of precipitation. The damping factor *f* in the modified leaf-water equation does not account for all of the "upstream" damping of the precipitation $\delta^{18}O$ values in individual trees, but does appear to account for most of the variation at a given location. Variations in $\delta^{18}O$ time series between individual trees have often been considered noise and are diminished by averaging $\delta^{18}O$ time series for several trees. It is necessary to select an average soil moisture residence time that is equivalent to the growing season, in this case an average of both species, in order to accurately reconstruct growing season conditions; however, there is still important information about climate process recorded by the difference between the two $\delta^{18}O$ time series such as changes in snow melt timing and magnitude and seasonal variations in atmospheric conditions. It is also essential to calibration the $\delta^{18}O$ values recorded in tree-ring α-cellulose with meteorological and precipitation isotope data in order to validate reconstructions source water $\delta^{18}O$ values.

Reconstruction of source water $\delta^{18}O$ values is limited by the availability of temperature and relative humidity data; in order to extend source water into the past it is necessary to develop proxies of relative humidity and temperature. Tree-ring chronologies as well as $\delta^{13}C$ and δD time series from tree-ring α-cellulose offer the potential to develop proxies of relative humidity and temperature and therefore the possibility to generate $\delta^{18}O$ precipitation records where instrumental records are not available, and further work is currently underway to develop these proxies. Additionally, $\delta^{18}O$ values in the white spruce time series do record seasonal changes in atmospheric circulation associated with the position of the circumpolar vortex and dominate modes of atmospheric variability such as the NAO and PDO.

4.8 Acknowledgements

This research was supported by a National Science Foundation – Graduate Research Fellowship J. Dodd, a Geologic Society of America Graduate Research Grant for J. Dodd, and Natural Sciences and Engineering Research Council of Canada Grant #203538 to W. Patterson. I would like to thank T. Prokopiuk for his invaluable assistance in the collecting of samples as well as A. Diefendorf, T. Prokopiuk, K. Dietrich, and A. Csank, for reading early drafts of the manuscript and help with analyses at the Saskatchewan Isotope Laboratory. Thanks also to J. Miller and K. Dietrich for help with the micromilling apparatus and software.

4.9 References

Allison, G.B., Gat, J.R., Leaney, F.W.J., 1985. The relationship between deuterium and oxygen-18 delta values in leaf water, Chemical Geology: 145-146.

Anderson, W.T., Bernasconi, S.M., McKenzie, J.A., Saurer, M., and Schweingruber, F., 2002. Model evaluation for reconstructing oxygen isotopic composition in precipitation from tree ring cellulose over the last century, Chemical Geology 182: 121-137.

Aucour, A.-M., Hillaire-Marcel, C., and Bonnefille, R., 1996. Oxygen isotopes in cellulose from modern and Quaternary intertropical peat bogs: implications for paleohydrology, Chemical Geology 129: 341-359.

Bowen, G.J., and Revenaugh, J., 2003. Interpolating the isotopic composition of modern meteoric precipitation, Water Resources and Research 39: 1299–1312.

Brendel, O., Iannetta, P.P.M ., Stewart, D., 2000. A rapid and simple method to isolate pure alpha-cellulose, Phytochem. Anal. 11: 7-10.

Buhay, W.M., and Edawards, T.W.D., 1995. Climate in Southwestern Ontario, Canada, between AD 1610 and 1885 inferred from oxygen and hydrogen isotopic measurements of wood cellulose from trees in different hydrological settings, Quat. Res. 44: 438-466.

Buhay, W.M., Edwards, T.W.D., and Aravena, R., 1996. Evaluating kinetic fractionation factors used for ecological and paleoclimatatic reconstructions from oxygen and hydrogen isotope ratios in plant water and cellulose, Geochim. Cosmochim. Acta 60: 2209-2218.

Burk, R.L., and Stuiver, M., 1981. Oxygen isotopes in trees reflect mean annual temperature and humidity, Science 211: 1417-1419.

Burnett, A., 1993. Size variations and long-wave circulation within the January Northern Hemisphere circumpolar vortex: 1946-89. J. of Clim. 6: 1914-1920.

R. D'Arrigo, R. Villalba, and G. Wiles, 2001. Tree-ring estimates of Pacific decadal climate variability, Climate Dynamics 18: 219-224.

Darling, W.G., 2004. Hydrological factors in the interpretation of stable isotope proxy data present and past: a European perspective, Quat. Sci. Rev. 23: 743-770.

DeNiro, M.J. and Epstein, S., 1979. Relationship between the oxygen isotope ratios of terrestrial plant cellulose, carbon dioxide, and water, Science 204: 51-53.

Dogmann, G., Nuernberg, H.W., Foestel, H., and Wagner, K., 1974. On the enrichment of $H_2{}^{18}O$ in the leaves of transpiring plants, Radiation and Environmental Biophysics 11: 41-52.

Environment Canada Climate Data Online, 2005 http://www.climate.weatheroffice.ec.gc.ca/prods_servs/cdcd_iso_e.html

Epstein, S., Thompson, P., and Yapp, C.J., 1977. Oxygen and hydrogen isotopic ratios in plant cellulose, Science 198: 1209-1215.

Evans, M.N. and Schrag, D.P., 2004. A stable isotope-based approach to tropical dendroclimatology, Geochim. Cosmochim. Acta 68: 3295-3305.

Frauenfeld, O.W., and Davis, R.E., 2003, Northern Hemisphere circumpolar vortex trends and climate change implications, Journal of Geophysical Research 108: 4423-4436.

Fritts, H.C., 1976. Tree Rings and Climate, Academic Press, New York.

Fritz, P., Drimmie, R.J., Frape, S.K., and O'Shea, K., 1987. The isotopic composition of precipitation and groundwater in Canada, in: Proceedings of an international symposium on the use of isotope techniques on water resource development, IAEA, Vienna, pp. 539-550.

Gabriel, H.C., 1971. The biplot display of matrices with application to principle component analysis, Biometrika 58: 453-467.

Gaudinski, J.B., Dawson, T. E., Quideau, S., Schuur, E.A.G., Roden, J.S., Trumbire, S.E., Sandquist, D.R., Oh, S., and Waslishen, R.E., 2005. Comparative analysis of cellulose preparation techniques for use with ^{13}C, ^{14}C, and ^{18}O Isotopic Measurements, Anal. Chem.: 7212-7224.

Gibson, J.J., 2001. Forest-tundra water balance signals traced by isotopic enrichment in lakes, J. of Hydro. 251: 1-12.

Girardin, M-P., Tardif, J., Flannigan, M.D., and Bergeron, Y., 2004. Multicentury reconstruction of the Canadian Drought Code from eastern Canada and its relationship with paleoclimatic indices of atmospheric circulation, Climate Dynamics 23: 99-115.

Girardin, M-P., and Tardiff, J., 2005, Sensitivity of tree growth to atmospheric vertical profile in the Boreal Plains of Manitoba, Canada, Canadian Journal of Forestry Research 35: 48-64.

Grinsted, A., Moore, J.C., and Jevrejeva, S., 2004. Application of the cross wavelet transform and wavelet coherence to geophysical time series, Nonlinear Processes in Geophysics 11: 561-566.

Hurrell, J. W., 1995. Decadal trends in the North Atlantic Oscillation regional temperatures and precipitation, Science 269: 267-679 ttp://www.cgd.ucar.edu/cas/jhurrell/indices.html.

Hurrell, J.W., 1996, Influence of variations in extratropical winter-time teleconnections on Northern Hemisphere temperatures, Geophysical Research Letters 23: 665-668.

IAEA/WMO, Global Network for Isotopes in Precipitation, 2001. The GNIP Database, Release 3, International Atomic Energy Agency /World Meteorological Organization http://www.iaea.org/programs/ri/gnip/gnipmain.htm.

Johnson, D., Kershaw, L., MacKinnon, A., and Pojar, J., 1995. Plants of the Western Boreal Forest and Aspen Parkland, Lone Pine Publisher, Edmonton.

Leavitt, S. W., and Danzer, S.R., 1993. Method for batch processing small wood samples to holocellulose for stable-carbon isotope analysis, Anal. Chem. 65: 87-89.

Manjoube, M., 1971, Fractionation en oxygèn 18 et deutérium entre l'eau et sa vapeur, Journal of Chimie Physique: 1423-1436.

Mantua, N.J., Hare, S.R., Zhang, Y., Wallace, J.M. and Francis, R.C., 1997. A Pacific interdecadal climate oscillation with impacts on salmon production. Bulletin of the American Meteorological Society 78:1069-1079. http://www.atmos.washington.edu/~mantua/abst.PDO.html

McCarroll, D., and Loader, N.J., 2004. Stable isotopes in tree rings, Quat. Sci. Rev. 23: 771-801.

Miller, D.L., Mora, C.I., Grissino-Mayer, H.D., Mock, C.J., Uhle, M.E., and Sharp, Z. A tree ring oxygen isotope record of hurricanes and droughts, Proc. Natl. Acad. Sci (in press).

NCEP Reanalysis data provided by the NOAA-CIRES Climate Diagnostics Center, Boulder, Colorado, USA, (2000) http://www.cdc.noaa.gov

Roden, J.S., Lin, G., and Ehleringer, J.R., 2000. A mechanistic model for interpretation of hydrogen and oxygen isotope ratios in tree-ring cellulose, Geochim. Cosmochim. Acta 64: 21-35.

Sauchyn, D.J., and Skinner, W.R., 2001. A Proxy PDSI record for the southwest Canadian Plains, Can. Water Res. J. 26: 253-272.

Saurer, M., 2003, The influence of climate on the oxygen isotopes in tree rings, Isotopes Environ. Health Stud. 39: 105-112.

Schindler, D.W., and Donahue, W.F., 2006. An impending water crisis in Canada's western prairie provinces, Proc. Natl. Acad. Sci.:1-7. (www.pnas.org/cgi/doi/10.1073/pnas.0601568103)

Sternberg, L.S.L., DeNiro, M.J., and Savidge, R.A., 1986. Oxygen isotopes exchange between metabolites and water during biochemical reactions leading to cellulose synthesis, Plant Physiology 82: 423-427.

Tang, K., and Feng X., 2001. The effect of soil hydrology on the oxygen and hydrogen isotopic compositions of plats' source water, Earth and Planetary Science Letters 185: 335-367.

Torrence, C., and Compo, G.P., 1998. A practical guide to wavelet analysis, Bulletin of the American Meteorological Society 79: 61-78.

Waterhouse, J.S., Switsur, V.R., Barker, A.C., Carter, A.H.C., and Robertson, I., 2002. Oxygen and hydrogen isotope ratios in tree rings: how well do models predict observed values? Earth and Planet. Sci. Lett. 201: 421-430.

Weigou, L., Xiahong, F., Yu, L., Quingle, Z., and Zhisheng, A., 2004. $\delta^{18}O$ values of tree rings as a proxy of monsoon precipitation in arid Northwest China, Chemical Geology 206: 73-80.

Wilson, A.T., and Grinsted, M.J., 1977. 12C/13C in cellulose and lignin as paleothermimeters, Nature 265: 133-135.

Yakir, D., and DeNiro, M.J., 1990, Oxygen and hydrogen isotope fractionation during cellulose metabolism in *Lemma gibba* L., Plant Physiol. 93: 325-332.

Zhang, Y., Wallace, J.M., and Battisti, D.S., 1997. ENSO-like interdecadal variability: 1900-93, Journal of Climate 10: 1004-1020.

4.10 Manuscript's Relationship to Thesis

Chapter 4 presents a 110yr record of seasonal variations in meteorological and atmospheric conditions preserved in the $\delta^{18}O$ time series of tree-ring α-cellulose. Chapter 4 demonstrates the usefulness of $\delta^{18}O$ time series in tree-ring α-cellulose as a record for temperature, relative humidity and atmospheric variability associated with changes in the NAO, PDO, and circumpolar vortex.

CHAPTER 5. DISCUSSION AND RELATION OF MANUSCRIPTS TO THE THESIS

Each chapter in the main body of the thesis (Chapters 2-3) offers a detailed examination of different aspects of stable isotope proxies, specifically those in surface water reservoirs, precipitation, and tree-ring cellulose as records of past climate change.

Chapter 2, *Survey of oxygen and hydrogen isotope values in Tasmanian precipitation and surface waters*, provides the first regional study of surface water $\delta^{18}O$ and δD values for Tasmania, Australia. Isotope values of Tasmanian surface waters provide useful information about modern meteorological and physical parameters that influence the spatial variation in $\delta^{18}O/\delta D$ values in Tasmanian precipitation. Additionally, this study provides critical information about the modification of precipitation isotope values by surficial processes such as evaporation, hydrologic residence time, and the time averaging of seasonal variability. Perhaps most importantly, development and interpretation of multi-proxy records of climate change in Tasmania and elsewhere will benefit significantly by surface water surveys such as this, in that they permit selection of the most appropriate study sites and proxy materials.

Chapter 3, *A new tool for obtaining sub-seasonal samples of tree-ring cellulose for isotope studies: advantages of robotic micromilling*, is the first study to implement a robotic micromill to produce high-resolution, intra-ring samples of tree-ring cellulose. Intra-ring sampling of tree-ring cellulose has previously been hampered by the methods used to sample the cellulose, such as a scalpel or microtome. The micromilling approach allows for growth bands to be accurately mapped and sampled, preventing crosscutting of growth bands as would often be the case if a razor based sampling system were used. The micromill also allows for the sampling of very narrow or highly curved rings that would otherwise be difficult to sample. The seasonal cyclicity observed in the intra-ring variations in $\delta^{18}O$, δD, and $\delta^{13}C$ values indicate that high-resolution sampling of tree-ring cellulose offers the potential to reconstruct sub-seasonal changes in temperature, relative humidity, and precipitation. Tree-ring isotope studies such as this are one of the only

seasonally resolved proxy records that are continuous at the centennial and millennial scale.

Chapter 4, *A 110yr seasonal precipitation and atmospheric circulation record: evidence from $\delta^{18}O$ values of tree-ring α–cellulose in modern spruce*, incorporates the concepts discussed in Chapters 2 and 3. The $\delta^{18}O$ values of α-cellulose in white and black spruce from Saskatchewan record changes in the $\delta^{18}O$ values of growing season precipitation, as well as relative humidity and temperature. The reconstructed $\delta^{18}O$ values of growing season precipitation are well correlated with $\delta^{18}O$ values record by the IAEA/WMO at The Pas, Manitoba. Additionally, the $\delta^{18}O$ time series from two spruce species (*Picea glauca* and *Picea mariana*) record winter precipitation amount (snow amount) and changes in temperature and relative humidity as a result of regime shifts in atmospheric circulation associated with the phase of the North Atlantic Oscillation (NAO) and Pacific Decadal Oscillation (PDO).

APPENDIX A. SURFACE WATER δD, $\delta^{18}O$, AND D-EXCESS DATA FOR TASMANIA, AUSTRALIA.

Sample Site	Date	Sample #	Latitude (S, dec. deg.)	Longitude (E, dec. deg.)	Sample Elevation (m)	Elevation of streamhead (m)	Estimated Mean Ann. Precip. (mm)	δD (‰) VSMOW	$\delta^{18}O$ (‰) VSMOW	d-excess (‰)
Rubicon River	07/03/04	44	41.451	146.565	180	300	1000	-27.4	-5.65	17.78
Meander River	07/03/04	45	41.525	146.659	242	1250	1200	-42.1	-7.00	13.93
Marakoopa Cave Creek	07/03/04	46	41.578	146.289	482	482	1600	-40.6	-7.07	15.98
Lobster Rivulet	07/03/04	47	41.553	146.478	263	1400	1600	-40.2	-6.78	14.07
Mt. Projection Bluff	07/03/04	48	41.721	146.725	1097	1097	1200	-54.3	-8.96	17.42
Liffy River Headwaters	07/03/04	49	41.770	146.709	1180	1400	1200	-48.1	-8.33	18.46
Great Lake	07/03/04	50	41.989	146.688	1034	1034	1600	-41.2	-6.22	8.52
Arthurs Lake	07/03/04	51	41.993	146.860	952	952	800	-56.1	-8.66	13.22
Shannon River	07/03/04	52	42.050	146.762	923	1034	1000	-55.2	-8.5	12.65
Penstock Lagoon	07/03/04	53	42.086	146.767	929	929	800	-51.3	-8.18	14.11
Ouse River	07/03/04	54	42.149	146.753	544	1151	1200	-53.1	-8.1	11.97
Bashan Plains Rivulet	07/03/04	55	42.209	146.758	683	1000	800	-51.1	-8.08	13.55
Kenmere Creek	07/03/04	56	42.309	146.707	594	950	800	-52.2	-8.31	14.30
Dee Lagoon	07/03/04	57	42.310	146.697	656	656	800	-40.5	-6.1	8.39
Echo Lake	07/03/04	58	42.308	146.668	826	846	600	-41.2	-6.52	10.99
Highland Lake	07/03/04	59	42.307	146.559	742	742	1200	-36.1	-4.77	2.07
Bradys Lake	07/03/04	60	42.306	146.546	651	651	1000	-49.9	-7.8	12.74
Lake Binney	07/03/04	61	42.301	146.506	659	659	1000	-42.8	-6.94	12.72
Nive River	07/03/04	62	42.300	146.458	368	1000	1600	-49.8	-8.05	14.56
Laughing Jack Canal	07/03/04	63	42.308	146.422	628	659	1000	-41.9	-6.76	12.11
Black Bob Rivulet	07/03/04	64	42.387	146.591	324	650	1200	-50.9	-7.9	12.23
Clyde River	07/03/04	65	42.562	146.828	96	822	600	-49.6	-7.1	7.19
Coal River	07/04/04	66	42.734	147.441	12	550	600	-38.9	-5.9	8.64
Orielton Rivulet	07/04/04	67	42.762	147.542	6	300	600	-36.4	-5.7	8.96

Table 1. (*continued*)

Sample Site	Date	Sample #	Latitude (S, dec. deg.)	Longitude (E, dec. deg.)	Sample Elevation (m)	Elevation of streamhead (m)	Estimated Mean Ann. Precip. (mm)	δD (‰) VSMOW	$\delta^{18}O$ (‰) VSMOW	d-excess (‰)
Allans Creek	07/04/04	68	43.063	147.864	26	438	800	-30.6	-5.88	16.40
Mt. Arthur Creek	07/04/04	69	43.119	147.758	0	400	800	-35.9	-6.14	13.25
Parsons Bay Creek	07/04/04	70	43.113	147.749	2	488	800	-34.4	-5.7	11.41
Saltwater River Pond	07/04/04	71	43.051	147.680	94	94	600	-6.2	0.4	-9.26
Carlton River	07/04/04	72	42.816	147.791	73	400	600	-32.5	-4.7	4.84
Griffiths Rivulet	07/04/04	73	42.708	147.841	214	600	800	-33.9	-5.8	12.09
Flash Tier Creek	07/04/04	74	42.651	147.898	18	300	800	-34.6	-5.9	12.35
Prosser River	07/04/04	75	42.559	147.871	3	600	600	-12.5	-1.8	1.83
Mountain River	07/05/04	76	42.995	147.065	33	1260	1000	-46.9	-7.4	12.70
Russel River	07/05/04	77	43.018	147.042	12	1260	1600	-48.1	-7.3	10.42
Huon River	07/05/04	78	43.034	147.048	6	309	2400	-49.0	-7.7	12.98
Crookes River	07/05/04	79	43.165	146.939	15	300	1200	-49.4	-7.6	11.05
Kermandie River	07/05/04	80	43.167	146.926	34	500	1200	-48.0	-7.46	11.71
Esperance River	07/05/04	81	43.322	147.010	76	1254	2000	-46.0	-7.85	16.73
Creekton Rivulet	07/05/04	82	43.350	146.958	75	1226	2000	-44.4	-6.94	11.12
South Port Creek	07/05/04	83	43.413	146.919	4	200	1600	-43.0	-6.69	10.50
Lune River	07/05/04	84	43.421	146.906	11	900	2000	-47.6	-7.73	14.21
Sugarloaf Creek	07/05/04	85	43.430	146.904	10	514	2400	-42.2	-6.56	10.32
D'Entrecasteaux River	07/05/04	86	43.507	146.876	46	1000	2400	-44.6	-7.37	14.36
Catamaran River	07/05/04	87	43.555	146.885	1	800	2000	-41.4	-6.99	14.51
Rileys Creek	07/05/04	88	43.176	146.924	40	450	2000	-41.2	-6.81	13.28
Crabtree Rivulet	07/06/04	89	42.927	147.047	217	900	2000	-46.1	-7.63	15.01
Snow Pond	07/06/04	90	42.910	147.048	692	692	1000	-46.1	-7.61	14.78
Rocky Creek	07/06/04	91	42.887	147.051	653	1000	1000	-46.0	-7.70	15.54

Table 1. (*continued*)

Sample Site	Date	Sample #	Latitude (S, dec. deg.)	Longitude (E, dec. deg.)	Sample Elevation (m)	Elevation of streamhead (m)	Estimated Mean Ann. Precip. (mm)	δD (‰) VSMOW	$\delta^{18}O$ (‰) VSMOW	d-excess (‰)
Lachlan River	07/06/04	92	42.844	147.033	151	700	1200	-48.3	-7.96	15.34
Derwent River	07/06/04	93	42.779	147.031	12	720	1600	-48.8	-8.00	15.22
Plenty River	07/06/04	94	42.739	146.957	18	850	1200	-49.1	-8.14	16.05
Tyenna River	07/06/04	95	42.674	146.790	97	800	1200	-46.3	-7.79	16.09
Kallista Creek	07/06/04	96	42.768	146.567	291	500	1200	-44.3	-7.47	15.43
Wedge River	07/06/04	97	42.859	146.229	335	1147	2000	-43.6	-7.54	16.71
Lake Pedder	07/06/04	98	42.851	146.175	309	309	2400	-26.8	-4.63	10.21
Lake Gorden	07/06/04	99	42.759	146.298	408	308	2000	-47.4	-7.78	14.89
River Styx	07/06/04	100	42.700	146.891	42	1245	1600	-47.0	-7.72	14.79
South Esk River	07/07/04	101	41.440	147.127	28	900	1200	-35.5	-6.59	17.21
Liffy River	07/07/04	102	41.514	147.063	150	1034	1600	-34.8	-6.65	18.40
Macquarie River	07/07/04	103	41.533	147.002	150	900	600	-39.1	-6.50	12.89
Quamby Brooke	07/07/04	104	41.526	146.827	176	1200	1200	-36.9	-6.39	14.22
Forth River	07/07/04	105	41.158	146.168	6	1500	2400	-2.5	-0.02	-2.36
Gawler River	07/07/04	106	41.172	146.254	18	400	2400	-41.6	-6.93	13.86
Emu River	07/07/04	107	41.077	145.924	17	700	1600	-34.5	-6.17	14.88
Maldon Creek	07/07/04	108	41.051	145.831	10	250	1600	-30.5	-5.12	10.41
Cam River	07/07/04	109	41.044	145.838	13	500	1600	-33.0	-5.81	13.45
Seabrook Creek	07/07/04	110	41.008	145.765	15	300	1600	-30.7	-5.28	11.46
Big Creek	07/07/04	111	40.996	145.703	21	300	1200	-30.0	-5.20	11.60
Inglis River	07/07/04	112	40.974	145.696	16	500	1600	-30.5	-5.42	12.83
Flowerdale River	07/07/04	113	40.971	145.658	19	550	1200	-31.2	-5.56	13.28
Wilsons Creek	07/07/04	114	40.918	145.485	49	200	1200	-29.4	-5.24	12.48
Detention River	07/07/04	115	40.880	145.452	10	554	1200	-23.8	-4.23	10.08

APPENDIX B. TREE RING DATA FOR WHITE AND BLACK SPRUCE FROM LIMESTONE LAKE, SASKATCHEWAN

Seasonal (early and late wood) $\delta^{18}O$ values for black spruce (*Picea mariana*) and white (*P. glauca*) as well as tree ring index, temperature, relative humidity (RH) measurements that were used to calculate the dampening factor *f*, and modeled source water $\delta^{18}O$ values. The calculated source water $\delta^{18}O$ values were compared to the weighted seasonal average $\delta^{18}O$ value of precipitation from The Pas, MB.

		Black Spruce (B.S)		White Spruce (W.S.)		Average	Meteor. Data The Pas, MB		B.S. Modeled Source H2O		W.S. Modeled Soruce H2O		Ave. Modeled Source H2O	Weighted Seasonal GNIP
Year	Seas.	$\delta^{18}O$	Ring Index	$\delta^{18}O$	Ring Index	$\delta^{18}O$	T (ºC)	RH	*f*	$\delta^{18}O$	f	$\delta^{18}O$	f	$\delta^{18}O$	$\delta^{18}O$
2005	early	--	--	23.5	0.10	23.5	12.4	0.67	--	--	0.01	-15.9	--	--	--
2004	late	--	--	23.7	0.31	23.7	12.3	0.76	--	--	-0.10	-13.4	-0.10	-13.4	--
2004	early	--	--	24.8	0.77	24.8	9.6	0.62	--	--	0.08	-15.5	0.08	-15.5	--
2003	late	--	0.15	24.7	0.33	24.7	15.5	0.74	0.01	--	0.03	-11.8	0.02	-11.9	--
2003	early	25.0	0.19	24.6	0.70	24.8	13.3	0.57	0.20	-15.1	0.25	-14.6	0.23	-14.9	--
2002	late	--	0.16	23.8	0.35	23.8	14.0	0.70	0.03	--	0.05	-14.2	0.04	-14.4	--
2002	early	24.3	0.46	24.5	0.69	24.4	10.8	0.58	0.15	-16.6	0.17	-15.9	0.16	-16.2	--
2001	late	--	0.31	22.1	0.75	22.1	15.6	0.68	0.12	--	0.17	-15.1	0.14	-15.4	--
2001	early	23.9	0.44	23.3	1.07	23.6	13.0	0.61	0.16	-15.6	0.23	-15.1	0.19	-15.4	--
2000	late	24.5	0.90	23.4	1.58	24.0	13.2	0.69	0.10	-13.1	0.16	-13.5	0.13	-13.3	--
2000	early	25.3	0.85	25.3	0.82	25.3	11.3	0.64	0.12	-14.0	0.12	-14.0	0.12	-14.0	--
1999	late	25.5	1.17	24.6	0.82	25.0	13.8	0.75	0.05	-10.5	0.01	-11.8	0.03	-11.1	--
1999	early	25.6	1.01	25.6	1.06	25.6	12.8	0.67	0.14	-12.5	0.15	-12.3	0.14	-12.4	--
1998	late	25.3	0.86	24.0	1.68	24.6	15.2	0.72	0.11	-11.2	0.19	-11.6	0.15	-11.4	--
1998	early	24.8	1.94	23.7	1.13	24.3	13.6	0.58	0.38	-12.1	0.30	-14.5	0.34	-13.3	--
1997	late	25.2	1.39	23.2	1.27	24.2	14.4	0.77	0.07	-9.9	0.05	-12.0	0.06	-10.9	--
1997	early	24.7	1.85	24.7	1.34	24.7	11.3	0.62	0.25	-13.2	0.20	-14.0	0.22	-13.6	--
1996	late	26.1	1.36	24.2	1.27	25.2	14.5	0.75	0.11	-9.6	0.10	-11.6	0.10	-10.6	--
1996	early	26.5	1.42	26.4	1.20	26.4	11.3	0.62	0.20	-12.1	0.18	-12.5	0.19	-12.3	--
1995	late	24.6	1.33	24.2	1.26	24.4	13.8	0.74	0.10	-11.5	0.09	-12.0	0.10	-11.8	--
1995	early	25.7	1.86	24.5	1.15	25.1	11.4	0.61	0.27	-12.2	0.19	-14.5	0.23	-13.3	--
1994	late	25.2	2.08	26.1	2.05	25.6	14.3	0.71	0.23	-10.3	0.23	-9.5	0.23	-9.9	--
1994	early	26.8	2.11	24.0	1.55	25.4	11.4	0.60	0.31	-10.8	0.26	-14.4	0.28	-12.6	--
1993	late	23.7	1.02	24.1	1.99	23.9	11.7	0.70	0.06	-14.2	0.17	-12.5	0.11	-13.4	--
1993	early	--	1.24	25.8	1.44	25.8	11.0	0.64	0.15	--	0.17	-12.6	0.16	-12.8	--
1992	late	24.4	1.74	24.2	1.91	24.3	12.1	0.70	0.15	-12.6	0.18	-12.4	0.16	-12.5	--
1992	early	23.7	1.19	24.7	1.26	24.2	10.0	0.58	0.20	-16.2	0.21	-15.0	0.20	-15.6	--
1991	late	23.9	1.21	24.5	0.37	24.2	14.4	0.72	0.12	-12.5	0.03	-12.9	0.08	-12.7	--
1991	early	24.3	1.42	25.1	0.98	24.7	13.5	0.62	0.26	-13.4	0.22	-13.1	0.24	-13.2	--
1990	late	23.9	1.42	24.9	1.05	24.4	14.4	0.70	0.18	-12.5	0.14	-11.9	0.16	-12.2	--
1990	early	24.7	1.08	24.7	0.94	24.7	11.7	0.59	0.22	-14.5	0.21	-14.8	0.21	-14.6	--

1989	late	25.3	0.92	24.4	1.33	24.9	13.5	0.68	0.13	-12.5	0.18	-12.7	0.16	-12.6	--
1989	early	24.9	1.04	26.2	1.05	25.6	12.3	0.58	0.25	-14.2	0.26	-12.8	0.25	-13.5	--
1988	late	24.6	1.58	25.4	1.57	25.0	14.0	0.66	0.24	-12.3	0.25	-11.3	0.24	-11.8	--
1988	early	26.7	1.24	26.6	0.69	26.7	13.4	0.57	0.32	-11.5	0.27	-12.6	0.29	-12.0	--
1987	late	23.6	1.32	23.1	1.49	23.4	13.2	0.67	0.17	-13.8	0.20	-13.9	0.19	-13.9	--
1987	early	25.8	1.42	26.1	0.83	25.9	12.9	0.60	0.29	-12.3	0.23	-12.9	0.26	-12.6	--
1986	late	25.1	1.29	24.4	1.41	24.8	12.6	0.69	0.12	-12.3	0.14	-12.7	0.13	-12.5	--
1986	early	25.2	1.13	25.0	1.34	25.1	11.7	0.60	0.21	-13.9	0.24	-13.7	0.22	-13.8	--
1985	late	25.0	0.84	24.4	1.60	24.7	11.6	0.67	0.07	-13.7	0.17	-13.1	0.12	-13.4	--
1985	early	26.0	1.30	26.2	1.42	26.1	11.3	0.57	0.27	-13.1	0.29	-12.6	0.28	-12.9	--
1984	late	23.9	1.03	23.8	1.26	23.9	13.7	0.71	0.10	-13.1	0.13	-12.8	0.11	-13.0	--
1984	early	24.9	0.41	24.8	1.07	24.8	13.2	0.58	0.22	-14.9	0.29	-13.7	0.25	-14.3	--
1983	late	25.3	1.00	24.3	0.48	24.8	15.2	0.71	0.14	-11.2	0.09	-12.9	0.11	-12.1	--
1983	early	24.6	0.50	25.8	0.86	25.2	11.3	0.63	0.09	-15.4	0.13	-13.6	0.11	-14.5	--
1982	late	24.4	1.37	25.8	0.68	25.1	12.7	0.72	0.09	-12.3	0.01	-11.6	0.05	-12.0	--
1982	early	25.2	0.95	25.2	0.69	25.2	10.6	0.61	0.15	-14.6	0.12	-15.0	0.14	-14.8	-14.8
1981	late	25.3	0.96	24.9	0.86	25.1	14.9	0.75	0.07	-10.7	0.07	-11.1	0.07	-10.9	-11.2
1981	early	24.9	1.27	27.3	0.75	26.1	11.7	0.61	0.21	-13.8	0.16	-12.2	0.19	-13.0	-12.9
1980	late	23.3	1.87	23.0	0.82	23.2	12.4	0.72	0.14	-13.0	0.03	-14.5	0.09	-13.8	-13.4
1980	early	24.0	1.30	25.1	0.90	24.5	13.0	0.57	0.32	-14.3	0.28	-13.9	0.30	-14.1	-14.0
1979	late	23.8	0.91	25.2	0.78	24.5	12.3	0.76	-0.03	-12.6	-0.04	-11.3	-0.03	-12.0	-14.2
1979	early	24.3	1.24	24.8	0.87	24.6	10.2	0.61	0.16	-15.1	0.12	-15.2	0.14	-15.2	-15.3
1978	late	25.9	0.71	25.5	0.94	25.7	12.3	0.76	-0.05	-10.7	-0.03	-10.8	-0.04	-10.8	-11.9
1978	early	24.4	1.03	27.0	0.96	25.7	11.0	0.63	0.13	-14.8	0.13	-12.3	0.13	-13.5	-12.5
1977	late	23.7	0.87	23.9	0.90	23.8	11.1	0.71	0.00	-14.2	0.01	-14.0	0.00	-14.1	-14.4
1977	early	25.4	1.14	24.7	0.75	25.1	12.4	0.60	0.23	-13.3	0.19	-14.7	0.21	-14.0	-14.5
1976	late	23.7	0.85	24.2	0.86	24.0	14.2	0.65	0.19	-14.3	0.19	-13.7	0.19	-14.0	-14.1
1976	early	22.3	1.45	24.4	0.79	23.3	13.0	0.61	0.27	-15.6	0.20	-14.6	0.24	-15.1	-15.2
1975	late	22.7	1.17	24.6	0.83	23.7	11.7	0.72	0.03	-14.5	0.00	-12.9	0.02	-13.7	-14.0
1975	early	22.7	1.18	24.5	0.88	23.6	11.2	0.65	0.13	-16.0	0.10	-14.7	0.11	-15.3	-15.1
1974	late	22.9	0.98	24.5	0.80	23.7	11.2	0.68	0.06	-15.6	0.05	-14.2	0.06	-14.9	--
1974	early	24.1	0.99	25.6	0.90	24.8	10.7	0.62	0.13	-15.4	0.12	-14.0	0.13	-14.7	--
1973	late	24.0	1.43	25.3	0.77	24.7	14.6	0.73	0.14	-11.9	0.07	-11.3	0.11	-11.6	--
1973	early	25.4	1.08	26.8	0.84	26.1	11.6	0.62	0.18	-13.7	0.15	-12.6	0.16	-13.1	--
1972	late	24.7	0.62	24.1	0.45	24.4	11.5	0.68	0.03	-14.2	0.01	-15.0	0.02	-14.6	--
1972	early	25.2	0.85	25.3	0.71	25.3	11.7	0.63	0.14	-14.0	0.13	-14.2	0.13	-14.1	--
1971	late	24.8	1.06	26.1	0.87	25.4	14.2	0.71	0.12	-12.1	0.11	-11.0	0.12	-11.6	--
1971	early	24.7	0.81	26.1	0.82	25.4	11.9	0.63	0.15	-14.6	0.15	-13.1	0.15	-13.8	--
1970	late	24.0	1.48	24.0	0.56	24.0	13.6	0.74	0.10	-11.9	0.01	-13.0	0.06	-12.5	--
1970	early	23.7	1.11	25.8	0.64	24.7	11.5	0.66	0.12	-14.9	0.07	-13.5	0.10	-14.2	--
1969	late	23.6	1.16	24.7	0.68	24.1	13.6	0.81	-0.03	-11.1	-0.08	-10.2	-0.06	-10.7	--
1969	early	23.5	0.69	26.0	0.76	24.7	11.4	0.61	0.14	-16.4	0.15	-13.7	0.15	-15.1	--
1968	late	23.4	1.13	23.9	0.53	23.6	12.7	0.79	-0.04	-12.0	-0.10	-12.0	-0.07	-12.0	--
1968	early	22.2	0.76	25.1	0.80	23.7	10.4	0.65	0.05	-17.3	0.06	-14.4	0.06	-15.9	--
1967	late	22.4	0.69	23.7	0.78	23.0	15.6	0.75	0.06	-13.5	0.07	-12.1	0.06	-12.8	--
1967	early	22.9	0.97	25.2	1.06	24.0	9.8	0.62	0.11	-17.1	0.12	-14.7	0.12	-15.9	--
1966	late	23.1	1.08	25.4	1.01	24.3	14.9	0.70	0.15	-13.5	0.15	-11.4	0.15	-12.5	--

1966	early	24.2	1.16	26.8	1.18	25.5	10.7	0.66	0.10	-14.6	0.10	-11.9	0.10	-13.2	--
1965	late	26.6	1.98	25.5	2.48	26.0	11.0	0.71	0.13	-10.3	0.19	-10.6	0.16	-10.4	--
1965	early	27.4	1.64	28.2	1.43	27.8	11.2	0.68	0.14	-10.3	0.12	-9.7	0.13	-10.0	--
1964	late	25.0	1.03	25.1	0.61	25.1	11.2	0.75	-0.04	-11.8	-0.08	-12.2	-0.06	-12.0	--
1964	early	23.6	1.10	25.5	1.25	24.6	11.6	0.64	0.16	-15.2	0.17	-13.1	0.16	-14.1	--
1963	late	22.7	0.63	25.0	0.48	23.9	14.8	0.74	0.04	-13.8	0.03	-11.7	0.04	-12.8	--
1963	early	23.0	0.89	24.2	1.04	23.6	12.2	0.66	0.11	-15.6	0.13	-14.1	0.12	-14.8	--
1962	late	23.6	0.86	22.6	0.94	23.1	12.9	0.72	0.05	-13.8	0.06	-14.6	0.05	-14.2	--
1962	early	24.3	0.78	25.3	1.04	24.8	11.1	0.63	0.11	-15.2	0.14	-13.8	0.12	-14.5	--
1961	late	24.1	0.60	24.2	0.58	24.1	12.7	0.74	-0.02	-13.2	-0.02	-13.1	-0.02	-13.1	--
1961	early	24.9	0.82	24.2	1.10	24.6	11.5	0.60	0.17	-14.8	0.20	-14.9	0.19	-14.8	--
1960	late	24.7	1.17	23.7	0.92	24.2	14.2	0.72	0.12	-11.8	0.09	-13.1	0.11	-12.5	--
1960	early	24.9	0.71	24.5	1.23	24.7	11.8	0.66	0.08	-14.1	0.14	-13.7	0.11	-13.9	--
1959	late	25.4	0.80	23.6	1.14	24.5	12.4	0.78	-0.06	-10.8	-0.02	-12.2	-0.04	-11.5	--
1959	early	25.4	1.15	25.3	1.19	25.4	10.8	0.68	0.06	-12.9	0.07	-12.9	0.07	-12.9	--
1958	late	24.4	1.01	23.6	1.13	24.0	12.6	0.79	-0.05	-11.1	-0.04	-11.8	-0.05	-11.5	--
1958	early	22.4	0.94	24.4	1.21	23.4	11.1	0.67	0.07	-16.4	0.10	-14.0	0.09	-15.2	--
1957	late	24.2	1.09	23.2	1.34	23.7	12.7	0.72	0.06	-12.8	0.08	-13.5	0.07	-13.2	--
1957	early	22.1	0.93	23.9	1.05	23.0	10.5	0.66	0.07	-17.1	0.09	-15.1	0.08	-16.1	--
1956	late	23.5	0.85	24.1	0.89	23.8	12.1	0.74	-0.01	-13.7	0.00	-13.0	0.00	-13.3	--
1956	early	24.2	1.16	25.8	1.55	25.0	10.6	0.67	0.08	-14.5	0.13	-12.3	0.11	-13.4	--
1955	late	23.1	0.73	22.5	2.21	22.8	13.9	0.71	0.07	-14.2	0.23	-13.0	0.15	-13.6	--
1955	early	22.6	1.13	24.9	1.42	23.7	13.3	0.66	0.18	-15.2	0.21	-12.5	0.19	-13.9	--
1954	late	22.7	0.92	22.9	0.88	22.8	12.4	0.75	-0.01	-14.1	-0.01	-13.8	-0.01	-13.9	--
1954	early	22.0	0.87	23.8	1.02	22.9	9.4	0.68	0.00	-17.4	0.02	-15.3	0.01	-16.4	--
1953	late	22.1	1.19	22.0	0.88	22.0	14.0	0.78	0.03	-13.1	-0.01	-13.6	0.01	-13.4	--
1953	early	22.3	0.78	24.1	1.05	23.2	10.8	0.72	-0.02	-15.8	0.01	-13.7	-0.01	-14.7	--
1952	late	22.1	0.78	23.2	1.10	22.6	13.4	--	--	--	--	--	--	--	--
1952	early	22.7	1.34	25.3	0.95	24.0	12.4	--	--	--	--	--	--	--	--
1951	late	--	--	22.8	0.88	61.4	12.1	--	--	--	--	--	--	--	--
1951	early	--	--	24.4	0.94	23.2	10.9	--	--	--	--	--	--	--	--
1950	late	--	--	23.2	0.66	23.2	12.7	--	--	--	--	--	--	--	--
1950	early	--	--	25.6	0.97	25.6	9.7	--	--	--	--	--	--	--	--
1949	late	--	--	23.9	1.33	23.9	14.3	--	--	--	--	--	--	--	--
1949	early	--	--	26.9	1.08	26.9	12.3	--	--	--	--	--	--	--	--
1948	late	--	--	24.1	0.56	24.1	15.8	--	--	--	--	--	--	--	--
1948	early	--	--	25.0	0.73	25.0	11.2	--	--	--	--	--	--	--	--
1947	late	--	--	23.9	1.01	23.9	13.1	--	--	--	--	--	--	--	--
1947	early	--	--	25.8	0.84	25.8	10.6	--	--	--	--	--	--	--	--
1946	late	--	--	23.0	0.91	23.0	13.1	--	--	--	--	--	--	--	--
1946	early	--	--	24.3	0.95	24.3	11.4	--	--	--	--	--	--	--	--
1945	late	--	--	22.9	1.15	22.9	13.7	--	--	--	--	--	--	--	--
1945	early	--	--	26.1	1.02	26.1	9.3	--	--	--	--	--	--	--	--
1944	late	--	--	22.8	3.49	22.8	13.4	--	--	--	--	--	--	--	--
1944	early	--	--	24.6	1.18	24.6	12.1	--	--	--	--	--	--	--	--
1943	late	--	--	23.8	0.94	23.8	--	--	--	--	--	--	--	--	--
1943	early	--	--	25.3	0.75	25.3	--	--	--	--	--	--	--	--	--

1942	late	--	--	24.8	0.96	24.8	--	--	--	--	--	--	--	--	--
1942	early	--	--	24.5	1.05	24.5	--	--	--	--	--	--	--	--	--
1941	late	--	--	24.3	0.61	24.3	--	--	--	--	--	--	--	--	--
1941	early	--	--	24.3	0.69	24.3	--	--	--	--	--	--	--	--	--
1940	late	--	--	21.8	1.00	21.8	--	--	--	--	--	--	--	--	--
1940	early	--	--	23.9	0.57	23.9	--	--	--	--	--	--	--	--	--
1939	late	--	--	22.7	0.25	22.7	--	--	--	--	--	--	--	--	--
1939	early	--	--	25.4	0.51	25.4	--	--	--	--	--	--	--	--	--
1938	late	--	--	25.5	0.39	25.5	--	--	--	--	--	--	--	--	--
1938	early	--	--	25.6	0.54	25.6	--	--	--	--	--	--	--	--	--
1937	late	--	--	24.6	1.33	24.6	--	--	--	--	--	--	--	--	--
1937	early	--	--	25.3	1.00	25.3	--	--	--	--	--	--	--	--	--
1936	late	--	--	24.0	0.96	24.0	--	--	--	--	--	--	--	--	--
1936	early	--	--	25.5	1.06	25.5	--	--	--	--	--	--	--	--	--
1935	late	--	--	24.0	1.13	24.0	--	--	--	--	--	--	--	--	--
1935	early	--	--	23.2	1.29	23.2	--	--	--	--	--	--	--	--	--
1934	late	--	--	25.3	1.45	25.3	--	--	--	--	--	--	--	--	--
1934	early	--	--	25.3	1.29	25.3	--	--	--	--	--	--	--	--	--
1933	late	--	--	24.6	1.50	24.6	--	--	--	--	--	--	--	--	--
1933	early	--	--	26.7	1.35	26.7	--	--	--	--	--	--	--	--	--
1932	late	--	--	26.6	0.77	26.6	--	--	--	--	--	--	--	--	--
1932	early	--	--	25.2	1.05	25.2	--	--	--	--	--	--	--	--	--
1931	late	--	--	24.7	0.80	24.7	--	--	--	--	--	--	--	--	--
1931	early	--	--	24.5	0.65	24.5	--	--	--	--	--	--	--	--	--
1930	late	--	--	24.3	0.83	24.3	--	--	--	--	--	--	--	--	--
1930	early	--	--	25.0	0.84	25.0	--	--	--	--	--	--	--	--	--
1929	late	--	--	25.1	1.04	25.1	--	--	--	--	--	--	--	--	--
1929	early	--	--	25.4	0.89	25.4	--	--	--	--	--	--	--	--	--
1928	late	--	--	25.5	0.54	25.5	--	--	--	--	--	--	--	--	--
1928	early	--	--	23.8	1.83	23.8	--	--	--	--	--	--	--	--	--
1927	late	--	--	23.9	0.95	23.9	--	--	--	--	--	--	--	--	--
1927	early	--	--	26.0	1.41	26.0	--	--	--	--	--	--	--	--	--
1926	late	--	--	24.6	0.59	24.6	--	--	--	--	--	--	--	--	--
1926	early	--	--	24.5	1.01	24.5	--	--	--	--	--	--	--	--	--
1925	late	--	--	24.1	0.62	24.1	--	--	--	--	--	--	--	--	--
1925	early	--	--	25.5	0.74	25.5	--	--	--	--	--	--	--	--	--
1924	late	--	--	24.8	0.87	24.8	--	--	--	--	--	--	--	--	--
1924	early	--	--	25.6	0.92	25.6	--	--	--	--	--	--	--	--	--
1923	late	--	--	23.9	0.69	23.9	--	--	--	--	--	--	--	--	--
1923	early	--	--	23.8	1.17	23.8	--	--	--	--	--	--	--	--	--
1922	late	--	--	24.6	0.97	24.6	--	--	--	--	--	--	--	--	--
1922	early	--	--	24.5	1.91	24.5	--	--	--	--	--	--	--	--	--
1921	late	--	--	--	0.51	--	--	--	--	--	--	--	--	--	--
1921	early	--	--	24.6	4.26	24.6	--	--	--	--	--	--	--	--	--
1921	late	--	--	--	0.81	--	--	--	--	--	--	--	--	--	--
1920	early	--	--	26.1	-5.59	26.1	--	--	--	--	--	--	--	--	--
1919	late	--	--	24.5	0.86	24.5	--	--	--	--	--	--	--	--	--

1919	early	--	--	22.9	-1.39	22.9	--	--	--	--	--	--	--	--	--
1918	late	--	--	22.7	0.30	22.7	--	--	--	--	--	--	--	--	--
1918	early	--	--	23.9	-1.22	23.9	--	--	--	--	--	--	--	--	--
1917	late	--	--	23.2	0.97	23.2	--	--	--	--	--	--	--	--	--
1917	early	--	--	23.8	-0.85	23.8	--	--	--	--	--	--	--	--	--
1916	late	--	--	24.7	0.34	24.7	--	--	--	--	--	--	--	--	--
1916	early	--	--	26.7	-0.43	26.7	--	--	--	--	--	--	--	--	--
1915	late	--	--	25.7	1.80	25.7	--	--	--	--	--	--	--	--	--
1915	early	--	--	24.3	-0.55	24.3	--	--	--	--	--	--	--	--	--
1914	late	--	--	24.0	0.76	24.0	--	--	--	--	--	--	--	--	--
1914	early	--	--	23.5	-0.23	23.5	--	--	--	--	--	--	--	--	--
1913	late	--	--	--	1.19	--	--	--	--	--	--	--	--	--	--
1913	early	--	--	23.6	-0.17	23.6	--	--	--	--	--	--	--	--	--
1912	late	--	--	--	0.41	--	--	--	--	--	--	--	--	--	--
1912	early	--	--	23.3	-0.19	23.3	--	--	--	--	--	--	--	--	--
1911	late	--	--	23.0	0.86	23.0	--	--	--	--	--	--	--	--	--
1911	early	--	--	24.3	-0.20	24.3	--	--	--	--	--	--	--	--	--
1910	late	--	--	24.6	1.32	24.6	--	--	--	--	--	--	--	--	--
1910	early	--	--	24.2	-0.25	24.2	--	--	--	--	--	--	--	--	--
1909	late	--	--	24.0	1.78	24.0	--	--	--	--	--	--	--	--	--
1909	early	--	--	23.5	-0.10	23.5	--	--	--	--	--	--	--	--	--
1908	late	--	--	--	2.23	--	--	--	--	--	--	--	--	--	--
1908	early	--	--	23.8	-0.17	23.8	--	--	--	--	--	--	--	--	--
1907	late	--	--	24.6	0.88	24.6	--	--	--	--	--	--	--	--	--
1907	early	--	--	25.7	-0.18	25.7	--	--	--	--	--	--	--	--	--
1906	late	--	--	25.1	2.16	25.1	--	--	--	--	--	--	--	--	--
1906	early	--	--	25.2	-0.16	25.2	--	--	--	--	--	--	--	--	--
1905	late	--	--	24.8	1.67	24.8	--	--	--	--	--	--	--	--	--
1905	early	--	--	23.4	-0.14	23.4	--	--	--	--	--	--	--	--	--
1904	late	--	--	23.4	1.99	23.4	--	--	--	--	--	--	--	--	--
1904	early	--	--	24.4	-0.13	24.4	--	--	--	--	--	--	--	--	--
1903	late	--	--	--	1.12	--	--	--	--	--	--	--	--	--	--
1903	early	--	--	23.3	-0.12	23.3	--	--	--	--	--	--	--	--	--
1902	late	--	--	--	0.35	--	--	--	--	--	--	--	--	--	--
1902	early	--	--	24.4	-0.09	24.4	--	--	--	--	--	--	--	--	--
1901	late	--	--	--	1.61	--	--	--	--	--	--	--	--	--	--
1901	early	--	--	24.5	-0.11	24.5	--	--	--	--	--	--	--	--	--
1900	late	--	--	--	0.89	--	--	--	--	--	--	--	--	--	--
1900	early	--	--	23.9	-0.10	23.9	--	--	--	--	--	--	--	--	--
1899	late	--	--	--	0.81	--	--	--	--	--	--	--	--	--	--
1899	early	--	--	23.6	-0.13	23.6	--	--	--	--	--	--	--	--	--
1898	late	--	--	--	0.74	--	--	--	--	--	--	--	--	--	--
1898	early	--	--	24.5	-0.10	24.5	--	--	--	--	--	--	--	--	--
1897	late	--	--	--	0.89	--	--	--	--	--	--	--	--	--	--
1897	early	--	--	24.7	-0.09	24.7	--	--	--	--	--	--	--	--	--
1896	late	--	--	--	0.81	--	--	--	--	--	--	--	--	--	--
1896	early	--	--	24.3	-0.08	24.3	--	--	--	--	--	--	--	--	--

1895	late	--	--	--	0.91	--	--	--	--	--	--	--	--	--	--
1895	early	--	--	24.1	-0.08	24.1	--	--	--	--	--	--	--	--	--

Justin Dodd

114 Science Place
Department of Geological Sciences
University of Saskatchewan
Saskatoon, SK S7N 5E2 Canada
Office: (306) 966-5737 Lab: (306) 966-5712
jpd058@mail.usask.ca

Education

2003 – 2006 University of Saskatchewan – Saskatoon, Saskatchewan, Canada
M.Sc., Geological Sciences (06/06/06) GPA 4.0/4.0
Thesis – **Isotopic Records of Meteorological and Atmospheric Conditions from Sub-Annually Resolved Tree-Ring Cellulose, Precipitation, and Surface Waters**

1999 – 2003 Beloit College -- Beloit, Wisconsin, USA
B.S., Geological Sciences *Magna Cum Laude*, GPA 3.71/4.0
Thesis – **Climate Change in Western Ireland During the Holocene: Evidence from Stable Isotope Ratios of Carbon and Oxygen in Lacustrine Sediments**
B.S., Anthropology *Magna Cum Laude*, GPA 3.71/4.0

Academic Awards and Achievements

2005 **Geological Society of America Research Grant**
2004 **National Science Foundation Graduate Research Fellowship**
2003 **Graduate Student Scholarship**, College of Graduate Studies, University of Saskatchewan
2003 Phi Beta Kappa Honor Society
2003 Outstanding Student Research in Geology, Beloit College
2002 Outstanding Student Research in Anthropology, Beloit College
2002 Outstanding Teaching Assistant in Geology, Beloit College
2001 Mineralogy Student Award, Beloit College
1999 **Beloit College Presidential Scholarship**, Beloit College

Field Experience

2005 **Northern Saskatchewan, Canada** - Fieldwork and Tree Sample Collection
2004 **Australia -** Fieldwork and Water Sample Collection (6 week field session)
2004 **Yucatán Peninsula, Mexico** - International Field School and Sample Collection
2003 **Northern Saskatchewan and Manitoba, Canada** - Fieldwork and Sample Collection
2002 **Western Ireland** - Keck Geology Consortium Research Program (4 week field session)
2001 **Dar es Salaam and Serengeti National Park, Tanzania** - Associated Colleges of the Midwest Study Abroad Program (6 month field session)
2001 **Red Lodge, MT** - Yellowstone-Bighorn Research Association Field School (6 week field session)

Field Experience (*continued)*

2000 **Atacama Desert, Chile** - Beloit College Archeological Field School (6 week field session)

1997 **Lower Illinois River Valley** - Center for American Archeology/ National Science Foundation Young Scholars Program (2 month field session)

Papers in Review

Dodd, J.P., Patterson, W.P, 2006, Survey of Oxygen and Hydrogen Isotope Values in Tasmanian Precipitation and Surface waters, Journal of Hydrology.

Published Abstracts

Patterson, W.P., Brasseur, J., **Dodd, J.P.**, Eglington, B.E., 2006, The use of robotics in deriving high resolution climate/environmental information from tree rings. The 7th International Conference on Dendrochronology, Beijing, China.

Dodd, J.P., Patterson, W.P., and Holmden, C.E., 2005. Reconstructing meteorological conditions from tree-ring cellulose at sub-annual resolution using a multi-isotope approach American Geophysical Union Fall Meeting, San Francisco, CA.

Dodd, J.P., Patterson, W.P., and Holmden, C.E., 2005. Calibration of carbon and oxygen isotope values of modern tree-ring cellulose from Saskatchewan with meteorological records. Geological Society of America, Earth System Processes 2 Meeting, Calgary, Alberta.

Dodd, J.P., Patterson, W.P., and Holmden, C. E., 2005. Comparison of stable carbon and oxygen isotope values of modern pine (*Pinus banksiana*) tree-ring cellulose to meteorological records: a proxy for reconstructing mid- to high-latitude continental climate. 35th Annual International Arctic Workshop. Edmonton, Alberta, Canada.

Glemser, C.*, **Dodd, J.P.**, Patterson, W.P., and Holmden, C.E., 2005. Paleoclimate Reconstruction of the Yucatán Peninsula from Lacustrine Sediments: Stable Isotope Evidence of Drought Cyclicity. Western Inter-University Geological Conference. Saskatoon, SK, Canada.
*** undergraduate student research co-supervised by Dodd, Patterson, and Holmden**

Dodd, J.P., Patterson, W.P., Martini, A. Tiber, N., 2003, Climate Change in Western Ireland During the Holocene as Indicated by Stable Isotope Ratios of Carbon and Oxygen in Lacustrine Sediments, 16th Annual Keck Research Symposium in Geology Proceedings. Beloit, WI.

Dodd, J.P., Wirth, K., Mabulla, A., 2001, The Role of Kopjes in the Regional Settlement Patterns of the Serengeti Plain, Associated Colleges of the Midwest – Tanzania Program, Dar es Salaam, Tanzania.